UNIVERSITÀ DEGLI STUDI DI MILANO

Scuola di Dottorato in Scienze Biologiche e Molecolari

XXVIII Ciclo

Unravelling the molecular mechanisms of impaired limb development: role of ΔNp63α in Split-Hand/Foot Malformation type 4 and in thalidomide teratogenicity

Elisa Molinari

PhD Thesis

Scientific tutor: Dr. Luisa Francesca Guerrini

Academic year: 2014-2015

SSD: BIO/11

Thesis performed at the Department of Biosciences, University of Milan (Italy), in collaboration with the Department of Nanoparticle Translational Research, Tokyo Medical University (Japan)

Table of contents

Part I

Part II

Part III

Part I

1. Abstract

The p63 transcription factor, homolog to the p53 tumour suppressor, plays a key role in limb, epithelial and cranio-facial development. p63 activity and stability are tightly modulated to guarantee correct development of such structures and an impairment of this regulative mechanism can result in severe malformations. The control of p63 function is achieved not only through the regulation of its gene expression but also through a complex network of post-translational modifications. Acetylation, phosphorylation and ubiquitination affect p63 half-life, the specificity and efficiency of protein-protein interactions and overall modulate the transcriptional activity of the protein.

Here we describe two pathways that, by post-translationally modifying ΔNp63α protein, modulate its stability and function.

One such pathway involves FGF8, c-Abl and p300 which cooperate in controlling the stability and function of ΔNp63α protein by leading to its acetylation on lysine 193 (K193). Interestingly, K193 is mutated into glutamic acid (K193E) in patients affected by Split Hand/Foot Malformation (SHFM) type 4. c-Abl kinase activity is required to transduce the signal induced by FGF8 leading to ΔNp63α stabilization and transcriptional activation, through its acetylation mediated by p300. The ΔNp63α-K193E mutant, which cannot be acetylated by this pathway, displays promoter-specific loss of DNA binding activity and consequent altered expression of development-associated ΔNp63α target genes. Our results, elucidating an important regulatory pathway activated by FGF8 and essential for ΔNp63α activation and stabilization, shed new light on the molecular mechanism that could be at the basis of the SHFM4 pathogenesis.

The other pathway that we here present is a degradative pathway promoted by the teratogenic drug thalidomide that leads to proteasome-mediated degradation of ΔNp63α, resulting in a lack of activation of ΔNp63α development-related target genes. In cell lines, thalidomide treatment induces a downregulation of ΔNp63α protein via the action of GSK3 kinase and FBWX7 ubiquitin ligase. Upon thalidomide treatment, GSK3 kinase is required to phosphorylate ΔNp63α on the residues serine 383 and threonine 397. This phosphorylation is recognized as a signal by FBWX7 which in turn ubiquitinates ΔNp63α, leading to its proteasome-mediated degradation. Thalidomide treatment induces a downregulation of ΔNp63α protein levels also *in vivo* in zebrafish embryos, where it results in a phenotypical and molecular impairment of fin development. Importantly, the microinjection of *zp63*-mRNA into zebrafish embryos treated with thalidomide rescues both the phenotypical and molecular defects induced by the drug, indicating that the downregulation of ΔNp63α is, at least in part, at the bases of thalidomide-induced malformations. Our results, by demonstrating that ΔNp63α is a molecular target of thalidomide teratogenicity, provide a fundamental missing piece in the

description of the drug molecular mechanism of action. Thalidomide is now used for the treatment of multiple myeloma and leprosy: a better understanding of its mechanism of action might pave the way for the design of related compounds with equal therapeutic properties but devoid of teratogenic activity.

2. State of the art

2.1 The p53 family

p53, located on chromosome 17 (17p13), is the principal tumor-suppressor gene, being mutated in 50% of human cancers (1). The p53 protein exhibits high amino acid identity with the other members of the family, p63 and p73, which are encoded by two genes located respectively on chromosome 3 (3q27-29) and 1 (1q36). The highest identity among the protein of the family is in their TransActivation (TA) domain, DNA-Binding Domain (DBD), and tetramerization (ISO) domain. Unlike p53, p63 and p73 are not classical tumour suppressors, rather, they act as key regulators in development. p73 is involved in the development of neuronal and pheromonal pathways (2) and p63 in limb, epithelial, and craniofacial development (2,3). p73 KO mice display high mortality rate within 2 months after birth, suffering from hydrocephals, indicative of abnormal cerebrospinal fluid dynamics, immunological problems characaterized by chronic infectious and inflammation and nervous system abnormalities related to hippocampal dysgenesis, olfactory neuron defects and loss of sympathetic neurons (4). $p63^{-/-}$ mice are born alive, but they die soon after birth because of dehydration. Moreover, they display an impairment in limb development as well as of stratified epidermis and of other ectodermal derivatives such as salivary, lacrimal and mammary glands, prostate, teeth and hair follicles (2,3).

p63 and *p73* encode several different isoforms. Both *p63* and *p73,* encode two primary transcripts, as they can be transcribed under two different promoters: one is located in a non-coding region of exon 1 and the other in intron 3. The product of the first promoter contains the TA domain (the TA isotypes) whilst the product of the second promoter lacks this domain (the ΔN isotypes). Additionally, extensive alternative splicing involves the 3' end, resulting in five different variants for p63 (α, β, γ, δ, ε) and seven for p73 (α, β, γ, δ, ε, ζ, η).

2.2 The p63 transcription factor

2.2.1 Protein structure

All p63 isoforms contain the DNA-binding domain (**DBD**), which is rensponsible for the binding of p63 to its responsive elements and the tetramerization (**ISO**) domain that allows the formation of omo- and etero-tetramer, which is essential for p63 transactivational functions.

On the contrary, the transactivation (**TA**) domain is present only in the products of the promoter contained in exon 1 (TA isoforms). It was initially considered as the only responsible for the activation of p63 target genes. In fact, the ΔN isoforms were thought to act as dominant-negative

isoforms, which, lacking the TA domain, inhibited the transactivational function of the tetramer. However, it has been demonstrated that also the ΔN isoforms were able to modulate directly p63 target genes as they possess a second transactivation (**TA2**) domain, located between the aminoacids 410 and 512 (5). The extended 3' coding sequences of the α-isoforms of *p63* encode a protein-protein-interaction motif that resembles the sterile-α-motif (**SAM**) domain (6,7), which is not present in p53. SAM domains are small globular protein-protein interaction modules that are usually involved in homo- and hetero-oligomerization with other SAM domains. In the extended carboxy-terminal portion of α-isoforms is also present a C-terminal inhibitor domain (**TID**) which is able, by binding to the N-terminal region of the protein, to mask the TA domain, leading to a reduction of the transactivational activity of TAp63α isoform.

Besides these major structural protein motifs, all p63 isoforms present, in the N-terminal portion, **proline-rich domains**, which are involved in pro-apoptotic activity and in the capacity to activate target sequences (8). A **second proline-rich region** is located between the ISO and SAM domains in p63 and p73 but not in p53. This proline-rich domain is engaged in a physical association with the YES-associated protein YAP (9) (Fig. 1).

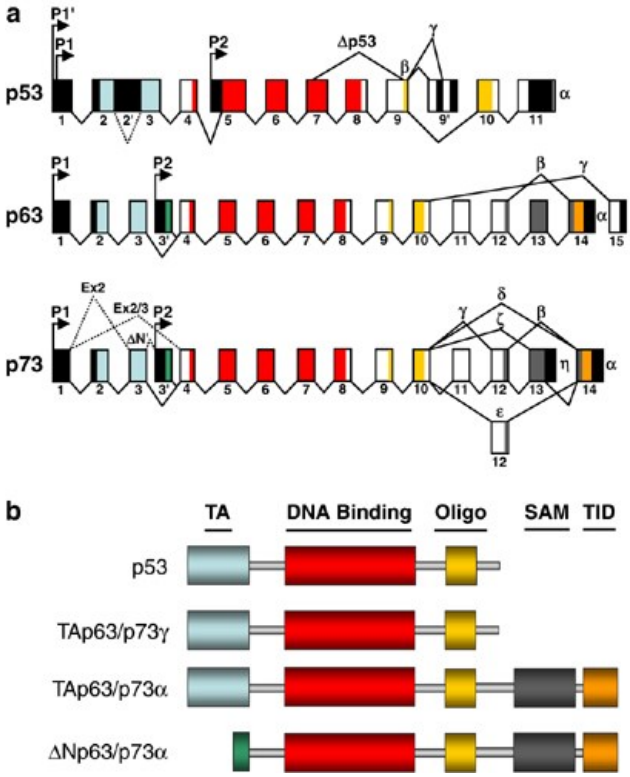

Figure 1. Structure and expression of p53 family members. **(a)** Structure of p53, p63 and p73 transcription units. Numbered boxes indicate exons, and black shading denotes untranslated sequences. The approximate regions encoding the transactivation (TA) domain (light blue), ΔN-specific region (green), DNA-binding domain (red), oligomerization domain (yellow), sterile alpha motif (SAM, grey), and transactivational inhibitory domain (TID, orange) are indicated. Distinct transcription start sites are indicated by arrows. N-terminal alternative splicing for p53 and p73 are indicated by dotted lines, and C-terminal splicing events are indicated by solid lines and Greek letter designation. **(b)** Protein domains of p53 family members. All three family members share a homologous DNA-binding domain and oligomerization domain (oligo). The TA domain is shared by p53, TAp63, and TAp73 isoforms. TAp63$^{\gamma}$/TAp73$^{\gamma}$ isoforms most closely resemble p53. N-terminally truncated ΔN isoforms possess unique N-terminal sequences. Alpha isoforms of p63 and p73 possess a C-terminal SAM domain followed by a transactivational inhibitory domain (TID). Other isoforms of p53, p63 and p73 are not shown (10).

2.2.2 p63 expression and functions

Despite the homology between *p53* and *p63*, the latter is not considered a classical tumour suppressor, rather it has a key role in limb, craniofacial and epithelial development. In fact, mice lacking *p63* are born alive but have striking developmental defects. Their forelimbs are truncated and hindlimbs are completely absent (2,3). These limb defects are caused by a failure of the Apical Ectodermal Ridge (AER) to differentiate. AER is a structure of stratified ectoderm with a key role in limb bud emergence and progression; sections of *p63*$^{-/-}$ specimens provide no evidence of a discernible stratified ectoderm along the interface of dorsal and ventral surfaces of the limb bud. Instead, mutant limb buds have a single-layered epithelium at the distal tip, indistinguishable from the surrounding ectoderm.

Moreover, *p63* KO mice die soon after birth because of dehydration as *p63*$^{-/-}$ mice lack epidermis. They also have no squamous epithelia (prostate, urothelium) or epithelial appendages, such as mammary, salivary and lachrymal glands, hair follicles and teeth (Fig. 2).

The phenotype of *p63* KO embryos correlates well with its pattern of expression.

p63 is expressed as early as embryonic day 9.5 (E9.5) within the oral ectoderm, limb buds and tail bud region. At later stages of gestation, *p63* is expressed primarily within the ectoderm; expression is evident within the basal region of the interfollicular epidermis of the skin and within the outer root-sheath of hair follicles. In adult mice, *p63* is expressed in skin, tongue, tail and skeletal muscle.

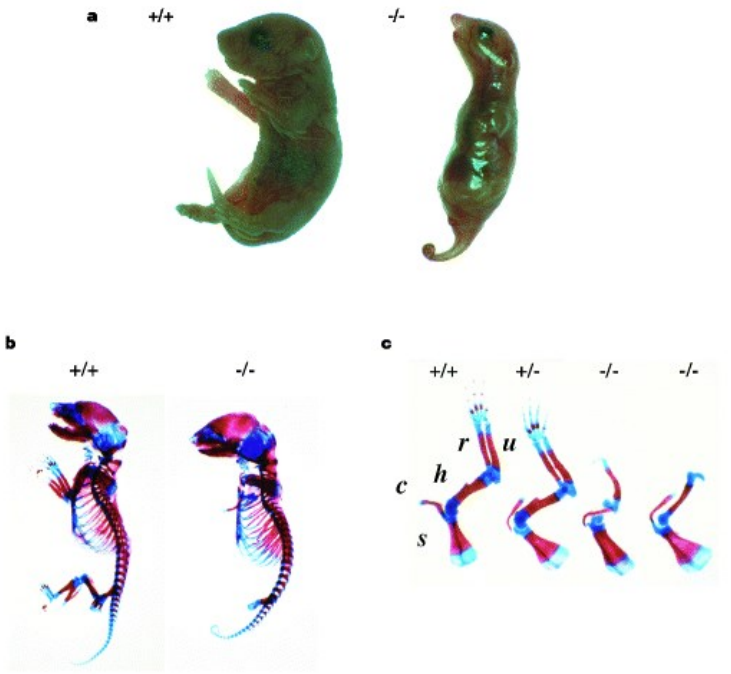

Figure 2. The phenotype of p63-deficient newborn mice. **(a)** Matings between p63-heterozygous mice produce wild-type and heterozygous offspring that are overtly normal and p63-deficient mice that have severe limb and skin defects. **(b)** Skeletons of wild-type, p63-heterozygous and p63-homozygous mutant animals were stained for cartilage (blue) and bone (red). **(c)** Forelimbs of p63-homozygous mutant mice are truncated; the phalanges, radius and ulna are absent and the humerus is deformed. Abbreviations: c, clavicle; h, humerus; r, radius; s, scapula; u, ulna (3).

2.2.3 Conserved sequence and role for the *p63* gene in zebrafish (*Danio rerio*)

In 2002, Bakkers et al. (11) cloned three different p63 isoforms in zebrafish, all encoding for ΔNp63 proteins lacking the N-terminal transactivating (TA) domain. In their C terminus, the two longer ΔNp63 isoforms (α1 and α2) correspond to the mammalian α splice products, containing the SAM domain and the entire C-terminal tail, while the shorter isoform corresponds to γ splice variants, with a C-terminal truncation starting before the SAM domain. The amino acid sequence alignment demonstrates that ΔNp63α is highly conserved from fish to mammals (11,12). Of the major domains

identified in p63, the DNA binding domain is 96% identical, the oligomerization domain is 67% identical and the SAM domain is 68% identical between mouse and zebrafish (11) (Fig. 3).

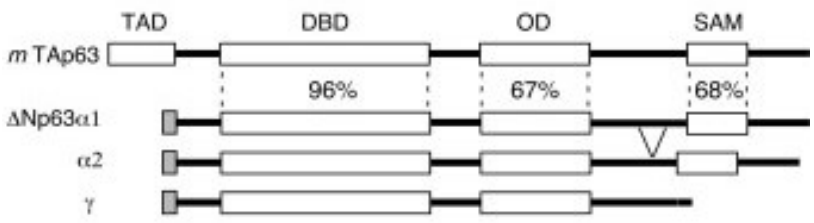

Figure 3. Diagram of isolated p63 isoforms. Structure of the longest version of mouse p63 and the three isolated zebrafish ΔNp63 isoforms. TAD, transactivating domain; DBD, DNA binding domain; OD, oligomerization domain; SAM, sterile α motif. Numbers indicate the percentages of amino acid conservation of the different domains between mouse p63 and zebrafish ΔNp63α. Compared to ΔNp63α1, α2 lacks 12 amino acids at the indicated position upstream of the SAM domain (11).

The ΔNp63α versions are the most abundant, if not the only, p63 isoforms present during zebrafish embryogenesis. ΔNp63 is readily detectable at early gastrula stages and continues to be expressed at similar levels during the first few days of embryogenesis (11,12) (Fig. 4).

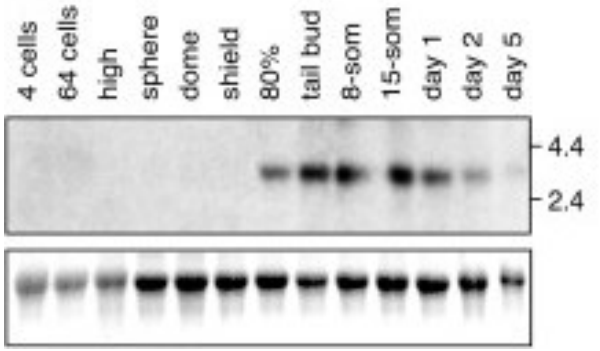

Figure 4. *p63* temporal expression in zebrafish embryos.

Whole-mount in situ hybridization revealed that *ΔNp63* expression is confined to the ventral ectoderm of gastrula embryos, which will give rise to epidermal, non-neural fates. Expression of *ΔNp63* in the prospective epidermal ectoderm is maintained throughout late gastrulation and early segmentation stages. At around 40 hours post fertilization (hpf), *ΔNp63* transcripts are present in the ectodermal components of the branchial arches and the pectoral fin buds. In the fin buds, *ΔNp63* is only expressed in the distal tip, called apical fold, which is homologous to the AER of higher vertebrates and not in the underlying mesenchyme. *ΔNp63* is also expressed in the cutaneous ectoderm (11,12) (Fig. 5).

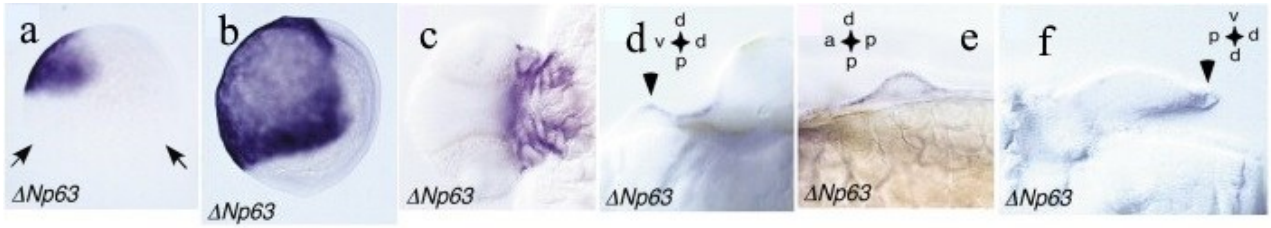

Figure 5. Stain by whole-mount in situ hybridization with indicated probe (*ΔNp63*). **(a)** 80% epiboly, lateral view, dorsal right, animal pole (anterior) up. Arrows point to margin of embryos. **(b)** Tailbud stage, dorsal right. **(c)** 48 hpf, ventral view on head region. **(d)** 38 hpf, optical transverse section through fin bud and trunk; axes of fin bud are indicated; distal up, proximal down, ventral left, dorsal right. The arrowhead points to presumptive apical fold. **(e)** 38 hpf, optical saggital section through finbud; axes of fin bud are indicated; distal up, proximal down, anterior left, posterior right. **(f)** 48 hpf, view on pectoral fin; axes of fin bud are indicated; ventral up, dorsal down, proximal left, distal right; arrowheads point to apical fold (11).

Consistent with the expression pattern of *ΔNp63*, its knock down in zebrafish embryos, obtained by microinjecting a specific morpholino, results in the absence of pectoral fins, probably due to the failure to maintain the apical fold. Moreover, skin lesions are noticeable and by days 4-5 post fertilization, the ΔNp63 morphants are susceptible to infection by microorganisms since the skin is no longer acting as a protective barrier from the outside environment. In morphant embryos skin cells fail to proliferate and are strongly reduced in number, but still express *cytokeratin8,* a marker for keratinocytes (11,12) (Fig. 6).

Overall, the phenotype is intriguingly similar to the effects observed in mice lacking the p63 gene, suggesting a conserved role for p63 in limb and epithelial development.

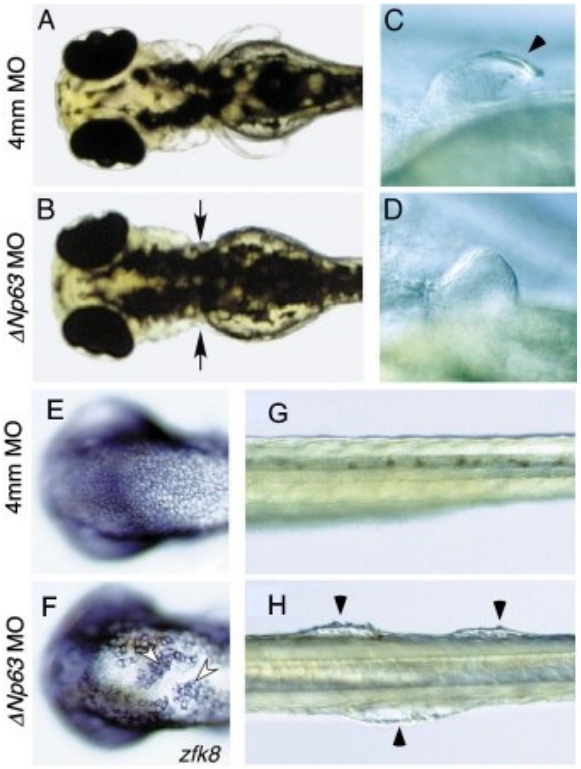

Figure 6. MO-based zebrafish *ΔNp63* knockdown affects pectoral fin and skin development. Upper panel of each block shows control animals injected with 4 mm MO; lower panel morphants injected with *ΔNp63* MOs. (a-d, g, and h) live larvae; (e and f) in situ hybridization with indicated probe (*zfk8*). **(a, b)** 72 hpf, dorsal view on anterior region. Arrows in (b) point to missing pectoral fins. **(c, d)** 48 hpf, view on pectoral fin. The arrowhead in (c) points to apical fold missing in (d). **(e, f)** *zfk8*, 48 hpf, dorsal view on head. White arrowheads in (f) point to clusters of *zfk8*-positive cells. **(g, h)** 54 hpf, dorsal view on trunk/tail. Arrowheads in (h) point to blisters in skin (10).

p63 overexpression in *ΔNp63* mRNA-injected embryos results in severe anterior CNS truncations, due to extended apopotosis among anterior neuroectodermal cells. Thus, *ΔNp63* mRNA-injected larvae lack forebrain and eyes, while other anterior structures like jaw and hatching glands and the rest of the embryo develop normally (11) (Fig. 7).

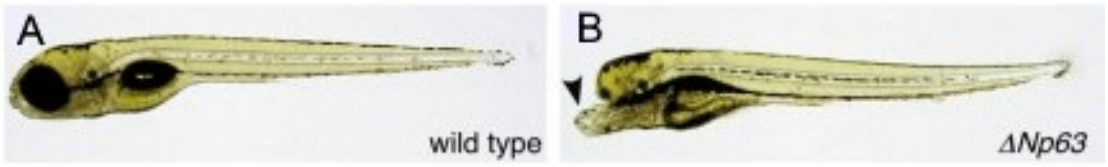

Figure 7. 120 hpf, lateral view. **(a)** Uninjected control. **(b)** Animal injected with *ΔNp63α* mRNA. Arrowhead points to jaw (11).

2.2.4 p63-associated syndromes and malformations

The phenotype of *p63* KO mice and zebrafish morphants correlates well with the defects displayed by patients affected by mutations in *p63* gene. There is a wide spectrum of *p63* mutations that underlie

five different human malformation conditions: Ectrodactyly-Ectodermal dysplasia-Clefting (EEC) syndrome (MIM 604292), Ankyloblepharon-Ectodermal dysplasia-Clefting (AEC) syndrome (MIM 106260), Limb-Mammary Syndrome (LMS [MIM 603543]), Acro-Dermato-Ungual Lacrimal-Tooth (ADULT) syndrome (MIM 103285), and nonsyndromic Split-Hand/Foot Malformation (SHFM) type 4 (13). All these disorders are caused by dominant mutations; it is likely that p63 mutant protein perturbs the activity of the wild type ones with which it can form tetramers.
It is noteworthy that the localization and functional effects of the mutations that underlie these syndromes establish a striking genotype-phenotype correlation (13,14) (Fig. 8).

Ectrodactyly-Ectodermal dysplasia-Clefting (EEC) syndrome

EEC are invariably affected by ectodermal dysplasia which can present as defects of hair, skin, nails teeth and glands. About two-thirds of these patients also have ectrodactyly, syndactyly is also frequent (43%). Cleft lip/palate is present in about 40% of the EEC patients, who occasionally also have mammary gland/nipple hypoplasia (14%) and hypohidrosis (11%).
Altogether 34 different EEC causing mutations have been reported, and 20 different amino acids are involved. However, they are almost all missense point mutations in the DBD of the *p63* gene and only two mutations are outside the DBD: one frameshift mutation consisting in a single nucleotide insertion in exon 13 (1572 InsA) and one point mutation (L563P) in the SAM domain.
Five frequently mutated amino acids: R204, R227, R279, R280 and R304 in the EEC population explain almost 90% of the EEC syndrome patients. The five p63 arginine hotspot mutations appear to impair the p63 protein binding to DNA, resulting in loss of p63 transactivational activity (13,15).

Limb-Mammary Syndrome (LMS)

The LMS phenotype resembles the EEC syndrome phenotype; about 70% of LMS patients have similar limb malformations as in EEC syndrome, and about 30% display orofacial clefting. However, the ectodermal manifestations are milder. Moreover, unlike in EEC patients, hair and skin defects are rarely detected in LMS patients a consistent feature of LMS is the mammary gland and/or nipple hypoplasia (100%). Lacrimal duct obstruction and dystrophic nails are also frequently observed (59 and 46% respectively), hypohydrosis and teeth defects are detected in about 30% of the patients.
Mutations in LMS are located in the N- and C-terminus of the *p63* gene. A large LMS family display G76W substitution in the ΔN-specific putative transactivation domain (TA2). One other missense point mutation (S90W) is located between the TA domain and DBD. In the C-terminus a TT deletion in the exon 13 and an AA deletion in exon 14 have been reported. These mutations will affect only

the p63α protein isoforms, where they are predicted to cause a frame shift and a premature stop codon. Also, a stop mutation in the TID (K632X) has been identified in a sporadic LMS patient and is predicted to impair the suppressive effect of the TI domain towards the TA domain, thus increasing p63 transactivational activity (13,15).

Acro-Dermato-Ungual Lacrimal-Tooth (ADULT) syndrome

As in LMS, ADULT syndrome phenotype is characterized by ectrodactyly and ectodermal defects, but hair (53%) and lacrimal duct defects (67%) are observed in ADULT patients more frequently than in LMS. Moreover, whilst teeth, skin and nail defects are only rarely observed in LMS, they are constantly present in ADULT syndrome (100, 93 and 100%, respectively). One other difference is the absence in ADULT syndrome of orofacial clefting. Four ADULT syndrome families and three sporadic cases have been reported. All the families and one of the sporadic cases have a missense point mutation in exon 8, changing R298 in the DNA binding domain into either a glutamine or a glycine. R298 is not located close to the DNA-binding interface, and mutation of this arginine does not affect DNA binding, but can confer transactivational activity to ΔNp63γ isoform. Two other mutations are located in the N-terminus: N6H mutation affects only the ΔN-isoforms and in another isolated patient a missense mutation G134D* is located just in front of the DBD in exon 4 (13,15).

Ankyloblepharon-Ectodermal dysplasia-Clefting (AEC) syndrome

Limb malformations are almost absent in AEC syndrome and ectrodactyly has never been reported, but 25% of patients have mild syndactyly. Approximately 80% of the patients have severe skin erosion at birth, which usually will recover in the first years of life. The eyelid fusion, also called ankyloblepharon, is present in about 45% of AEC patients. Nails and teeth defects are present in more than 80% of patients, and hair defects and/or alopecia are almost constant features (94%). Lacrimal duct obstruction is seen in 50% of patients, whereas mammary gland hypoplasia and hypohydrosis occur occasionally (both 13%). Interestingly, almost 40% of patients have hearing impairment and genito-urinary defects. Cleft lip is present in 44% and cleft palate in about 80%.
Mutations in 12 unrelated patients with AEC have been detected, and 10 of these are missense mutations within the SAM domain of p63. These mutations are predicted to disrupt protein-protein interactions, by either destroying the compact globular structure of the SAM domain or by substituting aminoacids that are crucial for such interactions. Missense mutations in AEC syndrome affect only the α isotypes of p63 (13,15).

Nonsyndromic Split-Hand Foot Malformation (SHFM) type 4

SHFM4 is a "pure" limb malformation (ectrodactyly and syndactyly) condition, thus without orofacial clefting or ectodermal dysplasia. SHFM is genetically heterogeneous, and three loci have previously been identified: 7q21-q22 (SHFM1), Xq26 (SHFM2) and 10q24 (SHFM3). In two affected families, SHFM chromosomal abnormalities did not map to any of these established loci but instead mapped to 3q27-q28, thereby indicating the existence of a fourth locus. Causative *p63* mutations were found in both families.

Five of the seven p63 mutations seen in patients with SHFM are unique to this syndrome: missense mutations K193E and K194E, nonsense mutations Q634X and E639X, and splice-site mutation IVS4-2ArC. Q634X and E639X are known to disrupt p63 sumoylation site, and therefore increase the stability and transcriptional activity of the p63α isoform. Two other mutations, R280C and R280H, have been found in both SHFM and EEC syndrome. This arginine is not in direct contact with the DNA, but the mutation might indirectly affect the DNA-binding capacity of p63 (13,15).

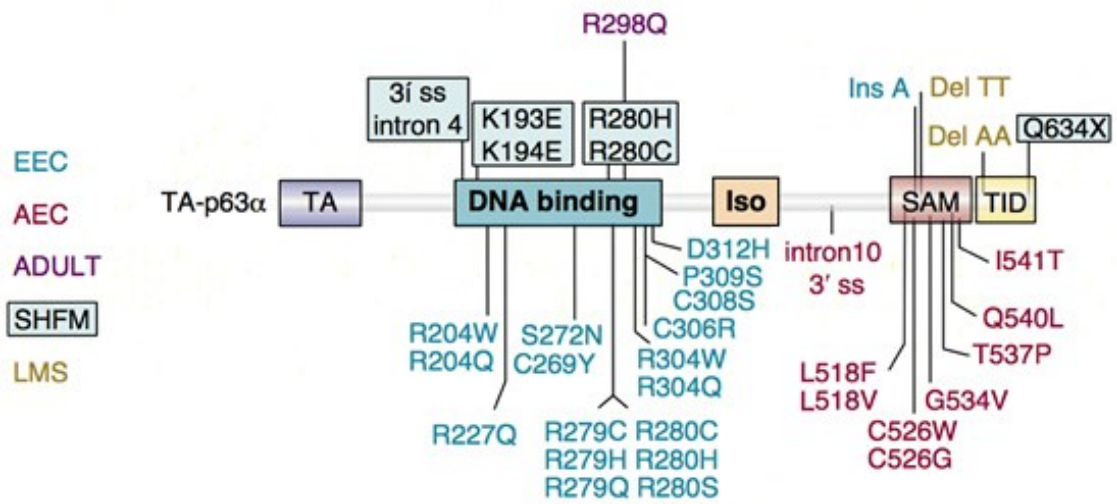

Figure 8. Illustration of p63 mutations in human syndromes establishing a clear genotype-phenotype correlation (16).

2.2.5 p63 downstream target genes

p63 is a transcriptional factor with a key role in limb development and epithelial stratification. It is likely that p63 exherts its function by regulating at a transcriptional level a series of target genes with a role in these processes. Many phenotype-relevant transcriptional targets of p63 have been identified through classical "candidate gene" approaches or by genome-wide screenings (14).

The best experimentally characterized function of p63 is to maintain the proliferative potential of epidermal progenitor cells. ΔNp63 can control distinct transcriptional networks depending on the

state of maturation of keratinocyte precursors. In proliferating keratinocytes of the basal layers, ΔNp63 promotes their amplification and controls the expression of basal layer keratins (*K5, K14*). Following a differentiation stimulus, ΔNp63 can change its transcriptional activity, activate genes required for cell cycle exit (*IKKa* and *IRF6*), and reorganize the transcription of adhesion molecules to allow keratinocytes to leave the basal layer and stratify (14).

DLX3

Many pieces of evidence suggest that a correct balance among different isoforms of p63 drives epithelial stratification. In particular, ΔNp63 is important for maintaining the proliferative potential of the basal layer, whereas TAp63 contributes by acting synergistically and/or subsequently to ΔNp63 to allow differentiation (2,3,17–20). TAp63α, but not ΔNp63α, is able to transactivate *distalless* homeodomain transcription factor *DLX3* (21). *DLX3* is expressed exclusively in the suprabasal differentiated layers of epidermis (22,23) where it activates a molecular mechanism that targets ΔNp63α for proteasome-mediated degradation. p63 functions as a molecular switch that initiates epithelial stratification while regulating keratinocytes proliferation and differentiation; DLX3-mediated ΔNp63α degradation may contribute to accomplish the program of terminal skin differentiation (24).

IKKa

IKKα is a protein kinase part of the IKK complex required for epidermal development and for the development of structures derived from the mesoderm and neural crest (25) and to switch on the differentiative program by favoring keratinocyte cell cycle arrest (26). *IKKα* is a direct transcriptional target of p63 in keratinocytes that is induced at early phases of terminal differentiation of primary keratinocytes (27,28). A failure by ΔNp63α to properly induce *IKKa* may play a role in the development of ectodermal dysplasias. Indeed, mutant p63 proteins expressed in ectodermal dysplasia patients exhibit defects in inducing *IKKα* (27). Consistently, *Ikkα*-deficient mice display developmental defects, including skin, craniofacial, and limb defects, showing some similarities with p63 null mice (2,3,29–31).

IRF6

IRF6 is a member of a family of interferon-dependent transcription factors (32) that control the proliferation-differentiation switch in epidermal cells (33–35); *Irf6*-null mice display an undifferentiated hyperplastic skin, due to the inability of *Irf6* mutant cells to exit the cell cycle (33,34).

IRF6 is also required for palate closure: mutations in *IRF6* are linked to a set of syndromes related to ectodermal dysplasia (36). *IRF6* has been demonstrated to be a ΔNp63 direct target gene. There is a feedback regulatory loop between *IRF6* and *p63*, in which p63 controls *IRF6* transcriptionally, while IRF6 controls p63 at the protein-stability level. *IRF6* expression is required to allow the onset of terminal differentiation by promoting the proteasome-dependent degradation of ΔNp63 (14,37).

REDD1

REDD1 is a transcriptional target of p63 which appears to function in the regulation of reactive oxygen species (ROS). During mouse embryogenesis, *Redd1* mirrors p63 tissue-specific pattern and in differentiating primary keratinocytes *p63* and *Redd1* expression are coordinately downregulated. *p63*-null embryos show no expression of *Redd1* and loss of p63 alters cellular ROS levels (38). In addition to effects on cellular stress and viability, subtle shifts in intracellular ROS levels can modulate cellular signalling through multiple tyrosine kinase growth factor receptors, including the epidermal growth factor receptor (EGF-R) (39–41). Regulation of EGF-dependent responses by ROS may therefore contribute to the effect of p63 on keratinocyte differentiation.

P-cadherin

P-cadherin (*CDH3* in human) is a cell-cell adhesion molecule, whose expression is highly associated with undifferentiated cells in normal adult epithelial tissues and is considered a marker of stem or progenitor cells of epithelial tissues (42,43). *P-cadherin* has been shown to be a transcriptional target of p63 (44), and is the disease gene for the Ectodermal Dysplasia-Ectrodactyly-Macular Dystrophy syndrome (EEM, MIM 225280) (45,46), characterized by the presence of the SHFM phenotype. However, no limb developmental functions of P-cadherin have been shown in mice (42).

PERP

PERP is a tetraspan membrane protein which, during embryogenesis, is expressed in an epithelial pattern, and its expression depends on p63. *Perp*$^{-/-}$ mice die postnatally, with dramatic blistering in stratified epithelia symptomatic of compromised adhesion. PERP localizes specifically to desmosomes, adhesion junctions important for tissue integrity, and numerous structural defects in desmosomes are observed in *Perp*-deficient skin, suggesting a role for PERP in promoting the stable assembly of desmosomal adhesive complexes. *PERP* is a direct p63 target gene, positively regulated by both TAp63 and ΔNp63 isoforms and is a key effector in the p63 developmental program, playing an essential role in an adhesion subprogram central to epithelial integrity and homeostasis (47).

DLX5 and DLX6

It is possible to link the role of p63 in epithelial stratification with its function in limb development. In fact, the AER, the ectodermal structure at the distal tip of the developing limbs essential for limb bud expansion and morphogenesis, is perhaps the first attempt of the embryonic ectoderm to organize into a multi-layered epithelial tissue (48). Indeed, the AER of *p63* null mice fails to organize as multilayer and there is experimental evidence that a failure to maintain the AER is the main pathogenic mechanism in the onset of the ectrodactyly phenotype (48,49).
Distalless-related homeogenes *DLX5* and *DLX6* are direct ΔNp63α transcriptional targets, whose regulation during limb development is needed to maintain the specialization and stratification of the AER cells; deletions of *DLX5* and *DLX6* can cause SHFM type 1 (14,50). In the limb buds of both *p63* and *Dlx5;Dlx6* murine models of SHFM, the AER is poorly stratified and FGF8 expression is severely reduced (51). In zebrafish embryos, *p63*-knockdown obtained by microinjecting a specific *p63*-morpholino causes a strong reduction in the expression of the *zdlx5a* and *zdlx6a* genes along with severe fin buds defects (52).
Furthermore, EEC and SHFM4 p63 mutants fail to transcriptionally activate *DLX5* and *DLX6* (50).

2.3 Limb development

As mentioned above, *p63* plays a key role in limb development. This is a delicate process driven by a complex network of several genes that control the correct timing and localization of limb morphogenesis.
The fore- and hind-limb buds emerge at defined somite positions perpendicular to the primary body axis because of continued growth of the flank mesoderm. The developing limb bud is a large embryonic field whose cells receive proliferative and positional cues from signals that allow their patterning along three axes: the Antero-Posterior (AP), Dorso-Ventral (DV), and Proximo-Distal (PD) axes. Three main limb skeletal compartments characterize the PD axis: the proximal stylopod, followed by the zeugopod and the distal autopod. The AP limb axis is congruent with the primary body axis and manifests itself in the distinct identities of the digits bearing autopod. Five distinct digits form in mice and humans with digit 1 (thumb) having the most anterior and digit 5 (little finger) the most posterior identities. It is generally accepted that the identities of the limb skeletal elements reflect the establishment of positional identities during limb-bud development (53–57) (Fig. 9).

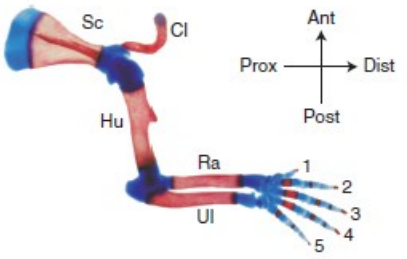

Figure 9. Skeletal preparation of a mouse forelimb at birth. Red and blue histological stains mark ossified bone and cartilage, respectively. (Proxdist) Proximodistal axis, (ant-post) anteroposterior axis, (Sc) scapula, (Cl) clavicle, (Hu) humerus, (Ra) radius, (Ul) ulna. Digit identities are indicated by numbers (57).

The first step in the development of a vertebrate limb is the determination of a group of embryonic cells that will give rise to the limb primordium (or limb bud). These so-called limb fields are initially composed of cells within the Lateral Plate Mesoderm (LPM) that are located in specific positions in the flank of the embryo by a combinatorial *HOX* genes expression which is in turn controlled by Retinoic Acid (RA) (58).

After the forelimb and hindlimb fields have been specified at precise locations along the embryonic flank, the corresponding cells in the LPM engage in active cell division, whereas cells in the non-limb flank LPM divide more slowly (59). This differential cell proliferation results in the development of a noticeable limb bud, consisting of a mass of mesenchymal cells encased in an ectodermal jacket. The mesenchymal cells of the prospective forelimb and hindlimb areas widely express *FGF-10.* FGF-10 protein signals to the overlying ectoderm to initiate a program of gene expression that includes activation of *FGF-8* transcription. These inductive signals from LPM cells of the limb bud area induce the overlying ectoderm to form a specialized structure (the AER), an ectodermal thickening that runs along the AP axis of the limb bud, separating the dorsal side of the limb from the ventral side (56). The establishment of the AER is the first step in the definition of the limb PD patterning.

2.3.1 Proximo-distal patterning

On the basis of the experimental evidence, many models were proposed to explain the processes that end up with the definition of the proximo-distal identities in the limb.

The progress zone model states that acquisition of PD identities depends on the time spent by proliferating undetermined cells in the distal mesenchyme (progress zone) under the influence of AER signals. As the progress zone is displaced distally, the more proximal cells are no longer under the influence of the AER, which causes determination of their positional identities. Mesenchymal cells “left behind” early acquire more proximal identities, whereas progenitor cells staying under influence of the AER longer acquire progressively more distal identities (60).

Another model accepted as a valid alternative to the progress zone model is the model proposed by Mercader et al. in 2000 (61). According to this model, PD limb-bud identities are specified by two early, opposing signals, namely RA, which is emanating from the embryonic flank/proximal limb bud, and AER-FGFs as proximalizing and distalizing signals, respectively. PD positional identities are likely specified as a consequence of cells integrating these signalling cues. During the onset of limb-bud development, the source of RA and AER-FGFs are very close, but their distance increases with outgrowth of the limb bud, such that proximal cells are exposed to RA for much longer than AER-FGFs, whereas the reverse applies to distal cells. In 2007, Tabin and Wolpert (62) proposed a modified model in which distal mesenchymal cells maintain an undifferentiated state during the proliferative expansion of the PD axis, because of exposure to AER-FGFs. As the PD limb axis expands distally, proximal mesenchymal cells are no longer under the influence of AER-FGFs, which results in the determination of their PD fates and initiation of differentiation. Therefore, the proximal limit of cells receiving AER-FGF signals at a given development time point defines a "differentiation front." This differentiation front prefigures the PD sequence by which the chondrogenic elements of the limb skeleton become apparent during subsequent mesenchymal condensation of the cartilage models.

2.3.2 Antero-posterior patterning

Growth and patterning along the AP axis appear to be tightly coordinated with the development of the PD axis, in a process mediated by specific interactions between the controller of limb outgrowth (the AER) and the AP organizer (the Zone of Polarizing Activity; ZPA). The ZPA is composed of a group of cells located in the posterior mesenchyme of the limb bud (63). In 1969 Wolpert (64) proposed that the ZPA specifies positional information in the limb-bud mesenchyme by secreting a diffusible molecule that forms a posterior (high) to anterior (low) gradient. Wolpert's model became famous as the "French Flag model" as it proposes that mesenchymal cells receive their positional identities by responding to specific thresholds of the morphogen gradient (Fig. 10).

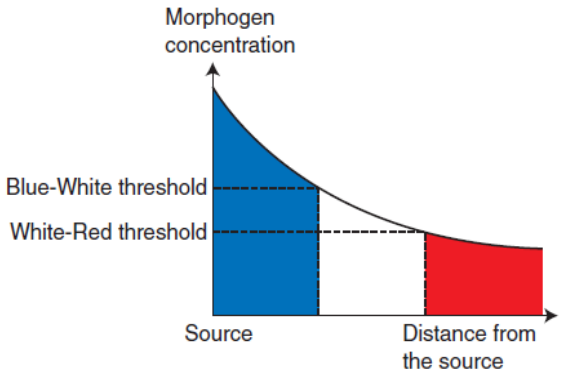

Figure 10. Wolpert's French flag model: A concentration gradient forms by diffusion of a morphogen from a source and positional information is determined in groups of cells by inducing distinct responses to specific concentration thresholds (indicated by blue, white, and red) (57).

In 1993, it was shown that the polarizing activity of the ZPA is mediated by *Sonic hedgehog* (*SHH*) (65–67), a gene that encodes a secreted factor homologous to the product of the *Drosophila* segment polarity gene *hedgehog* (*hh*), involved in many patterning processes in the embryo and imaginal discs (68). As first shown in the chick embryo, *Shh* expression is detected at stage 17 in the posterior margin shortly after the limb bud is induced, co-localizing with the ZPA. A similar pattern is observed in mouse, zebrafish, and other vertebrates (69–71). It is thought that SHH functions as a morphogen, possibly through an inductive effect on *BMP2* expression, and that the distance it diffuses depends upon post-translational modifications (72,73). The molecular mechanism by which SHH signalling regulates its target genes involves effects on GLI3, which functions either as transcriptional activator (GLI3A) or repressor (GLI3R). High levels of SHH prevent the formation of GLI3R and promote GLI3A function. Thus, the local concentration of SHH regulates target gene expression by controlling the balance of GLI3 repressor and activator forms (74,75).

SHH is not involved in patterning the most proximal limb structures, but *SHH* activity is absolutely required for the maintenance of growth and patterning of intermediate and distal limb structures and for the maintenance of the AER (56,76,77). In turn, maintenance of *SHH* expression in the posterior margin of the limb bud requires the integrity of the AER. Thus SHH seems to act in a regulatory loop with FGF proteins expressed in the AER to maintain cell growth and proliferation in the mesenchyme, and to maintain the integrity of the AER (78,79).

2.3.3 Dorso-ventral patterning

During limb development, DV patterning requires complex interactions between the ectoderm and mesoderm (80). Once DV patterning is established in the ectoderm, then it is the ectoderm that imposes the DV information on the mesoderm (80–82). The specification of DV polarity in the

ectoderm results in the establishment of specific domains of gene expression. The secreted factor encoded by the gene *WNT7a* is specifically expressed in the dorsal limb ectoderm and acts as a dorsalizing factor by imposing the expression of *LMX1b*, a LIM homeodomain-containing gene, in the underlying dorsal mesoderm (83–87). BMP signals, probably from the lateral mesoderm, are crucial for ventral patterning since they induce the expression of *Engrailed 1* in the ventral ectoderm, which acts to confine *WNT7a* expression to the dorsal ectoderm (88–90). This occurs in a narrow temporal window immediately prior to the initial outgrowth of the limb bud (91,92).

2.4 Fin development

Zebrafish paired pectoral fins and tetrapod limbs are considered to be homolog structures, in particular with respect to early patterning and gene expression (93). Numerous factors essential for limb development are involved with very similar functions in fin development. Fgf signalling is essential for limb outgrowth and it also plays crucial roles in pectoral fin bud formation. *Fgf10* is expressed in the mesenchyme of the pectoral fin bud-forming region and is required for pectoral fin bud outgrowth (94). *Fgf8* is also expressed in the AER of pectoral fin buds and plays a role in the pectoral fin bud formation (95). Likewise, a requirement for the essential antero-posterior organizing factor *shh* has been demonstrated in cell proliferation in the zebrafish pectoral fin bud (96,97).

Nevertheless, zebrafish fins and tetrapod limbs have obvious morphological differences in the skeletal structures. The paired pectoral fins of teleost fish contain two different bone elements. Endoskeletal elements are formed as chondral bone through endochondral ossification; exoskeletal elements (fin rays) are formed by intramembranous ossification (98). Fin rays are unique to, and common in, the fins of actinopterygians (e.g. teleosts) and basal sarcopterygians but this structure is never seen in tetrapod limbs. The endoskeletal elements proximal to fin rays in the teleost pectoral fin are poorly patterned along the PD axis, whereas limb endoskeletal elements exhibit a well-organized sequential pattern (stylopod, zeugopod and autopod) (99). Therefore, limb evolution involved both better endoskeletal element patterning and the elimination of fin rays. Many studies suggest that fin structures transformed into limbs by changes in genetic and developmental programs during tetrapod evolution (100–105). One major difference between fin and limb development is that the AER, which organizes limb development, in the fin bud transitions into a different, elongated organizing structure, the Apical Fold (AF) from the middle stage of fin development (106).

In zebrafish embryos it is possible to recognize a thickened single layer epidermis, a typical morphological trait of the AER, as early as at 30 hpf. By 34 hpf, the AER forms a small notch where two sheets of epidermis approach each other. At 36 hpf the notch starts to extend and makes a slit,

dividing the two epithelial layers. This distinctive morphological change marks the transformation of the AER into the AF. From now on, AF expresses *fgf4* and *fgf8*, which are AER markers in the amniote limb and starts growing considerably in the distal direction.

By 46 hpf, the distal fin mesenchyme starts migrating into the base of the AF, and continues to invade distally in a slit between the two layers of the AF. At 56 hpf, it is possible to distinguish between two portions of the AF with different tissue organization and gene functions: a distal region containing no mesenchyme (distal AF, dAF) and a proximal region with migrating mesenchyme (proximal AF, pAF) (107) (Fig. 11).

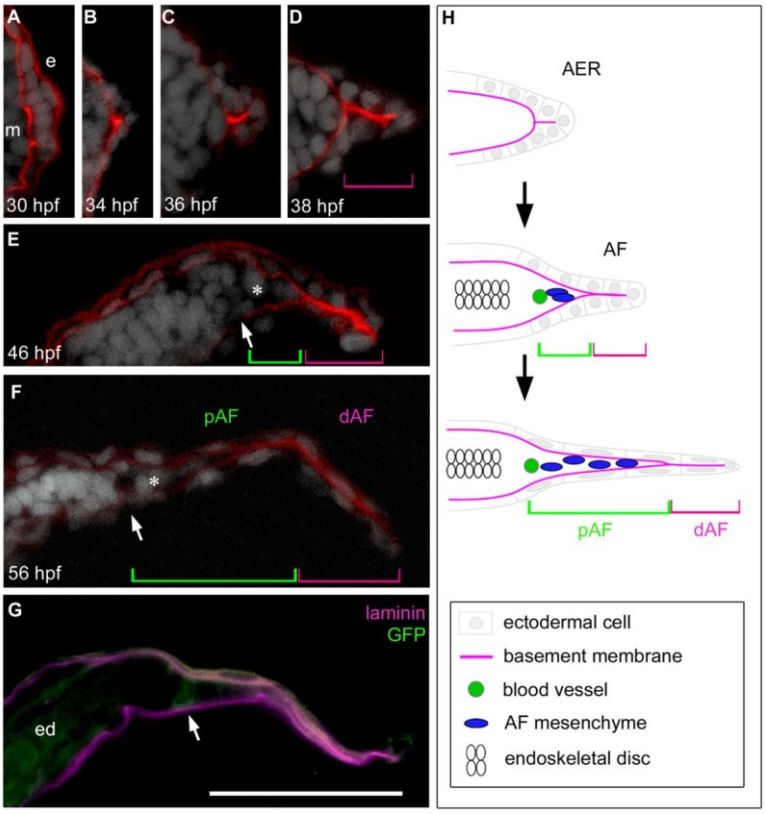

Figure 11. AER-AF transition and morphological features in pectoral fin development. (**a-g**) A series of transverse pectoral fin bud sections (distal is to the right and dorsal is to the top) at the indicated stages. The basement membrane (red), shown by Laminin α5 immunostaining, is located between the ectoderm (e) and mesoderm (m) **(a)**. Cell nuclei are visualized by DAPI (white). The distal portion of the AF (magenta brackets) consists of ectodermal cells only, and mesenchymal cells (asterisks) enter the notch of the AF within the proximal AF region (green brackets). The circumferential fin blood vessel (white arrows) is located at the base of the AF **(e-g)**, and is recognizable by GFP distribution in *fli1*:EGFP y1 transgenic fish **(g)**. ed, endoskeletal disc. Scale bar: 50 µm. (**h**) Diagram of transverse fin bud sections during AER/AF morphogenesis (107).

In contrast to what it happens in the tetrapod limb bud, where AER removal results in distal truncation of the limbs, in zebrafish embryos, repeated AF removal elongates the endoskeletal region along the PD axis. Interestingly, cellular proliferation status changes by AF removal. Mesenchymal cell

proliferation increases beneath a newly formed AER, which sends signals for morphogenesis into the endoskeletal region. The nature of these ectodermal signals remains unknown. AER signals before the transition are necessary for the survival, growth and maintenance of an undifferentiated state of 'mesenchyme', and experimental evidence suggest that dAF at the apex of the expanding AF might have the same function against the pAF. In fact, as fin development proceeds, dAF is distanced from the endoskeletal region and cannot continue to regulate its morphogenesis. Therefore, the region responding to the epidermal signals should change from the endoskeletal region to the pAF region at the time of the AER-to-AF transition (107) (Fig. 12).

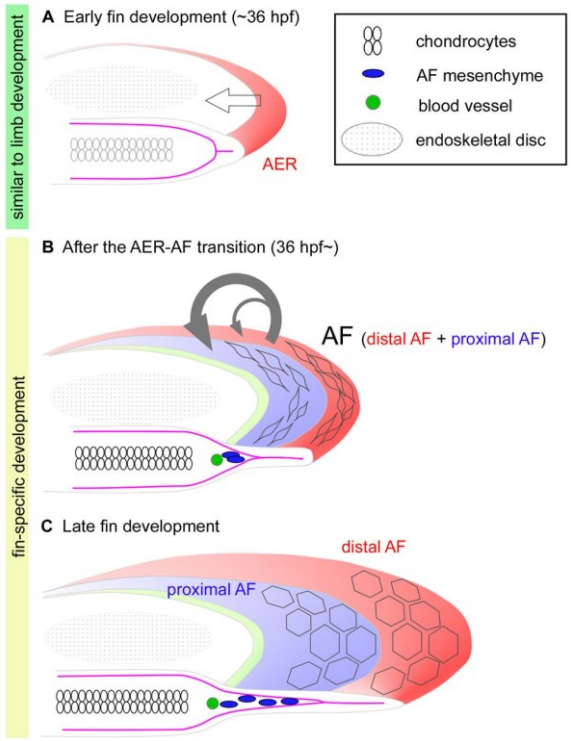

Figure 12. A model of pectoral fin development. (**a**) Until 36 hpf, the AER (red) is crucial for fin mesenchyme outgrowth (straight arrow). (**b**) After AER-AF transition, the dAF acts on the outgrowth of the AF (curved arrows). (**c**) Later, the dAF is distinguished from the pAF by tissue organization and gene expression. As fin buds develop distally, the ectodermal cell shape in the AF changes from a spherical and slender morphology **(b)** to a thin, polygonal one **(c)**.

In this scenario, a heterochronic shift of the timing of AER-to-AF transition in evolution (the so-called clock model) (108) might explain fin-to-limb transition. In teleost fins, AER signals regulate endochondral skeletal patterning during a short period of early fin development, resulting in a poor endoskeletal pattern; then the AF forms and fin rays develop. On the contrary, in tetrapod limbs, where AER signals regulate skeletal patterning through the entire period of limb development and an AER-to-AF transition never occurs, the proximal mesenchyme is exposed longer to AER signals,

resulting in a better patterning of endoskelatal elements and fin rays never develop (107,109) (Fig. 13).

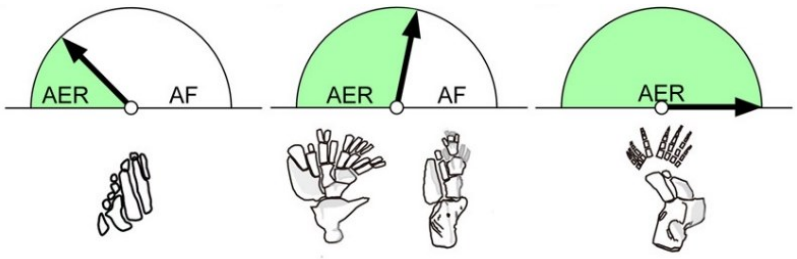

Figure 13. Clock model hypothesis. Hypothesized images of fin/limb development in the clock model (above), and endoskeletal patterns of the fin/limb (below). In teleost fins (left-most panel), AER signals regulate endochondral skeletal patterning during a short period of early fin development, resulting in a poor endoskeletal pattern; then the AF forms and fin rays develop. In the fins of lobe-fin fish (such as coelacanths and lungfish), basal actinopterygians (such as paddlefish and sturgeons) and chondrichthyans (such as sharks and skates, middle panel), regulation by AER signals continues for a longer period than in teleost fins, resulting in a better endoskeleton pattern and in the eventual transformation of the AER into the AF. In tetrapod limbs (right-most panel), AER signals regulate skeletal patterning through the entire period of limb development, an AER-to-AF transition never occurs, and fin rays never develop (107).

2.5 Thalidomide

Fifty years ago, the prescription of thalidomide to pregnant women caused a worldwide epidemic of multiple birth defects (Fig. 14).

Thalidomide (α-phthalimidoglutarimide) was developed and launched on the market by the German pharmaceutical company Grunenthal in 1957. Apparently, at that time, the drug had already been tested on rodents without observing any remarkable toxicity. Thalidomide was distributed and prescribed as a sedative and an antidote against morning sickness in over 40 countries. However, already in 1961 and 1962, two independent studies by W. McBride in Australia and W. Lenz in Germany reported limb and bowel malformations in children born to mothers who were exposed to thalidomide during pregnancy (153–159). The drug was immediately withdrawn from the market but many studies continued to investigate the mechanism of thalidomide action.

Figure 14. Child born to mother exposed to thalidomide during pregnancy.

Further investigation led to the discovery of several remarkable clinical effects of the drug which extended far beyond its sedative properties. In 1965, the Israeli physician, Sheskin, found thalidomide to be effective for the treatment of Erythema Nodosum Leprosum (ENL), an inflammatory complication of leprosy that results in painful skin lesions (160).

During the 1980s and early 1990s, investigators found that thalidomide was an effective treatment for certain autoimmune disorders, such as chronic graft versus host disease and rheumatoid arthritis (161–165). In the early 1990s, it was reported that thalidomide inhibits the production of Tumour Necrosis Factor-α (TNF-α) and replication of HIV (166–168). In addition to suppression of TNF-α, thalidomide effects the generation and elaboration of a cascade of pro-inflammatory cytokines that activate cytotoxic T-cells even in the absence of co-stimulatory signals (169). Furthermore, Vascular Endothelial Growth Factor (VEGF) and basic Fibroblast Growth Factor (bFGF) secretion and cellular response are suppressed by thalidomide, thus antagonizing neo-angiogenesis and altering the bone marrow stromal microenvironment in hematologic malignancies (170–172). In 1999, thalidomide was shown to be effective for the treatment of Multiple Myeloma (MM), a malignant B cell lymphoma (173). With respect to ENL and MM, thalidomide was approved for use by the US FDA in 1998 and 2006, respectively. Due to its serious teratogenicity, the prescription of thalidomide is strictly controlled by the System for Thalidomide Education and Prescribing Safety (STEPS) program (174). In South America, thalidomide is widely used for the treatment of leprosy. Sadly, many children have been born with severe birth defects due to poor patient understanding of the proper use of the drug and inconsistent contraceptive administration (175,176).

2.5.1 Thalidomide teratogenicity

The use of thalidomide during the first trimester of pregnancy led to serious embryotoxic effects; over 10,000 children were affected worldwide. A wide spectrum of birth defects such as malformations of the limb, ear, eye, internal organs, and central nervous system were documented (154,155,177). Limb malformations were the most frequently observed defects (157,177). Thalidomide induces two types of limb defects: amelia and phocomelia. Amelia is complete absence of the limb, and phocomelia consists of limbs with a stylopod, a truncated or absent zeugopod, and a nearly intact autopod (154). Ear defects were also frequent; ear malformations varied from anotia to mild malformation of the external ear. Cleft lip and ocular anomalies such as uveal coloboma, glaucoma, microphthalmia were also observed, and in internal organs, the most frequent defects were kidney malformations, heart defects, and structural chest defects (177). The mortality rate for babies born with thalidomide-induced defects was very high (about 30–40%). In addition, thalidomide caused an unknown number of miscarriages. Indeed, thalidomide induced several inoperable defects such as imperforate anus and

other gastrointestinal deformities, contributing significantly to early deaths (153,157,177–179). Facial nerve palsy was also common, and autism and mental retardation were reported even though the incidence was low (177) (Fig. 15). The individual type of thalidomide malformation depends on the time of intake. Indeed, thalidomide induced developmental defects only when taken between day 35 to day 49 after conception and the severity of malformations correlates with the timing of exposure (180).

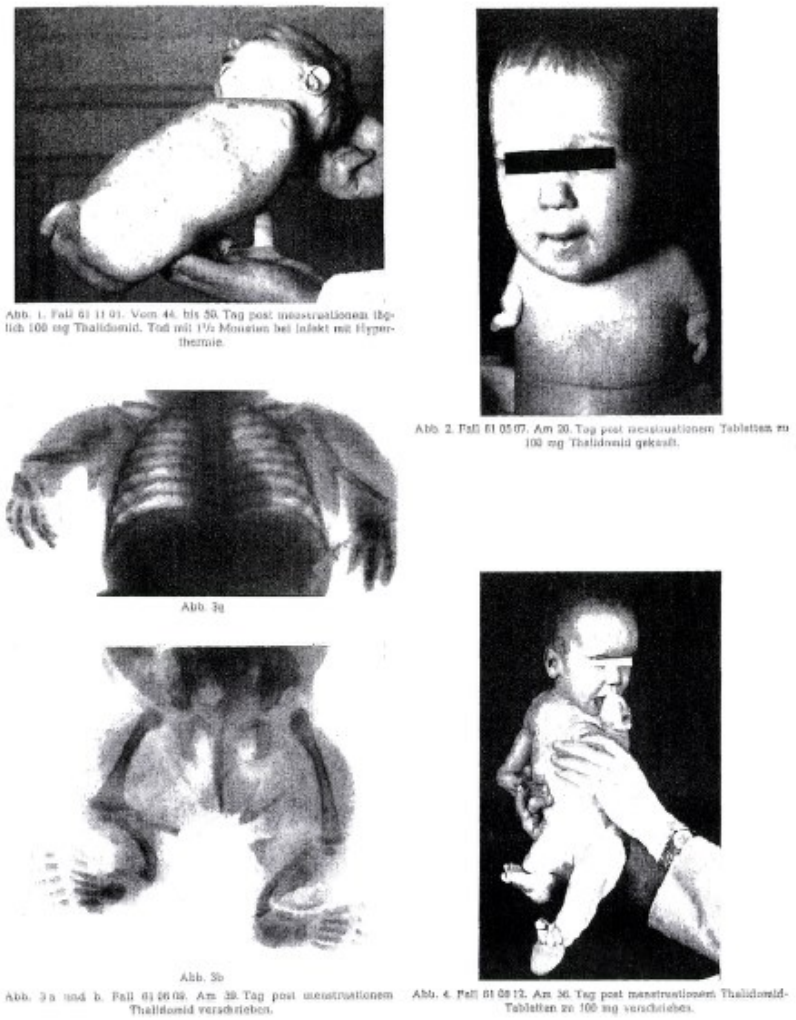

Figure 15. Phenotype of thalidomide victims (180).

Thalidomide is a derivative of glutamic acid and contains two imide rings: glutarimide and phthalimide with a single chiral center and is formulated as a racemic mixture of two active enantiomers: S (-) and R (+). The S (-) isomer was thought to work as a teratogen and the R (+) isomer as a sedative. However, both forms were found to be teratogenic in a rabbit model (181). Furthermore, both compounds rapidly interchange under physiological conditions and it is hard to isolate one form from the other (155,157,159). Thalidomide undergoes spontaneous non-enzymatic hydrolytic

breakdown into more than a dozen products under physiological conditions (155,157,159) and it is bio-transformed by liver cytochrome P450 (CYP450) into its hydroxylated products (155,157,159,182,183). It is still unclear whether the teratogenic activity is exerted by parental thalidomide or by its metabolites, though evidence exists that the bioactivation of thalidomide in the liver is not critically involved in its teratogenic action, at least in zebrafish and chicks (184–186).

Many efforts were spent during the past 50 years trying to understand the molecular mechanisms underlying thalidomide teratogenicity. More than 30 hypotheses have been proposed to explain how thalidomide causes limb defects (187–190). To mention some, it was proposed that at the basis of thalidomide teratogenicity there was folic acid antagonism, DNA intercalation or the disruption of molecular pathways such as acetylation of macromolecules and glutamate metabolism. Among the most possible and reasonable causes of thalidomide embryotoxicity are thalidomide-induced oxidative stress and anti-angiogenic action (170,185,187,191). Nevertheless, the details of thalidomide molecular mechanism of action remain elusive and scientists are still looking for a definitive model to explain thalidomide teratogenicity.

Anti-angiogenesis hypothesis

Thalidomide is able to exert anti-angiogenic effects by suppressing VEGF and bFGF secretion and cellular response and thalidomide-induced anti-angiogenesis seems to be an evolutionarily conserved mechanism which occurs in organisms from mammals to zebrafish (170,183,185,186). The first report of thalidomide anti-angiogenic properties was from D'Amato et al. (170). They found that thalidomide inhibits bFGF-induced angiogenesis in a rabbit cornea micropocket and postulated that the inhibition of angiogenesis caused limb defects, since blood vessel formation is crucial for limb development. Similarly, Vargesson et al. (185) demonstrated that inhibition of angiogenesis by CPS49, a synthetic thalidomide analogue (192), precedes changes in limb morphology, cell death, and inhibition of Fgf8/Fgf10 in chicks (185). Therefore, they suggested that inhibition of angiogenesis by thalidomide induces cell death and a reduction in the expression of essential growth factors such as Fgf8 and Fgf10, in turn resulting in mesenchymal loss in the limb bud (Fig. 16).

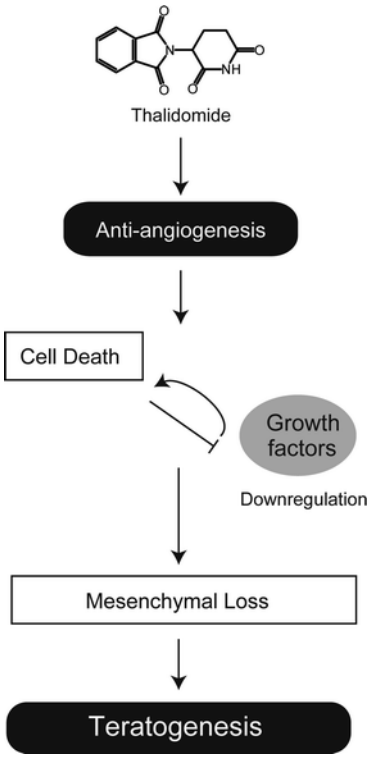

Figure 16. Schematic model of the anti-angiogenesis hypothesis. Antiangiogenesis induced by thalidomide leads to cell death and downregulation of growth factors including Fgf8/Fgf10. Disruption of growth factor signaling pathways is also likely to be involved in cell death. The sequence of events results in mesenchymal loss and in turn limb deformities (157,185,193).

Oxidative stress hypothesis

In 1999, Parman et al. (191) demonstrated that thalidomide generates reactive oxygen species (ROS), oxidizes DNA and accumulates 8-hydroxy-20-deoxyguanosine in rabbits. Moreover, by using a spin-trap reagent, α-phenyl-N-tertbutylnitrone (PBN), which has been shown to be effective in the *in vitro* trapping of free-radical intermediates of other teratogenic drugs, they suppressed both oxidation and limb defects induced by thalidomide in rabbits. Harris et al. (194) suggested that oxidative stress by thalidomide is likely to downregulate essential limb growth signalling. In fact, thalidomide treatment inhibits the expression of Fgf8 and Fgf10 and PBN pre-treatment is able to reverse this effect in rabbits. Fgf8 and Fgf10 have been shown to be downstream targets of Nuclear Factor-κB (NF-κB) (187,194). NF-κB is a redoxsensitive transcription factor whose function is affected by oxidative stress. Therefore, oxidative stress caused by thalidomide has been suggested to induce aberrant NF-κB activity, which in turn attenuates Fgf8 and Fgf10 expression, resulting in limb deformities (187). Thalidomide treatment also leads to the upregulation of other NF-κB targets, such as Bone morphogenic proteins (Bmps) and Dickkopf-1 (Dkk-1). This effect was shown to be involved in thalidomide teratogenicity and is reversed by PBN (195). Bmps are important factors for limb patterning, and have been demonstrated to stabilize phosphatase and tensin homolog (PTEN)

proteins, which block Akt survival signalling (92,196–198). In addition, Bmps have been shown to inhibit Fgf signalling in mouse limb development (199). Dkk-1 is a downstream target of Bmps and functions as an antagonist of Wnt, which regulates cell survival and proliferation (200). Thalidomide blocks Wnt signalling and increases Glycogen synthase kinase-3b (Gsk3b) activity through upregulation of Dkk-1 (195). Stabilization of PTEN also activates Gsk3b, which in the end promotes the programmed cell death pathway (201) (Fig. 17).

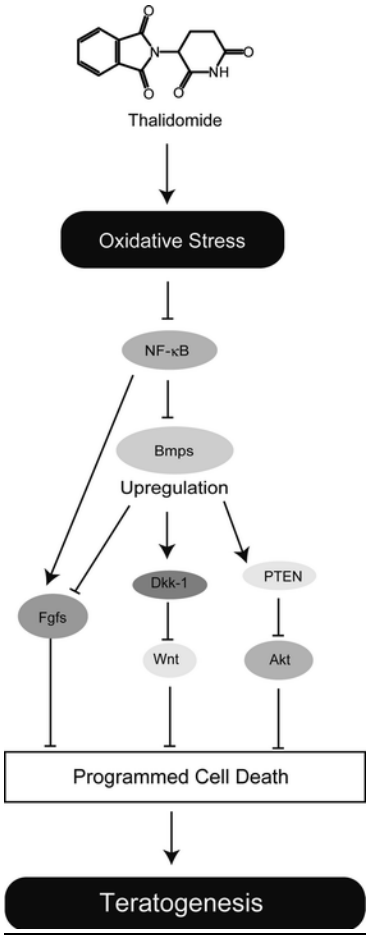

Figure 17. Schematic model of the oxidative stress hypothesis. Thalidomide induces ROS, and oxidative stress upregulates expression of Bmps through aberrant NF-κB activity. This alteration results in blocking Fgf (Fgf8/Fgf10), Akt, and Wnt pathways known to be important for cell survival and proliferation (154,187,193,198,202–204).

2.5.2 Cereblon

The above hypotheses seem to be both well supported by experimental data, but still do not provide an answer to what is the primary mediator of thalidomide teratogenicity.

Only in 2010 Ito et al. identified the direct target of thalidomide teratogenicity (186).

By employing high-performance affinity ferriteglycidyl methacrylate (FG) beads, covalently conjugated to the carboxylic thalidomide derivative FR259625, they were able to purify from HeLa cell extracts a direct target of thalidomide drug. By mass spectrometry, it was possible to identify this protein as CEREBLON (CRBN), a protein made up of 442 amino acids, evolutionarily conserved from plants to humans.

CRBN was first reported in 2004 as an autosomal recessive non-syndromic mild mental retardation (ARNSMR) gene. It is located at 3p25-pter and plays an important role in central nervous system development, being involved in memory and learning. The nomenclature of CRBN is based on its putative role in cerebral development and on the presence at the N-terminus of a large (237-aminoacids) highly conserved ATP-dependent Lon protease domain. However, whether this protein possesses ATP-dependent Lon protease activity or not has not been convincingly proved. Furthermore, CRBN protein sequence contains 11 casein kinase II phosphorylation sites, 4 protein kinase C phosphorylation sites, 1 N-linked glycosylation site and 2 myristoylation sites (205,206). CRBN is highly expressed in human brain (206,207) but it is also widely expressed in testis, spleen, prostate, liver, pancreas, placenta, kidney, lung, skeletal muscle, ovary, small intestine, peripheral blood leukocyte, colon, and retina (207–211). At a subcellular level, CRBN is located in cytoplasm, nucleus and peripheral membrane (186,208–212). The discovery by Ito et al. that CRBN directly interacts with damaged DNA binding protein 1 (DDB1), that it co-precipitates with all the components of the Cullin 4 (Cul4)-based E3 ubiquitin protein ligase complex and that it has intrinsic ubiquitination activity indicates that CRBN is a subunit of this E3 ubiquitin ligase complex. In the Cul4-based complex, CRBN functions as a substrate receptor, whilst regulator of cullins 1 (Roc1) and Cul4 form the catalytic core, and DDB1 works as an adaptor between Cul4 and the substrate receptor (186). Cul4-based E3 ubiquitin ligases have been shown to be important for DNA repair (213–219), DNA replication (220–223), transcription (224) and development (186). Thalidomide is able to inhibit CRBN autoubiquitination *in vitro*, suggesting that thalidomide is an inhibitor of its E3 ubiquitin ligase activity (186).

The *CRBN Y384A/W386A* (CRBNYW/AA) double point mutant (Fig. 18), unable to bind to thalidomide, does not display loss of autoubiquitination activity upon drug treatment, suggesting that thalidomide inhibits E3 function of the CRBN-containing complex by directly binding to CRBN (186).

```
Homo sapiens        326:CQETEITT-KNEIFSLSLCGPMAAYVNPHGYVHETLTVYKACNLNLI--GRPSTEHSWFP 382
Mus musculus        329:CQETEITT-KNEIFSLSLCGPMAAYVNPHGYVHETLTVYKASNLNLI--GRPSTVHSWFP 385
Gallus gallus       328:CQDTEITT-KNEIFSLSLCGPMAAYVNPHGYIHETLTVYKACNLNLS--GRPSTEHSWFP 384
Danio rerio         316:CQDTEITS-KNEIFSLSLYGPMAAYVNPHGYVHETLTVYKASNLNLI--GRPSTLHSWFP 372
D. melanogaster     458:CNSSLALCSDLFAMSKH--GVQTQYCNPEGYIHETNTVYRVISHAIGYSGEPSTKFSWFP 515
A. thaliana         447:CQTVI-ARRK-DMLVMSNEGPLGAYVNPHGYVHEIMTFYKANDIALR--GRPVKKDSWFP 502
                          * *
Homo sapiens        383:GYAWTVAQCKICASHIGWKFTATKKDMSPQKFWGLT----RSALLPTIPDTEDEISPD-- 436
Mus musculus        386:GYAWTIAQCKICASHIGWKFTATKKDMSPQKFWGLT----RSALLPTIPETEDEISPD-- 439
Gallus gallus       385:GYAWTIAQCRICGNHMGWKFTATKKDMSPQKFWGLT----RSALLPRIPEAEDELGHD-- 438
Danio rerio         373:GYAWTIAQCRTCSSHMGWKFSAVKKDLSPPRFWGLT----RSALLPTIPQGEEGVEGS-- 426
D. melanogaster     516:GYQWHIILCKFCAQHVGWEFKAVHPNLTPKVFFGLAGSSVRIGKASEYSPFNGTTYVVRN 575
A. thaliana         503:GYAWTIANCATCETQLGWHFTATNKKLKPSSFWAV-----RG--------SQVA-DDM-- 546
```

Figure 18. Evolutionary conservation of CRBN. Amino acid sequences of CRBN orthologs from six species are aligned. Bold letters indicate amino acids that are fully conserved among these species. Asterisks indicate amino acids that are critical for thalidomide binding (186).

In vivo studies on zebrafish embryos revealed that the microinjection in 2 cells-stage embryos of the mRNA encoding for *CRBN Y384A/W386A*, rescues the defects otherwise induced by thalidomide in ear and pectoral fin development (186) (Fig. 19).

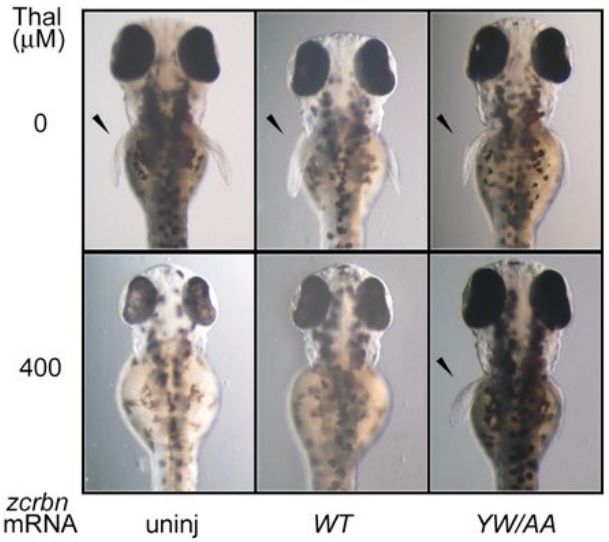

Figure 19. Expression of a drug binding-deficient form of CRBN suppresses thalidomide-induced teratogenicity in zebrafish. Dorsal views of pectoral fins of 72-hpf embryos. Fins are indicated by arrowheads. Uninjected control embryos in the left-most panel. Embryos injected with WT *zcrbn* mRNA in the middle panel. Embryos injected with WT *zcrbn*$^{YW/AA}$ mRNA in the right-most panel. After injection, embryos were allowed to develop in the presence (above) or absence (below) of thalidomide (186).

Collectively, all these pieces of evidence suggest that thalidomide exerts its teratogenic effects by binding to CRBN and inhibiting its function, indicating that CRBN is a primary target of thalidomide teratogenicity (186). However, the ubiquitously expressed CRBN protein cannot account alone for the tissue-specificity of thalidomide teratogenicity, indicating that CRBN is necessary but not

sufficient for thalidomide teratogenicity. Other molecules, perhaps downstream to CRBN E3 ubiquitin ligase activity, are likely to contribute to the effects of the drug and may define the tissue specificity of thalidomide teratogenicity. One such molecule might be fgf8 whose expression pattern is tissue-specific and results to be downregulated in zebrafish embryos upon thalidomide treatment. Ito et al. speculate that thalidomide might initiate teratogenic effects by inhibiting CRBN E3 ubiquitin ligase function, thus leading to the accumulation of unknown substrates that might be negative regulators of essential factors for correct limb/fin development, such as fgf8 (186) (Fig. 20).

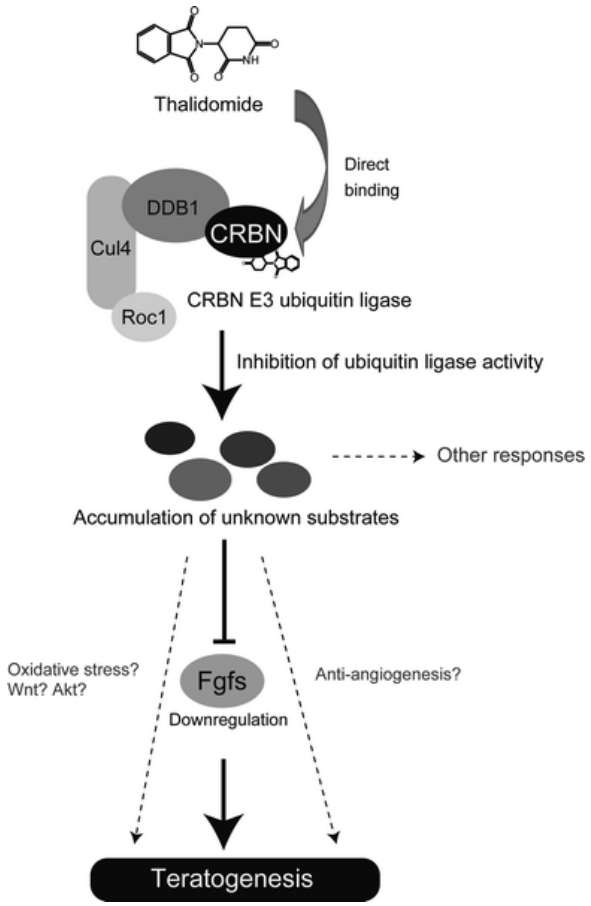

Figure 20. Schematic model of the molecular mechanisms of thalidomide teratogenicity from a CRBN-centric perspective. Thalidomide binds directly to CRBN and inhibits its E3 ubiquitin ligase activity. This inhibition results in aberrant accumulation of substrates (unknown), which in turn causes developmental defects such as limb deformities. Thalidomide-induced downregulation of Fgfs (Fgf8/Fgf10) might mediate the teratogenic effects of thalidomide-CRBN binding (186,193).

2.5.3 Species-specificity of thalidomide teratogenicity

Apparently, the first pharmacological trials performed on rodents did not reveal any remarkable toxic effect of the drug, which was therefore launched on the market in 1957. This tragic mistake was probably related to the characteristic species-specificity of thalidomide teratogenicity. Thalidomide induces limb/fin deformities in humans, monkeys, rabbits, chicks, and zebrafish (*Danio rerio*) (154,186).

In particular, amelia only occurs in chicks, whereas both amelia and phocomelia occur in monkeys. In zebrafish, thalidomide induces shortening along the proximo-distal axis of the pectoral fins, which are homolog structures to tetrapod limbs (see above) (93). On the contrary, rodents are resistant to limb deformities induced by thalidomide (154,155,157–159), even when administered at doses of up to 4,000 mg/kg (225). However, several reports have demonstrated the effects of thalidomide (e.g., anti-angiogenic effect) in cell lines and tissues from mice and rats (157,226,227). There is no clear explanation for rodents resistance. Mouse/rat CRBN is 95% homologous to human CRBN and has been shown to bind thalidomide (186). Hence, CRBN is unlikely to direct the species-specificity of thalidomide effects, but several other hypotheses have been proposed to explain why rodents are resistant to the teratogenic effects of thalidomide. One possibility is that differences in the pharmacokinetics of thalidomide metabolism among different species may reflect the diverse sensitivity. Indeed, the plasma elimination half-life of orally administered thalidomide is significantly shorter in mice (0.5 h) than in rabbits (2.2 h) and humans (7.3 h) (228). Thalidomide is rapidly hydrolyzed or metabolized into over a dozen products *in vitro* and *in vivo*, and many of the breakdown products are non-teratogenic (185); a more efficient thalidomide metabolism might confer to rodents resistance to the teratogenic effects of the drug. On the other side, if the breakdown or bioactivation of thalidomide is required for the induction of its embryotoxic effects, then again differences in the metabolism of the drug will explain the species-specificity of thalidomide teratogenicity. However, evidence exists that the bioactivation of thalidomide in the liver is not critically involved in its teratogenic action. In zebrafish, developmental defects were observed very early in development (around 30 hpf), when the liver is not functional yet (184). In chicks, thalidomide applied directly to one of the forelimb buds causes specific defects in the thalidomide-treated limb, but not in the other limb (185,186). Another chance is that thalidomide might be less efficient in causing ROS formation in the rodents. In support of this, the glutathione-dependent antioxidant response is stronger in mice and rats than in humans (229). Finally, interspecies differences in gestational development may result in different developmental toxic manifestations after exposure to thalidomide (230).

2.5.4 Immunomodulatory drugs and thalidomide analogues

The term IMiD (immunomodulatory drugs) refers to IMiDs licensed by Celgene Corporation (Summit, NJ, USA) for the treatment of several inflammatory and neoplastic diseases (158). The IMiDs were initially defined by their capacity to inhibit tumor necrosis factor (TNF)-α secretion (231). The second generation IMiDs CC-5013 (Revlimid, IMiD3, hereafter lenalidomide) and CC-4047 (Actimid, IMiD1, hereafter pomalidomide), are amino-phthaloyl-substituted thalidomide analogues developed on the basis of augmented TNF-α inhibition (232,233) (Fig. 21).

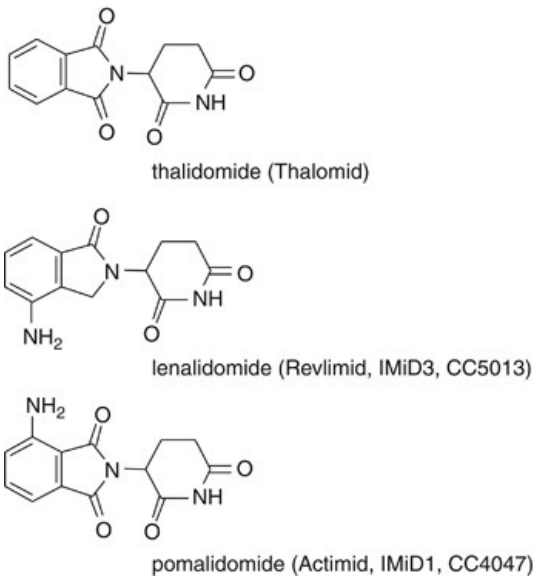

Figure 21. Chemical structures of the 'IMiDs', thalidomide and its amino-phthaloyl-substituted analogues (231).

Thalidomide, pomalidomide and lenalidomide display a wide range of overlapping and pleiotropic biological activities, including anti-angiogenic and teratogenic properties and multiple effects on the immune system, such as enhanced production of the cytokine interleukin-2 (IL-2) (which spurs T cell production), inhibition of the cytokine tumor necrosis factor (TNF), and the stimulation of natural killer cells (234). Importantly, IMiDs possess also anti-cancer activity with selectivity for molecularly defined subgroups of hematological malignancies, such as MM and other specifically mature B-cell neoplasms (231) (Fig. 22).

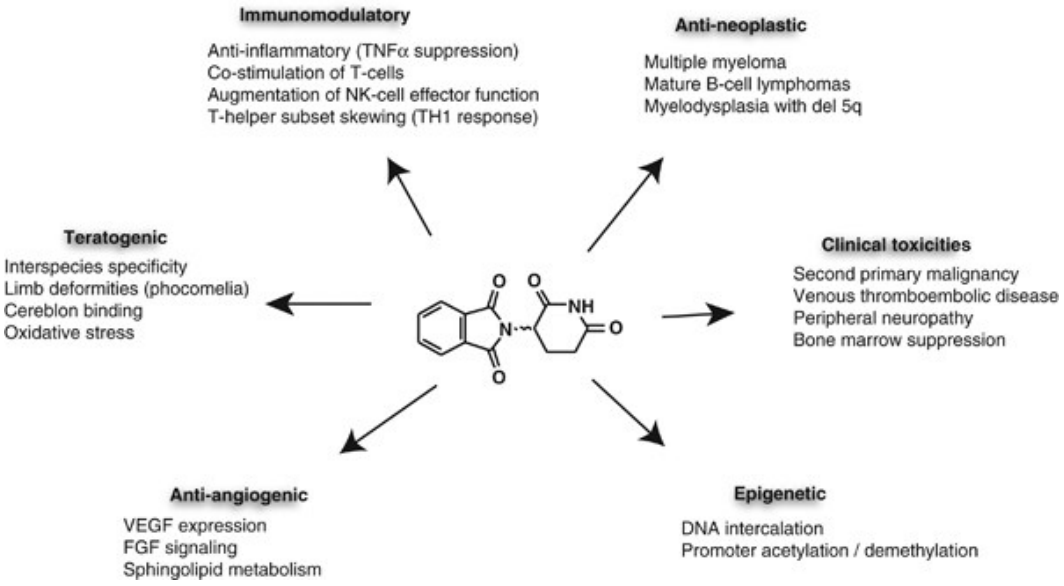

Figure 22. The pleotropic effects of thalidomide analogues.

MM is a malignancy of immunoglobulin producing plasma cells associated with systemic toxicities including renal failure, anemia, immunoparesis and destructive skeletal lesions (235).
Interestingly, low amounts of CRBN in multiple myeloma cells correlate with clinical drug resistance and poor survival outcomes (236), whilst high CRBN levels in myeloma cells are associated with increased responsiveness to IMiDs (236,237). Lu et al. and Krönke et al. demonstrated that the zinc finger–containing transcription factors Ikaros (IKZF1) and Aiolos (IKZF3) are selectively bound by CRBN. IKZF1 and IKZF3 are transcriptional regulators of B and T cell development (238,239). After direct binding, IMiDs activate cereblon E3 ligase activity, resulting in the rapid ubiquitination and degradation of IKZF1 and IKZF3. IMiDs-mediated loss of these two transcription factors is toxic for MM cells, thus explaining the molecular mechanism of IMiDs clinical effect on MM (240–242) (Fig. 23).

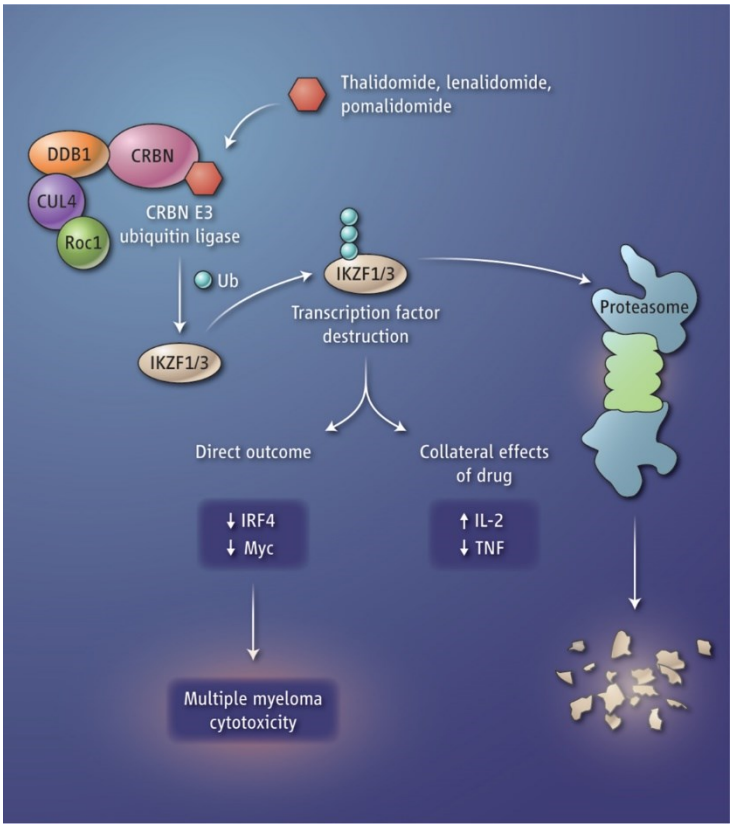

Figure 23. The small-molecule drugs thalidomide, lenalidomide and pomalidomide bind to the protein cereblon (CRBN), which activates the enzymatic activity of the CRBN E3 ubiquitin ligase complex. The transcription factors Ikaros (IKZF1) and Aiolos (IKZF3) are modified with ubiquitin (Ub) molecules, targeting them for proteolysis. This alters the function of T cells and B cells, with a toxic outcome for MM cells.

It is not clear how IMiDs binding to CRBN can promote the degradation of IKZF1 and IKZF3. It has been proposed that the underlying mechanism might conceptually resemble the auxin-induced degradation of members of the Aux/IAA repressor family by the ligase TIR1 (243). The CRL4CRBN architecture supports ubiquitination in its vicinity, a property that is exploited by viral proteins in

recruiting cellular targets for degradation by CRL4s (244). Small molecules such as thalidomide and its derivatives may mimic this behaviour, bringing novel substrates such as IKZF1 and IKZF3 in the vicinity of CRL4CRBN complex, thus promoting their degradation (245).

Studies on the crystallized structure of a chimaeric complex of human DDB1 and *Gallus gallus* (chicken) CRBN bound to thalidomide, lenalidomide and pomalidomide revealed that they bind to CRBN at the canonical substrate-binding site. Thus, IMiDs, by binding to CRBN, simultaneously confer to the E3 complex new substrate specificity while interfering with the recruitment of endogenous substrates (such as MEIS2) to CRL4CRBN, as they occupy the binding site (245) (Fig. 24).

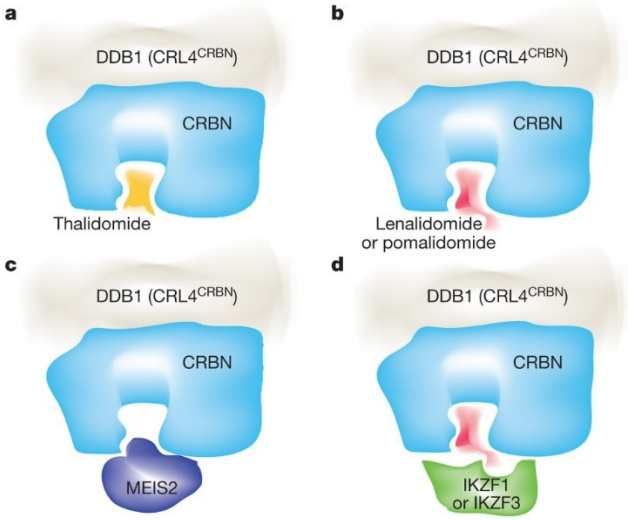

Figure 24. Molecular model of IMiDs function. **(a)** Thalidomide binds to CRBN at the canonical substrate-binding site. **(b)** The potent anti-myeloma drug thalidomide and its derivatives lenalidomide and pomalidomide occupy the same site but with different solvent-exposed moieties. **(c)** Binding of the endogenous substrate MEIS2 and the IMiDs to this site is mutually exclusive. **(d)** Direct interaction of lenalidomide or pomalidomide with IKAROS transcription factors (IKZF1 and IKZF3).

Overall, these observations suggest that IMiDs are not simply CRBN antagonists, as proposed by Ito et al. in 2010 (186), instead, they seem to more generally alter the substrate specificity of CRBN to include proteins important in myeloma (240,241).

To explain the complex, pleiotropic effects of thalidomide and its analogues, it is therefore necessary to consider both their inhibitory function on CRBN activity on its endogenous substrates and their ability to induce a CRBN gain of function towards *de novo* substrates.

2.6 Regulatory post-translational modifications of the p53 family members

Post-translational modifications are covalent processing events that change the properties of a protein by either proteolytic cleavage or by the addition of a modifying group to one or more aminoacids. These modifications can diversify proteins function and regulate their availability. Acetylation, sumoylation, phosphorylation and ubiquitination can affect the half-life, the specificity and efficiency of protein-protein interactions and overall modulate the transcriptional activity of the p53 family members (Fig. 25). In particular, to maintain p63 key role in the regulation of correct limb development, it is not only necessary the integrity of its DBD but also a tight control of the mechanisms that control its stability and activity.

2.6.1 Acetylation

Acetylation is a reversible process by which an acetyl group is covalently linked to the ε amino-group of lysine residues of a target protein. Acetylation was first discovered on histones; acetylation of internal lysine residues of core histone has been found associated with transcriptional activation in eukaryotes. However, acetylation process does not involve only histone proteins.

Acetylation and deacetylation have been described as fundamental mechanisms in the regulation of p53 activation and stability (110–117).

p53 is acetylated by Tip60/hMOF protein on lysine 120 (117) and by p300 acetyl-transferase on its C-terminus and on lysine 164 (K164) (110). Loss of acetylation at all these major sites completely abolishes p53 ability to activate p21 and suppresses cell growth (110). Moreover, acetylation blocks the interaction of p53 with its repressors MDM2 and MDMX and this event directly results in p53 activation (116). Interestingly, K164 in p53 corresponds to lysine 193 (K193) in p63, which is mutated to glutamic acid (K193E) in patients affected by SHFM4 (Fig. 26).

h p53 154 GTRVRAMAIY**K**QSQHMTEVVR 174
m p53 151 GSRVRAMAIY**K**KSQHMTEVVR 171
h p63 183 GAVIRAMPVY**K**KAEHVTDVVK 203
h p73 172 GTAIRAMPVY**K**KAEHVTDVVK 192

Figure 26. Alignment of the K164 flanking region of the human p53 protein with those of the murine protein and of human p63 and p73. The conserved lysine residue is marked in bold; h: human; m: mouse (110).

Acetylation has been largely demonstrated to be essential also for p73 regulation. p73 acetylation following DNA damage potentiates its apoptotic function by increasing its ability to activate the

transcription of proapoptotic target genes. Indeed, p73α is acetylated in a c-Abl-dependent manner by p300 in response to apoptotic concentrations of the DNA-damaging drug doxorubucin on three conserved lysines at positions 321, 327, and 331 and a non-acetylatable p73 mutant is impaired in the activation of the apoptotic gene *p53AIP1* (118,119).

2.6.2 Phosphorylation

Phosphorylation is the addition of a phosphate group to a serine, tyrosine or threonine residue which can alter the conformation and function of a protein by locally altering its charge and hydrophobicity. Multiple sites of phoshphorylation have been described in p53 protein and specific phosphorylation events can regulate specific biochemical and/or biological functions of p53.

The N-terminus of p53 is highly phosphorylated and is the target for a range of different protein kinases, each of which is activated through pathways responding to cellular stresses (such as DNA damage) or changes in growth status (120). The N-terminal 15 amino acids of p53 contain the most highly phosphorylated sites in the protein (121) which are substrates for several kinases such as DNA-activated Protein Kinase (DNA-PK) (122–124) and Casein Kinase 1α (CK1α) (125). The proline-rich and transactivation domains of p53 are also targets for members of the Mitogen-Activated Protein (MAP) kinase family (126,127) and of the related Stress-Activated Protein (SAP) kinase family (128), respectively. Moreover, three phosphorylation events take place at different locations within the C-terminus of p53, by Cyclin-Dependent protein Kinases (CDKs) (129,130), Protein Kinase C (PKC) (131–135) and Protein Pinase CK2 (136–140). Each of these modifications leads to stimulation of the sequence-specific DNA-binding function of the protein.

A tight regulation of protein expression and function is achieved through a complex cross-talk among different post-translational modification events. For instance, the above mentioned acetylation of p73 occurs after a phosphorylation events. c-Abl induces the phosphorylation of p73 on threonine residues adjacent to prolines, and this modification, together with a second phosphorylation mediated by p38 MAPK (141), in turn favors binding of PIN-1 prolyl isomerase, promoting a conformational change that stimulates p300-mediated acetylation of p73 upon genotoxic stress (142–145).

Also ΔNp63α is directly phosphorylated by c-Abl and this modification promotes increased binding to YAP, resulting in p63 increased stability. c-Abl phosphorylates p63 on multiple sites (Y55, Y137F and Y308) and the combined mutant construct with the three tyrosines mutated to phenylalanine displays greatly diminished binding to YAP compared with wild-type ΔNp63*α* (146).

In a similar way, Dlx3 tightly controls p63 isoforms availability during epithelial stratification upon Raf1 kinase-mediated p63 phosphorylation on serine 383 and threonine 397 residues (24) and PIN-1 regulates p63 protein levels in a phosphorylation-dependent manner (51).

2.6.3 Ubiquitination

Very well established is the cross-talk between phosphorylation and ubiquitination of p53 family members. Ubiquitination is an enzymatic process in which an ubiquitin protein is attached to a substrate protein. Usually, this process is divided into three steps: activation, conjugation and ligation, performed respectively by an ubiquitin-activating enzyme (E1), an ubiquitin-conjugating enzyme (E2) and an ubiquitin ligase (E3). In the last step, the glycine 76 residue of ubiquitin is covalently linked to a lysine of the substrate protein. Depending on the number of ubiquitin proteins attached to the substrate protein, ubiquitination can lead to different results. Mono-ubiquitination can modify protein localization, affect protein activity or promote the interaction with other proteins. On the contrary, poly-ubiquitination is usually associated to the proteasome targeting of the protein and consequently to its degradation.

The principal negative regulator of p53 is the E3 ubiquitin ligase MDM2 and phosphorylation of p53 disturbs the interaction with MDM2 thus leading to p53 accumulation and activation (147). Unlike p53, p73 and p63 bind to, but are not degraded by MDM2 (148,149). Both p73 and p63 levels are controlled by Itch, a Hect ubiquitin-protein ligase. Itch binds and ubiquitinates p73 and p63 but not p53, resulting in their rapid proteasome-dependent degradation (150–152). However, also MDM2 contributes to the regulation of p63 protein levels, even though it does not directly ubiquitinates the protein. In fact, upon DNA damage or keratynocytes differentiation, MDM2 cooperates with the FBWX7 E3-ubiquitin ligase to induce proteasome-mediated degradation of ΔNp63α. MDM2 promotes ΔNp63α translocation to the cytoplasm, where it is targeted for degradation by FBWX7-mediated ubiquitination. Efficient degradation of ΔNp63α by FBWX7 requires GSK3 kinase activity, which phosphorylates ΔNp63α on residue serine 383 (149).

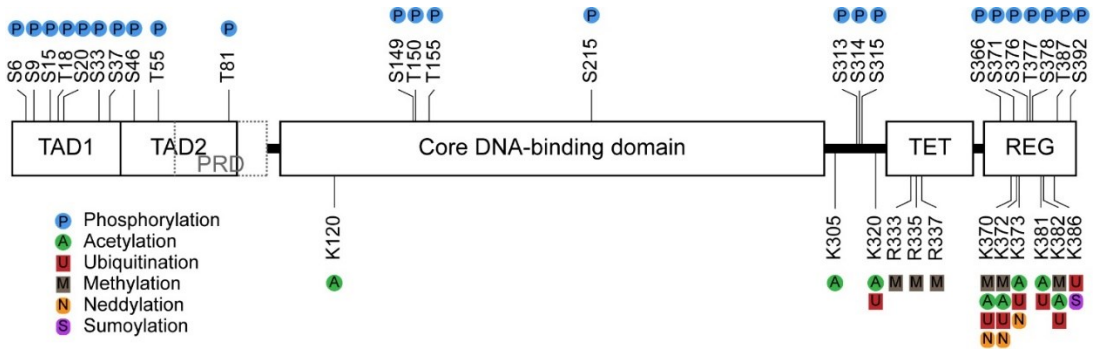

Figure 25. Sites of post-translational modifications on p53. Schematic representation of the 393 amino acid domain structure of human p53 showing the sites of post-translational modification including phosphorylation, acetylation, ubiquitination, methylation, neddylation, and sumoylation. Abbreviations: N-terminal transactivation domain (TAD); proline-rich domain (PRD); tetramerisation domain (TET); C-terminal regulatory domain (REG); arginine (R); lysine (K); serine (S); threonine (T).

3. Aim of the work

The p63 transcription factor, homolog to the p53 tumor suppressor, plays a pivotal role in limb, epithelial and cranio-facial development. The focus of our laboratory is to investigate the complex networks centered on p63 that govern limb and epithelia development. In particular, we are interested in the upstream signalling pathways that control p63 stability and activity in physiological and pathological conditions.

As mentioned before, the p53 family members are largely regulated by a huge numbers of post-translational modifications. Acetylation, sumoylation, phosphorylation and ubiquitination affect p63 stability and function and overall modulate the transcriptional activity of the protein. A perturbation of these regulative mechanisms can result in the alteration of p63 role in limb and epithelia development, in the end resulting in limb malformations and defective formation of the skin. Thus, investigating the upstream pathways and post-translational modifications that control p63 function is crucial to understand the genetic and molecular causes of those pathological conditions involving *p63*.

Dominant mutations in the *p63* gene give rise to several human congenital syndromes like Ectrodactyly-Ectodermal displasia-Cleft lip/palate (EEC), Ankyloblepharon-Ectodermal displasia-Clefting (AEC), Limb-Mammary Syndrome (LMS) and Split-Hand/Footh Malformation (SHFM) type 4 (13,246). Disease causing mutations can occur in the DNA Binding Domain (DBD) but can also reside in target sites for post-translational modifications. In 2008 was identified in the sequence of p53 protein a residue, lysine 164, which can be acetylated by acetyl-transferase CBP/p300 (110). The consideration that this lysine is conserved in p63 and that it corresponds to lysine 193 of ΔNp63α, which is mutated into glutamic acid (K193E) in patients affected by SHFM4, prompted us to verify whether ΔNp63α is acetylated on this residue and the relevance of this post-translational modification in limb development.

At the same time, the observation that the limb defects presented by EEC, LMS, ADULT and SHFM4 patients show a striking resemblance with the malformations induced by the teratogenic drug thalidomide prompted us to verify whether thalidomide could affect p63 function and/or stability. It has occurred that EEC patients have been wrongly referred as possible victims of thalidomide (189).

Indeed, our data indicate that ΔNp63α is a target of thalidomide teratogenicity and reveal that thalidomide is able to downregulate ΔNp63α protein. Furthermore, we set forth to investigate the upstream pathway through which thalidomide exerts its modulation of ΔNp63α levels and the post-translational modifications involved in this process. Finally, using zebrafish as a model system, we verified the *in vivo* relevance of ΔNp63α downregulation in the onset of thalidomide-induced malformations.

Thalidomide is now used for treatment of multiple myeloma and leprosy (160,173): a better understanding of its mechanism of action might pave the way for the design of related compounds with equal therapeutic properties but devoid of teratogenic activity.

Moreover, ΔNp63α was shown to be involved in several types of cancer such as Squamous Cell Carcinoma (SCC), pediatric neuroblastoma and osteosarcoma (247,248). The study of thalidomide ability to modulate ΔNp63α levels might also have therapeutic implications for those neoplastic conditions in which ΔNp63α is overexpressed.

4. Main results

4.1 FGF8, c-Abl and p300 participate in a pathway that controls stability and function of the ΔNp63α protein

Acetylation of p53 on lysine 164 (K164) by p300 is enhanced in response to DNA damage and correlates with p53 stabilization and activation (110). K164 in p53, corresponds to lysine 193 (K193) in ΔNp63α, which is mutated into glutamic acid (K193E) in SHFM4 (49,249).

Western blot analysis revealed that the p300 acetyl-transferase physically interacts with ΔNp63α and catalyzes its acetylation on K193. Indeed, overexpression of p300 stabilizes ΔNp63α in HaCaT cells and acetylation assay revealed that a synthetic p63 peptide centered on K193 is acetylated *in vitro*, whilst the levels of acetylation of the p63-K193R mutant were reduced.

Interestingly, qPCR analyses in U2OS cells stably transfected with either the wild-type ΔNp63α or the ΔNp63α-K193E revealed that the ΔNp63α-K193E mutant displays an altered transactivation activity on ΔNp63α target genes involved in development and apoptosis, while it behaves like the wild-type ΔNp63α on p53, involved in cell cycle regulation. Similarly, ChIP experiments showed that ΔNp63α-K193E mutant is not efficiently recruited on the Responsive Elements (RE) of genes relevant for developmental and apoptotic processes while it is normally recruited on RE of the p53 gene.

Moreover, Fibroblast Growth Factor-8 (FGF8), a morphogenetic signalling molecule essential for embryonic limb development, displayed the ability to stabilize ΔNp63α protein by increasing the binding of ΔNp63α to the tyrosine kinase c-Abl. HaCaT cells treated with FGF8 displayed a great increase in ΔNp63α-c-Abl interaction and also in the levels of ΔNp63α acetylation. Furthermore, co-immunoprecipitation experiments of p300 with wild-type ΔNp63α or with the ΔNp63α-3Y mutant, with the three tyrosines known to be phopshorylated by c-Abl mutated into phenylalanine (146,250), revealed that ΔNp63α-3Y mutant displays a drastically reduced interaction with p300. FGF8 appeared also to activate ΔNp63α transactivation functions and when we inhibited c-Abl kinase activity, ΔNp63α was unable to transactivate its target genes, even in the presence of FGF8.

These results link FGF8, c-Abl and p300 in a regulatory pathway that controls ΔNp63α protein stability and transcriptional activity. Notably, the natural mutant ΔNp63α-K193E, associated to SHFM4, cannot be acetylated by this pathway. Hence, our data, indicating that K193E mutation is likely to result in aberrant limb development via the combined action of altered protein stability and altered promoter occupancy, shed new light on the molecular mechanism that could be at the bases of the SHFM4 pathogenesis.

4.2 ΔNp63α is a molecular target of thalidomide teratogenicity

The phenotypic similarity between thalidomide-induced malformations and those due to mutations in *p63* gene prompted us to determine whether p63 could be a molecular target of the drug. Western blot analysis performed on lysates from human keratinocyte (HaCaT) cells treated with thalidomide revealed that the drug induces a reduction of ΔNp63α protein levels, which is not accompanied by a reduction of *ΔNp63α* transcript levels. This effects was blocked when the cells were treated with the proteasome inhibitor MG132, suggesting that thalidomide induces a proteasome-mediated degradation of ΔNp63α. The transfection of human osteosarcoma cells (U2OS), which do not endogenously express p63, with either ΔNp63α, ΔNp63β or ΔNp63γ isoforms revealed that thalidomide treatment efficiently leads to a downregulation of ΔNp63α and ΔNp63β isoforms but does not alter ΔNp63γ protein levels. Moreover, thalidomide acts specifically on p63 transcription factor, since the protein levels of NF-Y and p53 transcription factors were not altered by the treatment. By using a series of deletion mutants, we were able to identify the protein region responsible for mediating thalidomide effect on p63. In this region are present two residues indispensable for thalidomide-induced degradation of ΔNp63α: serine 383 and threonine 397. These two residues are centered on two predicted phosphodegrons for the FBWX7 E3 ubiquitin ligase, which promotes the degradation of ΔNp63α and ΔNp63β isoforms upon DNA damage or keratinocytes differentiation. FBWX7 binds to its targets in a phosphorylation-dependent manner and most of its known substrates are phosphorylated by Glycogen Synthase Kinase 3 (GSK3) (149). The silencing of endogenous *FBWX7* in HaCaT cells abolished ΔNp63α protein modulation upon thalidomide treatment as well as the inhibition of GSK3 kinase activity with the specific inhibitor SB216763, indicating that the thalidomide-induced downregulation of ΔNp63α requires the activity of FBWX7 E3 ubiquitin ligase and GSK3 kinase.

In 2010 Ito et al. demonstrated that thalidomide treatment induces fin defects in developing zebrafish embryos (186). Western blot analysis performed on total extracts from zebrafish embryos revealed that thalidomide is able to induce a downregulation of p63 also *in vivo*. In zebrafish, p63 is an important regulator of correct fin outgrowth and it is upstream to dlx5 in the control of fin development (11,12,52). Thalidomide treatment results in a downregulation of dlx5 protein in zebrafish embryos, indicating that thalidomide-induced downregulation of p63 results in a general impairment of the downstream fin developmental pathway.

Most importantly, the microinjection of *zp63*-mRNA into embryos, subsequently treated with thalidomide, was able to rescue the thalidomide-induced defects in pectoral fin development, strongly suggesting that p63 downregulation is at least in part responsible for the onset of the malformations

induced by the drug. Finally, Real Time qPCR performed on total RNA extracts from these embryos revealed that the microinjection of *zp63*-mRNA is able to restore the expression levels of *tbx5a* and *prrx1a*, two genes essential for correct fin development (251–253), otherwise altered by thalidomide treament. Thus, the restoration of p63 levels can rescue thalidomide-induced alterations in fin development not only at a phenotypical but also at a molecular level.

4.3 CRBN is a negative regulator of ΔNp63α protein

CRBN, which is substrate receptor in E3 ubiquitin ligase complex CRL4, is the only direct target of thalidomide identified so far (186). We were interested in verifying whether ΔNp63α could be downstream to CRBN in the teratogenic cascade initiated by thalidomide.

Western blot analysis revealed that silencing of endogenous *CRBN* results in an upregulation of ΔNp63α protein levels in U2OS cells. On the contrary, the overexpression of CRBN led to a reduction of transfected ΔNp63α protein and this effect was blocked when the cells were treated with the proteasome inhibitor MG132, indicating that CRBN is a negative regulator on ΔNp63α protein.

The transfection of U2OS cells with either ΔNp63α, ΔNp63β or ΔNp63γ isoforms revealed that CRBN overexpression leads specifically to a downregulation of ΔNp63α and ΔNp63β, whilst does not alter the levels of ΔNp63γ and p53, in a similar way as thalidomide treatment.

Crbn appears to function as a negative regulator of p63 also *in vivo* in zebrafish embryos, where its knockdown through the microinjection of a specific *crbn*-Morpholino leads to an increase of p63 protein levels.

CRBN is highly conserved from fish to mammals and can hardly account alone for the species-specificity of thalidomide teratogenicity. It is possible that other molecules, perhaps downstream targets of CRBN, may define the specificity of thalidomide teratogenicity. The overexpression of either human or mouse CRBN in a murine context (mouse embryonic fibroblast NIH3T3 cells) revealed that mouse CRBN is significantly less efficient in interacting with ΔNp63α and promoting its downregulation, compared to the human orthologous. Should ΔNp63α be a downstream target of CRBN in thalidomide teratogenic cascade, the differential sensitivity of ΔNp63α to CRBN orthologues from different species might provide a hint into the species-specificity of thalidomide teratogenicity.

5. Future perspectives

The results presented in this thesis indicate that thalidomide treatment induces a reduction of ΔNp63α protein levels and a downregulation of its target dlx5 not only *in vitro* but also *in vivo* and that this effect is, at least in part, at the basis of the phenotypical defects that we observed in the pectoral fins of the treated zebrafish embryos. In future, we plan to analyse the effects of thalidomide treatment in embryos microinjected with either *zΔNp63α*-mRNA or control-mRNA on the expression levels of other p63 target genes (*Ikka, Dlx5, Dlx6, Perp, Redd1*) (27,28,38,47,50) and on other genes known to be involved in zebrafish fin fold formation, such as *fgf8* and *shha* (95–97).

The mechanism through which thalidomide leads to a reduction of ΔNp63α protein levels is not completely clear but it is possible that the thalidomide primary target CRBN is involved in this process. The preliminary data I collected up to now indicate that CRBN is a negative regulator of ΔNp63α protein. In fact, CRBN overexpression in U2OS cells results in a decrease of transfected ΔNp63α protein levels, whilst CRBN knockdown results in an upregulation of ΔNp63α protein both in U2OS cells and in zebrafish embryos.

In future, I plan to verify if CRBN is involved in thalidomide-induced degradation of ΔNp63α by analysing the effects of thalidomide treatment on ΔNp63α protein levels in cells where CRBN has been silenced or overexpressed. Moreover, I plan to verify whether CRBN directly ubiquitinates ΔNp63α or it acts on a regulator of ΔNp63α stability. Finally, we previously demonstrated that thalidomide promotes p63 degradation via FBWX7 ubiquitin ligase activity. Should CRBN contribute to thalidomide-induced ΔNp63α downregulation, to fully appreciate the model it is necessary to understand whether CRBN interacts with FBWX7 or it functions through an independent pathway.

6. References

1. Levine AJ. p53, the cellular gatekeeper for growth and division. Cell. 1997 Feb 7;88(3):323–31.

2. Yang A, Schweitzer R, Sun D, Kaghad M, Walker N, Bronson RT, et al. p63 is essential for regenerative proliferation in limb, craniofacial and epithelial development. Nature. 1999 Apr 22;398(6729):714–8.

3. Mills AA, Zheng B, Wang XJ, Vogel H, Roop DR, Bradley A. p63 is a p53 homologue required for limb and epidermal morphogenesis. Nature. 1999 Apr 22;398(6729):708–13.

4. Yang A, Walker N, Bronson R, Kaghad M, Oosterwegel M, Bonnin J, et al. p73-deficient mice have neurological, pheromonal and inflammatory defects but lack spontaneous tumours. Nature. 2000 Mar 2;404(6773):99–103.

5. Ghioni P, Bolognese F, Duijf PHG, Van Bokhoven H, Mantovani R, Guerrini L. Complex transcriptional effects of p63 isoforms: identification of novel activation and repression domains. Mol Cell Biol. 2002 Dec;22(24):8659–68.

6. Schultz J, Ponting CP, Hofmann K, Bork P. SAM as a protein interaction domain involved in developmental regulation. Protein Sci Publ Protein Soc. 1997 Jan;6(1):249–53.

7. Bork P, Koonin EV. Predicting functions from protein sequences--where are the bottlenecks? Nat Genet. 1998 Apr;18(4):313–8.

8. Zhu J, Jiang J, Zhou W, Zhu K, Chen X. Differential regulation of cellular target genes by p53 devoid of the PXXP motifs with impaired apoptotic activity. Oncogene. 1999 Mar 25;18(12):2149–55.

9. Strano S, Munarriz E, Rossi M, Castagnoli L, Shaul Y, Sacchi A, et al. Physical interaction with Yes-associated protein enhances p73 transcriptional activity. J Biol Chem. 2001 May 4;276(18):15164–73.

10. Deyoung MP, Ellisen LW. p63 and p73 in human cancer: defining the network. Oncogene. 2007 Aug 9;26(36):5169–83.

11. Bakkers J, Hild M, Kramer C, Furutani-Seiki M, Hammerschmidt M. Zebrafish DeltaNp63 is a direct target of Bmp signaling and encodes a transcriptional repressor blocking neural specification in the ventral ectoderm. Dev Cell. 2002 May;2(5):617–27.

12. Lee H, Kimelman D. A dominant-negative form of p63 is required for epidermal proliferation in zebrafish. Dev Cell. 2002 May;2(5):607–16.

13. van Bokhoven H, Brunner HG. Splitting p63. Am J Hum Genet. 2002 Jul;71(1):1–13.

14. Guerrini L, Costanzo A, Merlo GR. A symphony of regulations centered on p63 to control development of ectoderm-derived structures. J Biomed Biotechnol. 2011;2011:864904.

15. Rinne T, Brunner HG, van Bokhoven H. p63-associated disorders. Cell Cycle Georget Tex. 2007 Feb 1;6(3):262–8.

16. Brunner HG, Hamel BCJ, Bokhoven Hv H van. P63 gene mutations and human developmental syndromes. Am J Med Genet. 2002 Oct 15;112(3):284–90.

17. Vanbokhoven H, Melino G, Candi E, Declercq W. p63, a story of mice and men. J Invest Dermatol. 2011 Jun;131(6):1196–207.

18. Dai X, Segre JA. Transcriptional control of epidermal specification and differentiation. Curr Opin Genet Dev. 2004 Oct;14(5):485–91.

19. Koster MI, Kim S, Roop DR. P63 deficiency: a failure of lineage commitment or stem cell maintenance? J Investig Dermatol Symp Proc Soc Investig Dermatol Inc Eur Soc Dermatol Res. 2005 Nov;10(2):118–23.

20. Candi E, Cipollone R, Rivetti di Val Cervo P, Gonfloni S, Melino G, Knight R. p63 in epithelial development. Cell Mol Life Sci CMLS. 2008 Oct;65(20):3126–33.

21. Radoja N, Guerrini L, Lo Iacono N, Merlo GR, Costanzo A, Weinberg WC, et al. Homeobox gene Dlx3 is regulated by p63 during ectoderm development: relevance in the pathogenesis of ectodermal dysplasias. Dev Camb Engl. 2007 Jan;134(1):13–8.

22. Koster MI, Roop DR. Mechanisms regulating epithelial stratification. Annu Rev Cell Dev Biol. 2007;23:93–113.

23. King KE, Ponnamperuma RM, Yamashita T, Tokino T, Lee LA, Young MF, et al. deltaNp63alpha functions as both a positive and a negative transcriptional regulator and blocks in vitro differentiation of murine keratinocytes. Oncogene. 2003 Jun 5;22(23):3635–44.

24. Di Costanzo A, Festa L, Duverger O, Vivo M, Guerrini L, La Mantia G, et al. Homeodomain protein Dlx3 induces phosphorylation-dependent p63 degradation. Cell Cycle Georget Tex. 2009 Apr 15;8(8):1185–95.

25. Sil AK, Maeda S, Sano Y, Roop DR, Karin M. IkappaB kinase-alpha acts in the epidermis to control skeletal and craniofacial morphogenesis. Nature. 2004 Apr 8;428(6983):660–4.

26. Descargues P, Sil AK, Sano Y, Korchynskyi O, Han G, Owens P, et al. IKKalpha is a critical coregulator of a Smad4-independent TGFbeta-Smad2/3 signaling pathway that controls keratinocyte differentiation. Proc Natl Acad Sci U S A. 2008 Feb 19;105(7):2487–92.

27. Marinari B, Ballaro C, Koster MI, Giustizieri ML, Moretti F, Crosti F, et al. IKKalpha is a p63 transcriptional target involved in the pathogenesis of ectodermal dysplasias. J Invest Dermatol. 2009 Jan;129(1):60–9.

28. Candi E, Terrinoni A, Rufini A, Chikh A, Lena AM, Suzuki Y, et al. p63 is upstream of IKK alpha in epidermal development. J Cell Sci. 2006 Nov 15;119(Pt 22):4617–22.

29. Hu Y, Baud V, Delhase M, Zhang P, Deerinck T, Ellisman M, et al. Abnormal morphogenesis but intact IKK activation in mice lacking the IKKalpha subunit of IkappaB kinase. Science. 1999 Apr 9;284(5412):316–20.

30. Li Q, Lu Q, Hwang JY, Büscher D, Lee KF, Izpisua-Belmonte JC, et al. IKK1-deficient mice exhibit abnormal development of skin and skeleton. Genes Dev. 1999 May 15;13(10):1322–8.

31. Takeda K, Takeuchi O, Tsujimura T, Itami S, Adachi O, Kawai T, et al. Limb and skin abnormalities in mice lacking IKKalpha. Science. 1999 Apr 9;284(5412):313–6.

32. Taniguchi T, Takaoka A. A weak signal for strong responses: interferon-alpha/beta revisited. Nat Rev Mol Cell Biol. 2001 May;2(5):378–86.

33. Richardson RJ, Dixon J, Malhotra S, Hardman MJ, Knowles L, Boot-Handford RP, et al. Irf6 is a key determinant of the keratinocyte proliferation-differentiation switch. Nat Genet. 2006 Nov;38(11):1329–34.

34. Ingraham CR, Kinoshita A, Kondo S, Yang B, Sajan S, Trout KJ, et al. Abnormal skin, limb and craniofacial morphogenesis in mice deficient for interferon regulatory factor 6 (Irf6). Nat Genet. 2006 Nov;38(11):1335–40.

35. Rahimov F, Marazita ML, Visel A, Cooper ME, Hitchler MJ, Rubini M, et al. Disruption of an AP-2alpha binding site in an IRF6 enhancer is associated with cleft lip. Nat Genet. 2008 Nov;40(11):1341–7.

36. Little HJ, Rorick NK, Su L-I, Baldock C, Malhotra S, Jowitt T, et al. Missense mutations that cause Van der Woude syndrome and popliteal pterygium syndrome affect the DNA-binding and transcriptional activation functions of IRF6. Hum Mol Genet. 2009 Feb 1;18(3):535–45.

37. Moretti F, Marinari B, Lo Iacono N, Botti E, Giunta A, Spallone G, et al. A regulatory feedback loop involving p63 and IRF6 links the pathogenesis of 2 genetically different human ectodermal dysplasias. J Clin Invest. 2010 May;120(5):1570–7.

38. Ellisen LW, Ramsayer KD, Johannessen CM, Yang A, Beppu H, Minda K, et al. REDD1, a developmentally regulated transcriptional target of p63 and p53, links p63 to regulation of reactive oxygen species. Mol Cell. 2002 Nov;10(5):995–1005.

39. Bae YS, Kang SW, Seo MS, Baines IC, Tekle E, Chock PB, et al. Epidermal growth factor (EGF)-induced generation of hydrogen peroxide. Role in EGF receptor-mediated tyrosine phosphorylation. J Biol Chem. 1997 Jan 3;272(1):217–21.

40. Finkel T. Redox-dependent signal transduction. FEBS Lett. 2000 Jun 30;476(1-2):52–4.

41. Meng T-C, Fukada T, Tonks NK. Reversible oxidation and inactivation of protein tyrosine phosphatases in vivo. Mol Cell. 2002 Feb;9(2):387–99.

42. Radice GL, Ferreira-Cornwell MC, Robinson SD, Rayburn H, Chodosh LA, Takeichi M, et al. Precocious mammary gland development in P-cadherin-deficient mice. J Cell Biol. 1997 Nov 17;139(4):1025–32.

43. Kolle G, Ho M, Zhou Q, Chy HS, Krishnan K, Cloonan N, et al. Identification of human embryonic stem cell surface markers by combined membrane-polysome translation state array analysis and immunotranscriptional profiling. Stem Cells Dayt Ohio. 2009 Oct;27(10):2446–56.

44. de Mollerat XJ, Gurrieri F, Morgan CT, Sangiorgi E, Everman DB, Gaspari P, et al. A genomic rearrangement resulting in a tandem duplication is associated with split hand-split foot malformation 3 (SHFM3) at 10q24. Hum Mol Genet. 2003 Aug 15;12(16):1959–71.

45. Shimomura Y, Wajid M, Shapiro L, Christiano AM. P-cadherin is a p63 target gene with a crucial role in the developing human limb bud and hair follicle. Dev Camb Engl. 2008 Feb;135(4):743–53.

46. Kjaer KW, Hansen L, Schwabe GC, Marques-de-Faria AP, Eiberg H, Mundlos S, et al. Distinct CDH3 mutations cause ectodermal dysplasia, ectrodactyly, macular dystrophy (EEM syndrome). J Med Genet. 2005 Apr;42(4):292–8.

47. Ihrie RA, Marques MR, Nguyen BT, Horner JS, Papazoglu C, Bronson RT, et al. Perp is a p63-regulated gene essential for epithelial integrity. Cell. 2005 Mar 25;120(6):843–56.

48. Fernandez-Teran M, Ros MA. The Apical Ectodermal Ridge: morphological aspects and signaling pathways. Int J Dev Biol. 2008;52(7):857–71.

49. Duijf PHG, van Bokhoven H, Brunner HG. Pathogenesis of split-hand/split-foot malformation. Hum Mol Genet. 2003 Apr 1;12 Spec No 1:R51–60.

50. Lo Iacono N, Mantero S, Chiarelli A, Garcia E, Mills AA, Morasso MI, et al. Regulation of Dlx5 and Dlx6 gene expression by p63 is involved in EEC and SHFM congenital limb defects. Dev Camb Engl. 2008 Apr;135(7):1377–88.

51. Restelli M, Lopardo T, Lo Iacono N, Garaffo G, Conte D, Rustighi A, et al. DLX5, FGF8 and the Pin1 isomerase control ΔNp63α protein stability during limb development: a regulatory loop at the basis of the SHFM and EEC congenital malformations. Hum Mol Genet. 2014 Jul 15;23(14):3830–42.

52. Kouwenhoven EN, van Heeringen SJ, Tena JJ, Oti M, Dutilh BE, Alonso ME, et al. Genome-wide profiling of p63 DNA-binding sites identifies an element that regulates gene expression during limb development in the 7q21 SHFM1 locus. PLoS Genet. 2010 Aug;6(8):e1001065.

53. Mariani FV, Martin GR. Deciphering skeletal patterning: clues from the limb. Nature. 2003 May 15;423(6937):319–25.

54. Towers M, Wolpert L, Tickle C. Gradients of signalling in the developing limb. Curr Opin Cell Biol. 2012 Apr;24(2):181–7.

55. Tanaka M. Molecular and evolutionary basis of limb field specification and limb initiation. Dev Growth Differ. 2013 Jan;55(1):149–63.

56. Capdevila J, Izpisúa Belmonte JC. Patterning mechanisms controlling vertebrate limb development. Annu Rev Cell Dev Biol. 2001;17:87–132.

57. Bénazet J-D, Zeller R. Vertebrate limb development: moving from classical morphogen gradients to an integrated 4-dimensional patterning system. Cold Spring Harb Perspect Biol. 2009 Oct;1(4):a001339.

58. Marshall H, Morrison A, Studer M, Pöpperl H, Krumlauf R. Retinoids and Hox genes. FASEB J Off Publ Fed Am Soc Exp Biol. 1996 Jul;10(9):969–78.

59. Searls RL, Janners MY. The initiation of limb bud outgrowth in the embryonic chick. Dev Biol. 1971 Feb;24(2):198–213.

60. Summerbell D, Lewis JH, Wolpert L. Positional information in chick limb morphogenesis. Nature. 1973 Aug 24;244(5417):492–6.

61. Mercader N, Leonardo E, Piedra ME, Martínez-A C, Ros MA, Torres M. Opposing RA and FGF signals control proximodistal vertebrate limb development through regulation of Meis genes. Dev Camb Engl. 2000 Sep;127(18):3961–70.

62. Tabin C, Wolpert L. Rethinking the proximodistal axis of the vertebrate limb in the molecular era. Genes Dev. 2007 Jun 15;21(12):1433–42.

63. Jr SJ, Gasseling MT. Ectoderm-mesenchymal interaction in the origins of wing symmetry. In: Epithelial-Mesenchymal Interactions. R Fleischmajer, RE Billingham; 1968. p. 289–314.

64. Wolpert L. Positional information and the spatial pattern of cellular differentiation. J Theor Biol. 1969 Oct;25(1):1–47.

65. Riddle RD, Johnson RL, Laufer E, Tabin C. Sonic hedgehog mediates the polarizing activity of the ZPA. Cell. 1993 Dec 31;75(7):1401–16.

66. Chang DT, López A, von Kessler DP, Chiang C, Simandl BK, Zhao R, et al. Products, genetic linkage and limb patterning activity of a murine hedgehog gene. Dev Camb Engl. 1994 Nov;120(11):3339–53.

67. López-Martínez A, Chang DT, Chiang C, Porter JA, Ros MA, Simandl BK, et al. Limb-patterning activity and restricted posterior localization of the amino-terminal product of Sonic hedgehog cleavage. Curr Biol CB. 1995 Jul 1;5(7):791–6.

68. Ingham PW. Transducing Hedgehog: the story so far. EMBO J. 1998 Jul 1;17(13):3505–11.

69. Echelard Y, Epstein DJ, St-Jacques B, Shen L, Mohler J, McMahon JA, et al. Sonic hedgehog, a member of a family of putative signaling molecules, is implicated in the regulation of CNS polarity. Cell. 1993 Dec 31;75(7):1417–30.

70. Roelink H, Augsburger A, Heemskerk J, Korzh V, Norlin S, Ruiz i Altaba A, et al. Floor plate and motor neuron induction by vhh-1, a vertebrate homolog of hedgehog expressed by the notochord. Cell. 1994 Feb 25;76(4):761–75.

71. Krauss S, Concordet JP, Ingham PW. A functionally conserved homolog of the Drosophila segment polarity gene hh is expressed in tissues with polarizing activity in zebrafish embryos. Cell. 1993 Dec 31;75(7):1431–44.

72. Drossopoulou G, Lewis KE, Sanz-Ezquerro JJ, Nikbakht N, McMahon AP, Hofmann C, et al. A model for anteroposterior patterning of the vertebrate limb based on sequential long- and short-range Shh signalling and Bmp signalling. Dev Camb Engl. 2000 Apr;127(7):1337–48.

73. Lewis PM, Dunn MP, McMahon JA, Logan M, Martin JF, St-Jacques B, et al. Cholesterol modification of sonic hedgehog is required for long-range signaling activity and effective modulation of signaling by Ptc1. Cell. 2001 Jun 1;105(5):599–612.

74. Litingtung Y, Dahn RD, Li Y, Fallon JF, Chiang C. Shh and Gli3 are dispensable for limb skeleton formation but regulate digit number and identity. Nature. 2002 Aug 29;418(6901):979–83.

75. Aza-Blanc P, Ramírez-Weber FA, Laget MP, Schwartz C, Kornberg TB. Proteolysis that is inhibited by hedgehog targets Cubitus interruptus protein to the nucleus and converts it to a repressor. Cell. 1997 Jun 27;89(7):1043–53.

76. Chiang C, Litingtung Y, Lee E, Young KE, Corden JL, Westphal H, et al. Cyclopia and defective axial patterning in mice lacking Sonic hedgehog gene function. Nature. 1996 Oct 3;383(6599):407–13.

77. Kraus P, Fraidenraich D, Loomis CA. Some distal limb structures develop in mice lacking Sonic hedgehog signaling. Mech Dev. 2001 Jan;100(1):45–58.

78. Laufer E, Nelson CE, Johnson RL, Morgan BA, Tabin C. Sonic hedgehog and Fgf-4 act through a signaling cascade and feedback loop to integrate growth and patterning of the developing limb bud. Cell. 1994 Dec 16;79(6):993–1003.

79. Niswander L, Jeffrey S, Martin GR, Tickle C. A positive feedback loop coordinates growth and patterning in the vertebrate limb. Nature. 1994 Oct 13;371(6498):609–12.

80. Chen H, Johnson RL. Dorsoventral patterning of the vertebrate limb: a process governed by multiple events. Cell Tissue Res. 1999 Apr;296(1):67–73.

81. Akita K. The effect of the ectoderm on the dorsoventral pattern of epidermis, muscles and joints in the developing chick leg: a new model. Anat Embryol (Berl). 1996 Apr;193(4):377–86.

82. Michaud JL, Lapointe F, Le Douarin NM. The dorsoventral polarity of the presumptive limb is determined by signals produced by the somites and by the lateral somatopleure. Dev Camb Engl. 1997 Apr;124(8):1453–63.

83. Dealy CN, Roth A, Ferrari D, Brown AM, Kosher RA. Wnt-5a and Wnt-7a are expressed in the developing chick limb bud in a manner suggesting roles in pattern formation along the proximodistal and dorsoventral axes. Mech Dev. 1993 Oct;43(2-3):175–86.

84. Parr BA, Shea MJ, Vassileva G, McMahon AP. Mouse Wnt genes exhibit discrete domains of expression in the early embryonic CNS and limb buds. Dev Camb Engl. 1993 Sep;119(1):247–61.

85. Parr BA, McMahon AP. Dorsalizing signal Wnt-7a required for normal polarity of D-V and A-P axes of mouse limb. Nature. 1995 Mar 23;374(6520):350–3.

86. Riddle RD, Ensini M, Nelson C, Tsuchida T, Jessell TM, Tabin C. Induction of the LIM homeobox gene Lmx1 by WNT7a establishes dorsoventral pattern in the vertebrate limb. Cell. 1995 Nov 17;83(4):631–40.

87. Vogel A, Rodriguez C, Warnken W, Izpisúa Belmonte JC. Dorsal cell fate specified by chick Lmx1 during vertebrate limb development. Nature. 1995 Dec 14;378(6558):716–20.

88. Cygan JA, Johnson RL, McMahon AP. Novel regulatory interactions revealed by studies of murine limb pattern in Wnt-7a and En-1 mutants. Dev Camb Engl. 1997 Dec;124(24):5021–32.

89. Logan C, Hornbruch A, Campbell I, Lumsden A. The role of Engrailed in establishing the dorsoventral axis of the chick limb. Dev Camb Engl. 1997 Jun;124(12):2317–24.

90. Loomis CA, Kimmel RA, Tong CX, Michaud J, Joyner AL. Analysis of the genetic pathway leading to formation of ectopic apical ectodermal ridges in mouse Engrailed-1 mutant limbs. Dev Camb Engl. 1998 Mar;125(6):1137–48.

91. Ahn K, Mishina Y, Hanks MC, Behringer RR, Crenshaw EB. BMPR-IA signaling is required for the formation of the apical ectodermal ridge and dorsal-ventral patterning of the limb. Dev Camb Engl. 2001 Nov;128(22):4449–61.

92. Pizette S, Abate-Shen C, Niswander L. BMP controls proximodistal outgrowth, via induction of the apical ectodermal ridge, and dorsoventral patterning in the vertebrate limb. Dev Camb Engl. 2001 Nov;128(22):4463–74.

93. Ito T, Handa H. Deciphering the mystery of thalidomide teratogenicity. Congenit Anom. 2012 Mar;52(1):1–7.

94. Ng JK, Kawakami Y, Büscher D, Raya A, Itoh T, Koth CM, et al. The limb identity gene Tbx5 promotes limb initiation by interacting with Wnt2b and Fgf10. Dev Camb Engl. 2002 Nov;129(22):5161–70.

95. Grandel H, Draper BW, Schulte-Merker S. dackel acts in the ectoderm of the zebrafish pectoral fin bud to maintain AER signaling. Dev Camb Engl. 2000 Oct;127(19):4169–78.

96. Prykhozhij SV, Neumann CJ. Distinct roles of Shh and Fgf signaling in regulating cell proliferation during zebrafish pectoral fin development. BMC Dev Biol. 2008;8:91.

97. Akimenko MA, Ekker M. Anterior duplication of the Sonic hedgehog expression pattern in the pectoral fin buds of zebrafish treated with retinoic acid. Dev Biol. 1995 Jul;170(1):243–7.

98. Farquharson C. Bones and Cartilage: Developmental and Evolutionary Skeletal Biology, Second Edition by Brian K. Hall. Br Poult Sci. 2015 Oct 1;

99. Tamura K, Yonei-Tamura S, Yano T, Yokoyama H, Ide H. The autopod: its formation during limb development. Dev Growth Differ. 2008 Jun;50 Suppl 1:S177–87.

100. Yonei-Tamura S, Abe G, Tanaka Y, Anno H, Noro M, Ide H, et al. Competent stripes for diverse positions of limbs/fins in gnathostome embryos. Evol Dev. 2008 Dec;10(6):737–45.

101. Metscher BD, Takahashi K, Crow K, Amemiya C, Nonaka DF, Wagner GP. Expression of Hoxa-11 and Hoxa-13 in the pectoral fin of a basal ray-finned fish, Polyodon spathula: implications for the origin of tetrapod limbs. Evol Dev. 2005 Jun;7(3):186–95.

102. Sakamoto K, Onimaru K, Munakata K, Suda N, Tamura M, Ochi H, et al. Heterochronic shift in Hox-mediated activation of sonic hedgehog leads to morphological changes during fin development. PloS One. 2009;4(4):e5121.

103. Sordino P, van der Hoeven F, Duboule D. Hox gene expression in teleost fins and the origin of vertebrate digits. Nature. 1995 Jun 22;375(6533):678–81.

104. Ahn D, Ho RK. Tri-phasic expression of posterior Hox genes during development of pectoral fins in zebrafish: implications for the evolution of vertebrate paired appendages. Dev Biol. 2008 Oct 1;322(1):220–33.

105. Woltering JM, Duboule D. The origin of digits: expression patterns versus regulatory mechanisms. Dev Cell. 2010 Apr 20;18(4):526–32.

106. Dane PJ, Tucker JB. Modulation of epidermal cell shaping and extracellular matrix during caudal fin morphogenesis in the zebra fish Brachydanio rerio. J Embryol Exp Morphol. 1985 Jun;87:145–61.

107. Yano T, Abe G, Yokoyama H, Kawakami K, Tamura K. Mechanism of pectoral fin outgrowth in zebrafish development. Dev Camb Engl. 2012 Aug;139(16):2916–25.

108. Thorogood, P. The development of the teleost fin and implications for our understanding of tetrapod evolution. In: Developmental Patterning Of The Vertebrate Lim. J. Hinchliffe, J. Hurle and D. Summerbell; 1991. p. 347–54.

109. Yano T, Tamura K. The making of differences between fins and limbs. J Anat. 2013 Jan;222(1):100–13.

110. Tang Y, Zhao W, Chen Y, Zhao Y, Gu W. Acetylation is indispensable for p53 activation. Cell. 2008 May 16;133(4):612–26.

111. Gu W, Roeder RG. Activation of p53 sequence-specific DNA binding by acetylation of the p53 C-terminal domain. Cell. 1997 Aug 22;90(4):595–606.

112. Luo J, Li M, Tang Y, Laszkowska M, Roeder RG, Gu W. Acetylation of p53 augments its site-specific DNA binding both in vitro and in vivo. Proc Natl Acad Sci U S A. 2004 Feb 24;101(8):2259–64.

113. Brooks CL, Gu W. Ubiquitination, phosphorylation and acetylation: the molecular basis for p53 regulation. Curr Opin Cell Biol. 2003 Apr;15(2):164–71.

114. Brooks CL, Gu W. The impact of acetylation and deacetylation on the p53 pathway. Protein Cell. 2011 Jun;2(6):456–62.

115. Luo J, Su F, Chen D, Shiloh A, Gu W. Deacetylation of p53 modulates its effect on cell growth and apoptosis. Nature. 2000 Nov 16;408(6810):377–81.

116. Li M, Luo J, Brooks CL, Gu W. Acetylation of p53 inhibits its ubiquitination by Mdm2. J Biol Chem. 2002 Dec 27;277(52):50607–11.

117. Sykes SM, Mellert HS, Holbert MA, Li K, Marmorstein R, Lane WS, et al. Acetylation of the p53 DNA-binding domain regulates apoptosis induction. Mol Cell. 2006 Dec 28;24(6):841–51.

118. Zeng X, Li X, Miller A, Yuan Z, Yuan W, Kwok RP, et al. The N-terminal domain of p73 interacts with the CH1 domain of p300/CREB binding protein and mediates transcriptional activation and apoptosis. Mol Cell Biol. 2000 Feb;20(4):1299–310.

119. Costanzo A, Merlo P, Pediconi N, Fulco M, Sartorelli V, Cole PA, et al. DNA damage-dependent acetylation of p73 dictates the selective activation of apoptotic target genes. Mol Cell. 2002 Jan;9(1):175–86.

120. Meek DW. Multisite phosphorylation and the integration of stress signals at p53. Cell Signal. 1998 Mar;10(3):159–66.

121. Meek DW. Post-translational modification of p53. Semin Cancer Biol. 1994 Jun;5(3):203–10.

122. Wang Y, Eckhart W. Phosphorylation sites in the amino-terminal region of mouse p53. Proc Natl Acad Sci U S A. 1992 May 15;89(10):4231–5.

123. Lees-Miller SP, Chen YR, Anderson CW. Human cells contain a DNA-activated protein kinase that phosphorylates simian virus 40 T antigen, mouse p53, and the human Ku autoantigen. Mol Cell Biol. 1990 Dec;10(12):6472–81.

124. Lees-Miller SP, Sakaguchi K, Ullrich SJ, Appella E, Anderson CW. Human DNA-activated protein kinase phosphorylates serines 15 and 37 in the amino-terminal transactivation domain of human p53. Mol Cell Biol. 1992 Nov;12(11):5041–9.

125. Milne DM, Palmer RH, Campbell DG, Meek DW. Phosphorylation of the p53 tumour-suppressor protein at three N-terminal sites by a novel casein kinase I-like enzyme. Oncogene. 1992 Jul;7(7):1361–9.

126. Milne DM, Campbell DG, Caudwell FB, Meek DW. Phosphorylation of the tumor suppressor protein p53 by mitogen-activated protein kinases. J Biol Chem. 1994 Mar 25;269(12):9253–60.

127. Jardine LJ, Milne DM, Dumaz N, Meek DW. Phosphorylation of murine p53, but not human p53, by MAP kinase in vitro and in cultured cells highlights species-dependent variation in post-translational modification. Oncogene. 1999 Dec 9;18(52):7602–7.

128. Milne DM, Campbell LE, Campbell DG, Meek DW. p53 is phosphorylated in vitro and in vivo by an ultraviolet radiation-induced protein kinase characteristic of the c-Jun kinase, JNK1. J Biol Chem. 1995 Mar 10;270(10):5511–8.

129. Bischoff JR, Friedman PN, Marshak DR, Prives C, Beach D. Human p53 is phosphorylated by p60-cdc2 and cyclin B-cdc2. Proc Natl Acad Sci U S A. 1990 Jun;87(12):4766–70.

130. Wang Y, Prives C. Increased and altered DNA binding of human p53 by S and G2/M but not G1 cyclin-dependent kinases. Nature. 1995 Jul 6;376(6535):88–91.

131. Baudier J, Delphin C, Grunwald D, Khochbin S, Lawrence JJ. Characterization of the tumor suppressor protein p53 as a protein kinase C substrate and a S100b-binding protein. Proc Natl Acad Sci U S A. 1992 Dec 1;89(23):11627–31.

132. Milne DM, McKendrick L, Jardine LJ, Deacon E, Lord JM, Meek DW. Murine p53 is phosphorylated within the PAb421 epitope by protein kinase C in vitro, but not in vivo, even after stimulation with the phorbol ester o-tetradecanoylphorbol 13-acetate. Oncogene. 1996 Jul 4;13(1):205–11.

133. Hupp TR, Lane DP. Regulation of the cryptic sequence-specific DNA-binding function of p53 by protein kinases. Cold Spring Harb Symp Quant Biol. 1994;59:195–206.

134. Takenaka I, Morin F, Seizinger BR, Kley N. Regulation of the sequence-specific DNA binding function of p53 by protein kinase C and protein phosphatases. J Biol Chem. 1995 Mar 10;270(10):5405–11.

135. Delphin C, Baudier J. The protein kinase C activator, phorbol ester, cooperates with the wild-type p53 species of Ras-transformed embryo fibroblasts growth arrest. J Biol Chem. 1994 Nov 25;269(47):29579–87.

136. Hupp TR, Meek DW, Midgley CA, Lane DP. Activation of the cryptic DNA binding function of mutant forms of p53. Nucleic Acids Res. 1993 Jul 11;21(14):3167–74.

137. Herrmann CP, Kraiss S, Montenarh M. Association of casein kinase II with immunopurified p53. Oncogene. 1991 May;6(5):877–84.

138. Filhol O, Baudier J, Delphin C, Loue-Mackenbach P, Chambaz EM, Cochet C. Casein kinase II and the tumor suppressor protein P53 associate in a molecular complex that is negatively regulated upon P53 phosphorylation. J Biol Chem. 1992 Oct 15;267(29):20577–83.

139. Hupp TR, Meek DW, Midgley CA, Lane DP. Regulation of the specific DNA binding function of p53. Cell. 1992 Nov 27;71(5):875–86.

140. Meek DW, Simon S, Kikkawa U, Eckhart W. The p53 tumour suppressor protein is phosphorylated at serine 389 by casein kinase II. EMBO J. 1990 Oct;9(10):3253–60.

141. Sanchez-Prieto R, Sanchez-Arevalo VJ, Servitja J-M, Gutkind JS. Regulation of p73 by c-Abl through the p38 MAP kinase pathway. Oncogene. 2002 Jan 31;21(6):974–9.

142. Agami R, Blandino G, Oren M, Shaul Y. Interaction of c-Abl and p73alpha and their collaboration to induce apoptosis. Nature. 1999 Jun 24;399(6738):809–13.

143. Yuan ZM, Shioya H, Ishiko T, Sun X, Gu J, Huang YY, et al. p73 is regulated by tyrosine kinase c-Abl in the apoptotic response to DNA damage. Nature. 1999 Jun 24;399(6738):814–7.

144. Gong JG, Costanzo A, Yang HQ, Melino G, Kaelin WG, Levrero M, et al. The tyrosine kinase c-Abl regulates p73 in apoptotic response to cisplatin-induced DNA damage. Nature. 1999 Jun 24;399(6738):806–9.

145. Mantovani F, Piazza S, Gostissa M, Strano S, Zacchi P, Mantovani R, et al. Pin1 links the activities of c-Abl and p300 in regulating p73 function. Mol Cell. 2004 Jun 4;14(5):625–36.

146. Yuan M, Luong P, Hudson C, Gudmundsdottir K, Basu S. c-Abl phosphorylation of ΔNp63α is critical for cell viability. Cell Death Dis. 2010;1:e16.

147. Momand J, Zambetti GP, Olson DC, George D, Levine AJ. The mdm-2 oncogene product forms a complex with the p53 protein and inhibits p53-mediated transactivation. Cell. 1992 Jun 26;69(7):1237–45.

148. Bálint E, Bates S, Vousden KH. Mdm2 binds p73 alpha without targeting degradation. Oncogene. 1999 Jul 8;18(27):3923–9.

149. Galli F, Rossi M, D'Alessandra Y, De Simone M, Lopardo T, Haupt Y, et al. MDM2 and Fbw7 cooperate to induce p63 protein degradation following DNA damage and cell differentiation. J Cell Sci. 2010 Jul 15;123(Pt 14):2423–33.

150. Rossi M, De Laurenzi V, Munarriz E, Green DR, Liu Y-C, Vousden KH, et al. The ubiquitin-protein ligase Itch regulates p73 stability. EMBO J. 2005 Feb 23;24(4):836–48.

151. Rossi M, De Simone M, Pollice A, Santoro R, La Mantia G, Guerrini L, et al. Itch/AIP4 associates with and promotes p63 protein degradation. Cell Cycle Georget Tex. 2006 Aug;5(16):1816–22.

152. Rossi M, Aqeilan RI, Neale M, Candi E, Salomoni P, Knight RA, et al. The E3 ubiquitin ligase Itch controls the protein stability of p63. Proc Natl Acad Sci U S A. 2006 Aug 22;103(34):12753–8.

153. Lenz W. A short history of thalidomide embryopathy. Teratology. 1988 Sep;38(3):203–15.

154. Knobloch J, Rüther U. Shedding light on an old mystery: thalidomide suppresses survival pathways to induce limb defects. Cell Cycle Georget Tex. 2008 May 1;7(9):1121–7.

155. Franks ME, Macpherson GR, Figg WD. Thalidomide. Lancet Lond Engl. 2004 May 29;363(9423):1802–11.

156. McBride WG. Thalidomide embryopathy. Teratology. 1977 Aug;16(1):79–82.

157. Vargesson N. Thalidomide-induced limb defects: resolving a 50-year-old puzzle. BioEssays News Rev Mol Cell Dev Biol. 2009 Dec;31(12):1327–36.

158. Bartlett JB, Dredge K, Dalgleish AG. The evolution of thalidomide and its IMiD derivatives as anticancer agents. Nat Rev Cancer. 2004 Apr;4(4):314–22.

159. Melchert M, List A. The thalidomide saga. Int J Biochem Cell Biol. 2007;39(7-8):1489–99.

160. Sheskin J. THALIDOMIDE IN THE TREATMENT OF LEPRA REACTIONS. Clin Pharmacol Ther. 1965 Jun;6:303–6.

161. Gutiérrez-Rodríguez O. Thalidomide. A promising new treatment for rheumatoid arthritis. Arthritis Rheum. 1984 Oct;27(10):1118–21.

162. Hamza MH. Treatment of Behçet's disease with thalidomide. Clin Rheumatol. 1986 Sep;5(3):365–71.

163. McCarthy DM, Kanfer EJ, Barrett AJ. Thalidomide for the therapy of graft-versus-host disease following allogeneic bone marrow transplantation. Biomed Pharmacother Biomed Pharmacothérapie. 1989;43(9):693–7.

164. Vogelsang GB, Farmer ER, Hess AD, Altamonte V, Beschorner WE, Jabs DA, et al. Thalidomide for the treatment of chronic graft-versus-host disease. N Engl J Med. 1992 Apr 16;326(16):1055–8.

165. Atra E, Sato EI. Treatment of the cutaneous lesions of systemic lupus erythematosus with thalidomide. Clin Exp Rheumatol. 1993 Oct;11(5):487–93.

166. Moreira AL, Sampaio EP, Zmuidzinas A, Frindt P, Smith KA, Kaplan G. Thalidomide exerts its inhibitory action on tumor necrosis factor alpha by enhancing mRNA degradation. J Exp Med. 1993 Jun 1;177(6):1675–80.

167. Makonkawkeyoon S, Limson-Pobre RN, Moreira AL, Schauf V, Kaplan G. Thalidomide inhibits the replication of human immunodeficiency virus type 1. Proc Natl Acad Sci U S A. 1993 Jul 1;90(13):5974–8.

168. Sampaio EP, Sarno EN, Galilly R, Cohn ZA, Kaplan G. Thalidomide selectively inhibits tumor necrosis factor alpha production by stimulated human monocytes. J Exp Med. 1991 Mar 1;173(3):699–703.

169. Haslett PA, Corral LG, Albert M, Kaplan G. Thalidomide costimulates primary human T lymphocytes, preferentially inducing proliferation, cytokine production, and cytotoxic responses in the CD8+ subset. J Exp Med. 1998 Jun 1;187(11):1885–92.

170. D'Amato RJ, Loughnan MS, Flynn E, Folkman J. Thalidomide is an inhibitor of angiogenesis. Proc Natl Acad Sci U S A. 1994 Apr 26;91(9):4082–5.

171. Lentzsch S, LeBlanc R, Podar K, Davies F, Lin B, Hideshima T, et al. Immunomodulatory analogs of thalidomide inhibit growth of Hs Sultan cells and angiogenesis in vivo. Leukemia. 2003 Jan;17(1):41–4.

172. Dredge K, Marriott JB, Macdonald CD, Man H-W, Chen R, Muller GW, et al. Novel thalidomide analogues display anti-angiogenic activity independently of immunomodulatory effects. Br J Cancer. 2002 Nov 4;87(10):1166–72.

173. Singhal S, Mehta J, Desikan R, Ayers D, Roberson P, Eddlemon P, et al. Antitumor activity of thalidomide in refractory multiple myeloma. N Engl J Med. 1999 Nov 18;341(21):1565–71.

174. Zeldis JB, Williams BA, Thomas SD, Elsayed ME. S.T.E.P.S.: a comprehensive program for controlling and monitoring access to thalidomide. Clin Ther. 1999 Feb;21(2):319–30.

175. Castilla EE, Ashton-Prolla P, Barreda-Mejia E, Brunoni D, Cavalcanti DP, Correa-Neto J, et al. Thalidomide, a current teratogen in South America. Teratology. 1996 Dec;54(6):273–7.

176. Schuler-Faccini L, Soares RCF, de Sousa ACM, Maximino C, Luna E, Schwartz IVD, et al. New cases of thalidomide embryopathy in Brazil. Birt Defects Res A Clin Mol Teratol. 2007 Sep;79(9):671–2.

177. Miller MT, Strömland K. Teratogen update: thalidomide: a review, with a focus on ocular findings and new potential uses. Teratology. 1999 Nov;60(5):306–21.

178. Mellin GW, Katzenstein M. The saga of thalidomide. Neuropathy to embryopathy, with case reports of congenital anomalies. N Engl J Med. 1962 Dec 6;267:1184–92 contd.

179. Spouge D, Baird PA. Imperforate anus in 700,000 consecutive liveborn infants. Am J Med Genet Suppl. 1986;2:151–61.

180. Lenz W, Knapp K. [Thalidomide embryopathy]. Dtsch Med Wochenschr 1946. 1962 Jun 15;87:1232–42.

181. Eriksson T, Björkman S, Roth B, Höglund P. Intravenous formulations of the enantiomers of thalidomide: pharmacokinetic and initial pharmacodynamic characterization in man. J Pharm Pharmacol. 2000 Jul;52(7):807–17.

182. Braun AG, Harding FA, Weinreb SL. Teratogen metabolism: thalidomide activation is mediated by cytochrome P-450. Toxicol Appl Pharmacol. 1986 Jan;82(1):175–9.

183. Ando Y, Fuse E, Figg WD. Thalidomide metabolism by the CYP2C subfamily. Clin Cancer Res Off J Am Assoc Cancer Res. 2002 Jun;8(6):1964–73.

184. Field HA, Dong PDS, Beis D, Stainier DYR. Formation of the digestive system in zebrafish. II. Pancreas morphogenesis. Dev Biol. 2003 Sep 1;261(1):197–208.

185. Therapontos C, Erskine L, Gardner ER, Figg WD, Vargesson N. Thalidomide induces limb defects by preventing angiogenic outgrowth during early limb formation. Proc Natl Acad Sci U S A. 2009 May 26;106(21):8573–8.

186. Ito T, Ando H, Suzuki T, Ogura T, Hotta K, Imamura Y, et al. Identification of a primary target of thalidomide teratogenicity. Science. 2010 Mar 12;327(5971):1345–50.

187. Hansen JM, Harris C. A novel hypothesis for thalidomide-induced limb teratogenesis: redox misregulation of the NF-kappaB pathway. Antioxid Redox Signal. 2004 Feb;6(1):1–14.

188. Stephens TD, Fillmore BJ. Hypothesis: thalidomide embryopathy-proposed mechanism of action. Teratology. 2000 Mar;61(3):189–95.

189. Stephens TD, Bunde CJ, Fillmore BJ. Mechanism of action in thalidomide teratogenesis. Biochem Pharmacol. 2000 Jun 15;59(12):1489–99.

190. Stephens TD. Proposed mechanisms of action in thalidomide embryopathy. Teratology. 1988 Sep;38(3):229–39.

191. Parman T, Wiley MJ, Wells PG. Free radical-mediated oxidative DNA damage in the mechanism of thalidomide teratogenicity. Nat Med. 1999 May;5(5):582–5.

192. Ng SSW, Gütschow M, Weiss M, Hauschildt S, Teubert U, Hecker TK, et al. Antiangiogenic activity of N-substituted and tetrafluorinated thalidomide analogues. Cancer Res. 2003 Jun 15;63(12):3189–94.

193. Ito T, Ando H, Handa H. Teratogenic effects of thalidomide: molecular mechanisms. Cell Mol Life Sci CMLS. 2011 May;68(9):1569–79.

194. Hansen JM, Gong S-G, Philbert M, Harris C. Misregulation of gene expression in the redox-sensitive NF-kappab-dependent limb outgrowth pathway by thalidomide. Dev Dyn Off Publ Am Assoc Anat. 2002 Oct;225(2):186–94.

195. Knobloch J, Shaughnessy JD, Rüther U. Thalidomide induces limb deformities by perturbing the Bmp/Dkk1/Wnt signaling pathway. FASEB J Off Publ Fed Am Soc Exp Biol. 2007 May;21(7):1410–21.

196. Leslie NR, Downes CP. PTEN function: how normal cells control it and tumour cells lose it. Biochem J. 2004 Aug 15;382(Pt 1):1–11.

197. Knobloch J, Schmitz I, Götz K, Schulze-Osthoff K, Rüther U. Thalidomide induces limb anomalies by PTEN stabilization, Akt suppression, and stimulation of caspase-dependent cell death. Mol Cell Biol. 2008 Jan;28(2):529–38.

198. Scherz PJ, Harfe BD, McMahon AP, Tabin CJ. The limb bud Shh-Fgf feedback loop is terminated by expansion of former ZPA cells. Science. 2004 Jul 16;305(5682):396–9.

199. Pajni-Underwood S, Wilson CP, Elder C, Mishina Y, Lewandoski M. BMP signals control limb bud interdigital programmed cell death by regulating FGF signaling. Dev Camb Engl. 2007 Jun;134(12):2359–68.

200. Grotewold L, Rüther U. The Wnt antagonist Dickkopf-1 is regulated by Bmp signaling and c-Jun and modulates programmed cell death. EMBO J. 2002 Mar 1;21(5):966–75.

201. Beurel E, Jope RS. The paradoxical pro- and anti-apoptotic actions of GSK3 in the intrinsic and extrinsic apoptosis signaling pathways. Prog Neurobiol. 2006 Jul;79(4):173–89.

202. Moon AM, Capecchi MR. Fgf8 is required for outgrowth and patterning of the limbs. Nat Genet. 2000 Dec;26(4):455–9.

203. Wells PG, Winn LM. Biochemical toxicology of chemical teratogenesis. Crit Rev Biochem Mol Biol. 1996 Feb;31(1):1–40.

204. Ohuchi H, Nakagawa T, Yamamoto A, Araga A, Ohata T, Ishimaru Y, et al. The mesenchymal factor, FGF10, initiates and maintains the outgrowth of the chick limb bud through interaction with FGF8, an apical ectodermal factor. Dev Camb Engl. 1997 Jun;124(11):2235–44.

205. Higgins JJ, Rosen DR, Loveless JM, Clyman JC, Grau MJ. A gene for nonsyndromic mental retardation maps to chromosome 3p25-pter. Neurology. 2000 Aug 8;55(3):335–40.

206. Higgins JJ, Pucilowska J, Lombardi RQ, Rooney JP. A mutation in a novel ATP-dependent Lon protease gene in a kindred with mild mental retardation. Neurology. 2004 Nov 23;63(10):1927–31.

207. Aizawa M, Abe Y, Ito T, Handa H, Nawa H. mRNA distribution of the thalidomide binding protein cereblon in adult mouse brain. Neurosci Res. 2011 Apr;69(4):343–7.

208. Hohberger B, Enz R. Cereblon is expressed in the retina and binds to voltage-gated chloride channels. FEBS Lett. 2009 Feb 18;583(4):633–7.

209. Jo S, Lee K-H, Song S, Jung Y-K, Park C-S. Identification and functional characterization of cereblon as a binding protein for large-conductance calcium-activated potassium channel in rat brain. J Neurochem. 2005 Sep;94(5):1212–24.

210. Xin W, Xiaohua N, Peilin C, Xin C, Yaqiong S, Qihan W. Primary function analysis of human mental retardation related gene CRBN. Mol Biol Rep. 2008 Jun;35(2):251–6.

211. Higgins JJ, Tal AL, Sun X, Hauck SCR, Hao J, Kosofosky BE, et al. Temporal and spatial mouse brain expression of cereblon, an ionic channel regulator involved in human intelligence. J Neurogenet. 2010 Mar;24(1):18–26.

212. Lee KM, Jo S, Kim H, Lee J, Park C-S. Functional modulation of AMP-activated protein kinase by cereblon. Biochim Biophys Acta. 2011 Mar;1813(3):448–55.

213. Groisman R, Kuraoka I, Chevallier O, Gaye N, Magnaldo T, Tanaka K, et al. CSA-dependent degradation of CSB by the ubiquitin-proteasome pathway establishes a link between complementation factors of the Cockayne syndrome. Genes Dev. 2006 Jun 1;20(11):1429–34.

214. Wang H, Zhai L, Xu J, Joo H-Y, Jackson S, Erdjument-Bromage H, et al. Histone H3 and H4 ubiquitylation by the CUL4-DDB-ROC1 ubiquitin ligase facilitates cellular response to DNA damage. Mol Cell. 2006 May 5;22(3):383–94.

215. Kapetanaki MG, Guerrero-Santoro J, Bisi DC, Hsieh CL, Rapić-Otrin V, Levine AS. The DDB1-CUL4ADDB2 ubiquitin ligase is deficient in xeroderma pigmentosum group E and targets histone H2A at UV-damaged DNA sites. Proc Natl Acad Sci U S A. 2006 Feb 21;103(8):2588–93.

216. Groisman R, Polanowska J, Kuraoka I, Sawada J, Saijo M, Drapkin R, et al. The ubiquitin ligase activity in the DDB2 and CSA complexes is differentially regulated by the COP9 signalosome in response to DNA damage. Cell. 2003 May 2;113(3):357–67.

217. Nag A, Bondar T, Shiv S, Raychaudhuri P. The xeroderma pigmentosum group E gene product DDB2 is a specific target of cullin 4A in mammalian cells. Mol Cell Biol. 2001 Oct;21(20):6738–47.

218. Chen X, Zhang Y, Douglas L, Zhou P. UV-damaged DNA-binding proteins are targets of CUL-4A-mediated ubiquitination and degradation. J Biol Chem. 2001 Dec 21;276(51):48175–82.

219. Sugasawa K, Okuda Y, Saijo M, Nishi R, Matsuda N, Chu G, et al. UV-induced ubiquitylation of XPC protein mediated by UV-DDB-ubiquitin ligase complex. Cell. 2005 May 6;121(3):387–400.

220. Liu C, Powell KA, Mundt K, Wu L, Carr AM, Caspari T. Cop9/signalosome subunits and Pcu4 regulate ribonucleotide reductase by both checkpoint-dependent and -independent mechanisms. Genes Dev. 2003 May 1;17(9):1130–40.

221. Bondar T, Ponomarev A, Raychaudhuri P. Ddb1 is required for the proteolysis of the Schizosaccharomyces pombe replication inhibitor Spd1 during S phase and after DNA damage. J Biol Chem. 2004 Mar 12;279(11):9937–43.

222. Higa LAA, Mihaylov IS, Banks DP, Zheng J, Zhang H. Radiation-mediated proteolysis of CDT1 by CUL4-ROC1 and CSN complexes constitutes a new checkpoint. Nat Cell Biol. 2003 Nov;5(11):1008–15.

223. Hu J, McCall CM, Ohta T, Xiong Y. Targeted ubiquitination of CDT1 by the DDB1-CUL4A-ROC1 ligase in response to DNA damage. Nat Cell Biol. 2004 Oct;6(10):1003–9.

224. Wertz IE, O'Rourke KM, Zhang Z, Dornan D, Arnott D, Deshaies RJ, et al. Human De-etiolated-1 regulates c-Jun by assembling a CUL4A ubiquitin ligase. Science. 2004 Feb 27;303(5662):1371–4.

225. Brent RL. DRUG TESTING IN ANIMALS FOR TERATOGENIC EFFECTS. THALIDOMIDE IN THE PREGNANT RAT. J Pediatr. 1964 May;64:762–70.

226. Kenyon BM, Browne F, D'Amato RJ. Effects of thalidomide and related metabolites in a mouse corneal model of neovascularization. Exp Eye Res. 1997 Jun;64(6):971–8.

227. Fratta ID, Sigg EB, Maiorana K. TERATOGENIC EFFECTS OF THALIDOMIDE IN RABBITS, RATS, HAMSTERS, AND MICE. Toxicol Appl Pharmacol. 1965 Mar;7:268–86.

228. Chung F, Lu J, Palmer BD, Kestell P, Browett P, Baguley BC, et al. Thalidomide pharmacokinetics and metabolite formation in mice, rabbits, and multiple myeloma patients. Clin Cancer Res Off J Am Assoc Cancer Res. 2004 Sep 1;10(17):5949–56.

229. Knobloch J, Reimann K, Klotz L-O, Rüther U. Thalidomide resistance is based on the capacity of the glutathione-dependent antioxidant defense. Mol Pharm. 2008 Dec;5(6):1138–44.

230. Janer G, Verhoef A, Gilsing HD, Piersma AH. Use of the rat postimplantation embryo culture to assess the embryotoxic potency within a chemical category and to identify toxic metabolites. Toxicol Vitro Int J Publ Assoc BIBRA. 2008 Oct;22(7):1797–805.

231. Shortt J, Hsu AK, Johnstone RW. Thalidomide-analogue biology: immunological, molecular and epigenetic targets in cancer therapy. Oncogene. 2013 Sep 5;32(36):4191–202.

232. Muller GW, Corral LG, Shire MG, Wang H, Moreira A, Kaplan G, et al. Structural modifications of thalidomide produce analogs with enhanced tumor necrosis factor inhibitory activity. J Med Chem. 1996 Aug 16;39(17):3238–40.

233. Muller GW, Chen R, Huang SY, Corral LG, Wong LM, Patterson RT, et al. Amino-substituted thalidomide analogs: potent inhibitors of TNF-alpha production. Bioorg Med Chem Lett. 1999 Jun 7;9(11):1625–30.

234. Zhu YX, Kortuem KM, Stewart AK. Molecular mechanism of action of immune-modulatory drugs thalidomide, lenalidomide and pomalidomide in multiple myeloma. Leuk Lymphoma. 2013 Apr;54(4):683–7.

235. Kyle RA, Rajkumar SV. Multiple myeloma. Blood. 2008 Mar 15;111(6):2962–72.

236. Schuster SR, Kortuem KM, Zhu YX, Braggio E, Shi C-X, Bruins LA, et al. The clinical significance of cereblon expression in multiple myeloma. Leuk Res. 2014 Jan;38(1):23–8.

237. Zhang L-H, Kosek J, Wang M, Heise C, Schafer PH, Chopra R. Lenalidomide efficacy in activated B-cell-like subtype diffuse large B-cell lymphoma is dependent upon IRF4 and cereblon expression. Br J Haematol. 2013 Feb;160(4):487–502.

238. Morgan B, Sun L, Avitahl N, Andrikopoulos K, Ikeda T, Gonzales E, et al. Aiolos, a lymphoid restricted transcription factor that interacts with Ikaros to regulate lymphocyte differentiation. EMBO J. 1997 Apr 15;16(8):2004–13.

239. Georgopoulos K, Bigby M, Wang JH, Molnar A, Wu P, Winandy S, et al. The Ikaros gene is required for the development of all lymphoid lineages. Cell. 1994 Oct 7;79(1):143–56.

240. Lu G, Middleton RE, Sun H, Naniong M, Ott CJ, Mitsiades CS, et al. The myeloma drug lenalidomide promotes the cereblon-dependent destruction of Ikaros proteins. Science. 2014 Jan 17;343(6168):305–9.

241. Krönke J, Udeshi ND, Narla A, Grauman P, Hurst SN, McConkey M, et al. Lenalidomide causes selective degradation of IKZF1 and IKZF3 in multiple myeloma cells. Science. 2014 Jan 17;343(6168):301–5.

242. Stewart AK. Medicine. How thalidomide works against cancer. Science. 2014 Jan 17;343(6168):256–7.

243. Tan X, Calderon-Villalobos LIA, Sharon M, Zheng C, Robinson CV, Estelle M, et al. Mechanism of auxin perception by the TIR1 ubiquitin ligase. Nature. 2007 Apr 5;446(7136):640–5.

244. Li T, Chen X, Garbutt KC, Zhou P, Zheng N. Structure of DDB1 in complex with a paramyxovirus V protein: viral hijack of a propeller cluster in ubiquitin ligase. Cell. 2006 Jan 13;124(1):105–17.

245. Fischer ES, Böhm K, Lydeard JR, Yang H, Stadler MB, Cavadini S, et al. Structure of the DDB1-CRBN E3 ubiquitin ligase in complex with thalidomide. Nature. 2014 Aug 7;512(7512):49–53.

246. van Bokhoven H, McKeon F. Mutations in the p53 homolog p63: allele-specific developmental syndromes in humans. Trends Mol Med. 2002 Mar;8(3):133–9.

247. Bid HK, Roberts RD, Cam M, Audino A, Kurmasheva RT, Lin J, et al. ΔNp63 promotes pediatric neuroblastoma and osteosarcoma by regulating tumor angiogenesis. Cancer Res. 2014 Jan 1;74(1):320–9.

248. Hibi K, Trink B, Patturajan M, Westra WH, Caballero OL, Hill DE, et al. AIS is an oncogene amplified in squamous cell carcinoma. Proc Natl Acad Sci U S A. 2000 May 9;97(10):5462–7.

249. Ianakiev P, Kilpatrick MW, Toudjarska I, Basel D, Beighton P, Tsipouras P. Split-hand/split-foot malformation is caused by mutations in the p63 gene on 3q27. Am J Hum Genet. 2000 Jul;67(1):59–66.

250. Gonfloni S, Di Tella L, Caldarola S, Cannata SM, Klinger FG, Di Bartolomeo C, et al. Inhibition of the c-Abl-TAp63 pathway protects mouse oocytes from chemotherapy-induced death. Nat Med. 2009 Oct;15(10):1179–85.

251. Pi-Roig A, Martin-Blanco E, Minguillon C. Distinct tissue-specific requirements for the zebrafish tbx5 genes during heart, retina and pectoral fin development. Open Biol. 2014;4:140014.

252. Parrie LE, Renfrew EM, Wal AV, Mueller RL, Garrity DM. Zebrafish tbx5 paralogs demonstrate independent essential requirements in cardiac and pectoral fin development. Dev Dyn Off Publ Am Assoc Anat. 2013 May;242(5):485–502.

253. Hernández-Vega A, Minguillón C. The Prx1 limb enhancers: targeted gene expression in developing zebrafish pectoral fins. Dev Dyn Off Publ Am Assoc Anat. 2011 Aug;240(8):1977–88.

Part II

HMG Advance Access published June 1, 2015

OXFORD

Human Molecular Genetics, 2015, 1–13

doi: 10.1093/hmg/ddv151
Original Article

ORIGINAL ARTICLE

FGF8, c-Abl and p300 participate in a pathway that controls stability and function of the ΔNp63α protein

Michela Restelli[1], Elisa Molinari[1], Barbara Marinari[2], Daniele Conte[3], Nerina Gnesutta[1], Antonio Costanzo[2], Giorgio Roberto Merlo[3] and Luisa Guerrini[1,*]

[1]Department of Biosciences, Università degli Studi di Milano, 20133 Milano, Italy, [2]Dermatology Unit, NESMOS Department, Università di Roma La Sapienza, I-00189 Rome, Italy and [3]Department of Molecular Biotechnologies and Health Sciences, Università di Torino, I-10126 Torino, Italy

*To whom correspondence should be addressed at: Luisa Guerrini, Department of Biosciences, Università degli Studi di Milano, Via Celoria 26, 20133 Milan, Italy. Tel: +39 0250315000; Fax: +39 0250315044; Email: luisa.guerrini@unimi.it

Abstract

The p63 transcription factor, homolog to the p53 tumor suppressor gene, plays a crucial role in epidermal and limb development, as its mutations are associated to human congenital syndromes characterized by skin, craniofacial and limb defects. While limb and skin-specific p63 transcriptional targets are being discovered, little is known of the post-translation modifications controlling ΔNp63α functions. Here we show that the p300 acetyl-transferase physically interacts *in vivo* with ΔNp63α and catalyzes its acetylation on lysine 193 (K193) inducing ΔNp63α stabilization and activating specific transcriptional functions. Furthermore we show that Fibroblast Growth Factor-8 (FGF8), a morphogenetic signaling molecule essential for embryonic limb development, increases the binding of ΔNp63α to the tyrosine kinase c-Abl as well as the levels of ΔNp63α acetylation. Notably, the natural mutant ΔNp63α-K193E, associated to the Split-Hand/Foot Malformation-IV syndrome, cannot be acetylated by this pathway. This mutant ΔNp63α protein displays promoter-specific loss of DNA binding activity and consequent altered expression of development-associated ΔNp63α target genes. Our results link FGF8, c-Abl and p300 in a regulatory pathway that controls ΔNp63α protein stability and transcriptional activity. Hence, limb malformation-causing p63 mutations, such as the K193E mutation, are likely to result in aberrant limb development via the combined action of altered protein stability and altered promoter occupancy.

Introduction

The p63 transcription factor, highly related to the p53 and p73 transcription factors, plays a central role during development of the embryonic ectoderm and derived structures. *p63* is expressed in the embryonic ectoderm and in the proliferating stem cells of the adult epidermis, breast and oral epithelium (1,2). Accordingly, *p63* null mice show lack of epidermis stratification which causes death at birth, absence of nails and hairs, sweat and mammary glands and severe defects in limb and craniofacial development (3,4).

The limb defects observed in $p63^{-/-}$ mice are highly reminiscent of ectrodactily found in patients affected by the Ectrodactily-Ectodermal Dysplasia-Cleft palate syndrome (EEC) or in non-syndromic Ectrodactily, also known as Split-Hand Foot Malformation (SHFM) type-IV. Ectrodactily is characterized by the absence of the central rays of the limbs, resulting in a deep

Received: February 25, 2015. **Revised and Accepted:** April 21, 2015

medial cleft, missing or hypoplastic central fingers and fusion of the remaining ones (5–8), and has been associated with developmental failure of the Apical Ectodermal Ridge (AER) a transitory pluri-stratified ectodermal region required for limb outgrowth, and for the expression of key signaling molecules (1,2,5–9).

p63 is at the center of a complex molecular network. However, its regulation and tissue distribution remain issues not fully understood. The *p63* gene encodes for at least ten protein isoforms, which differ in their amino and carboxy-terminal regions as a consequence of alternative transcription start site and alternative splicing, respectively (10,11), with ΔNp63α being the most expressed isoform in the embryonic ectoderm. All p63 isoforms share with p53 and p73 homology in the DNA binding and the oligomerization domains (12–15), and indeed p53 and p63 regulate a number of common transcriptional targets, in particular those related to cell-cycle control. However, p63-specific target genes are known that justify its specific role in ectoderm development and epidermis stratification, and also explain the specific set of human diseases associated with *p63* mutations (16–18).

Interestingly, while some mutations of the *p63* gene occurring in the DNA Binding Domain (DBD) coding sequence (such as the R279H mutation) are causative of the EEC syndrome, which comprises ectrodactyly and several other skin and craniofacial developmental defects, others (such as the K193E mutation) result in non-syndromic ectrodactyly (or SHFM-type IV), with little or no skin/craniofacial anomalies (7,8). The logical question that arises is: why the EEC- and the SHFM-associated mutations cause limb developmental malformations, while p63 mutations found in AEC patients (i.e. the L518F mutation), localized in the SAM domain of the ΔNp63α protein, do not affect limb development? One possibility is related to the ability of the peptidyl-prolyl isomerase Pin1 to negatively regulate ΔNp63α stability, and to the activity of the key limb morphogen Fibroblast Growth Factor-8 (FGF8) (19–22) to counter-act this function (23). Mutant p63 proteins are differentially sensitive to Pin1-induced degradation (23). However, the correlation between specific p63 mutations, their stability, transcriptional activity and the onset of limb developmental anomalies remains not fully resolved.

It is becoming increasingly evident that the distinct functions of wild-type and mutant p63 protein(s) might reside not only in their specific DNA binding activity but also in their post-translational modifications such as sumoylation, phosphorylation and ubiquitylation (24–27). These modifications modulate ΔNp63α half-life, the specificity and efficiency of protein–protein interactions and overall modulate the transcriptional activity of the protein. The elucidation of these 'upstream' regulatory events is required for a full comprehension of the molecular network centered on p63, to explain the genotype–phenotype correlations observed in patients affected by syndromes associated to p63 mutations.

p53 and/or p73 protein activity and stability are finely regulated by several post-translational modifications (28–30), among which acetylation seems to play a pivotal role in regulating their biological functions (29,31–33). Acetylation is a reversible modification, catalyzed by histone acetyl-transferases, of lysine residues of a target protein and its function in transcriptional activation is well accepted (34). p73 is acetylated by p300 on lysines located in the DNA binding and oligomerization domains in response to DNA damage (35); acetylation enhances p73 ability to bind and activate proapototic target genes (36). Furthermore, p73–p300 interaction requires the activity of Pin1 that induces p73 conformational changes upon phosphorylation by the tyrosine kinase c-Abl (37). Acetylation of p53 is enhanced in response to DNA damage and well correlates with p53 stabilization and activation: indeed, acetylation of p53 antagonizes the MDM2 ubiquitin-ligase activity that keeps p53 protein at low levels in normal conditions. Moreover, acetylation of p53 by p300 was found to promote its sequence-specific DNA binding (31–33,38).

All considered, we set forth to examine ΔNp63α acetylation in the context of naturally occurring ΔNp63α missense mutations associated to SHFM-IV: one such mutation causes lysine 193 substitution with glutamic acid (K193E) (7,8). We noted that lysine K164 in p53, acetylated by p300 (38), correspond to K193 in ΔNp63α. Thus we raised the hypothesis that wild-type ΔNp63α could be acetylated by p300 on K193, and that mutations of this residue could prevent this post-translational modification with important developmental consequences.

Our results are consistent with this hypothesis and, for the first time, we show that FGF8 signaling participates in a regulatory pathway promoting the physical interaction of ΔNp63α with c-Abl and p300, leading to stabilization and transcriptional activation of ΔNp63α.

Results

Δnp63α is acetylated and stabilized in cultured cells

In order to assess whether p63 could be acetylated in human cells, we treated the human keratinocytes HaCaT cell line, expressing endogenous ΔNp63α, with Valproic-Acid (VPA), which selectively inhibits class I deacetylases, or with Trichostatin-A (TSA) which inhibits class I and II deacetylases. VPA and TSA treatments resulted in an increase in ΔNp63α abundance (Fig. 1A). Similar effects of ΔNp63α accumulation were also obtained when ΔNp63α was ectopically overexpressed in U2OS cells, a human osteosarcoma cell line devoid of endogenous *p63* expression (Supplementary Material, Fig. S1). Then, we performed immunoprecipitation of endogenous ΔNp63α from total protein extracts of HaCaT cells treated with TSA. The level of ΔNp63α acetylation was detected using an antibody against acetylated lysines: we observed that ΔNp63α is found acetylated at a basal level, as previously reported (39), and that its acetylation increased upon TSA treatment (Fig. 1B). These results show that the ΔNp63α protein is acetylated in human cells and that the acetylation levels of ΔNp63α correlate with its accumulation in human cells following deacetyl-transferases inhibition.

The acetyl-transferase domain of p300 is required to induce ΔNp63α protein stabilization

Acetylation of p53 and p73 proteins is required for their stabilization and transcriptional activation in response to DNA damage (31–33,35–38) and the p300 acetyl-transferase is known to be involved in this process (29,35,36,38). To determine whether p300 could acetylate ΔNp63α, we silenced endogenous p300 in HaCaT cells by transfecting a p300-specific shRNA plasmid. Depletion of p300 was clearly detected and, concomitant with p300 reduction, a significant decrease of ΔNp63α was also observed (Fig. 2A). Conversely, when p300 protein levels were increased by transient overexpression in HaCaT or U2OS cells, ΔNp63α protein was stabilized in a dose-dependent manner (Fig. 2B and C). In contrast, a construct expressing a mutated variant of p300, with a mutation affecting the Histone Acetyl-Transferase domain (LY-RR) (36), failed to stabilize endogenous ΔNp63α in HaCaT cells (Fig. 2B). These data clearly indicate that p300 and its acetyl-transferase activity are required for ΔNp63α protein levels regulation.

Accordingly, when we overexpressed ΔNp63α with p300 in U2OS cells and treated the cells with the protein synthesis

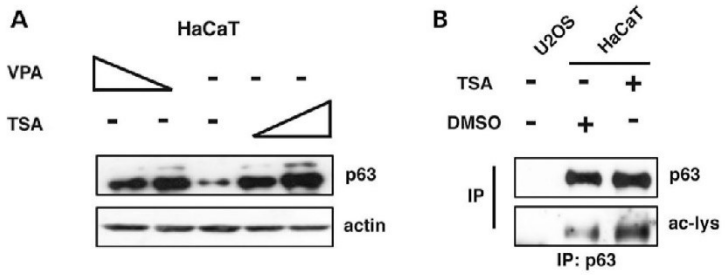

Figure 1. The ΔNp63α protein is acetylated in human keratynocytes. (**A**) Western Blot (WB) analysis of whole HaCaT cell extracts treated with increasing amounts of TSA (5 ng/ml and 10 ng/ml) for 5 h or VPA (0.5 mM and 1 mM) for 3 h. (**B**) Whole cell extracts from HaCaT cells treated with 5 ng/ml of Trichostatin (TSA) for 5 h were analyzed by immunoprecipitation of endogenous ΔNp63α with an anti-p63 antibody followed by WB analysis with an anti-acetylated lysines. U2OS cells, not expressing p63, were used as negative control.

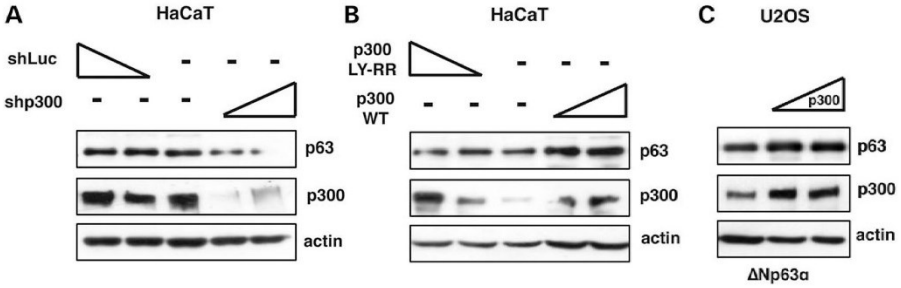

Figure 2. The acetyl-transferase domain of p300 is required to induce ΔNp63α protein stabilization. (**A**) WB analysis of whole HaCaT cell extracts transiently transfected with increasing amounts (20 ng and 40 ng) of shp300 or shLuc expression vectors (**B**) WB analysis of HaCaT whole cell extracts transiently co-transfected with equal amount of ΔNp63α expression vectors (30 ng) and increasing amounts of p300 encoding plasmids (p300 (WT) or p300-LY-RR, mutated in the HAT domain (10 and 20 ng). (**C**) WB analysis of U2OS whole cell extracts transiently co-transfected with equal amount of ΔNp63α expression vectors (30 ng) and increasing amounts of p300 expression vectors (10 and 20 ng).

inhibitor Cycloheximide (CHX), we observed an increase of ΔNp63α protein half-life (Fig. 3D). We also determined the effect of p300 silencing on ΔNp63α protein half-life in HaCaT cells, by transfecting p300-specific shRNA plasmid and treated the cells with CHX. As shown in Supplementary Material, Figure S2, the levels of ΔNp63α protein decreased upon p300 silencing with only a modest decrease of ΔNp63α half-life upon CHX addition.

P300 interacts with ΔNp63α in human cells and catalyzes *in vitro* acetylation of lysine K193

To assess whether the observed stabilization of ΔNp63α by p300 was due to a direct interaction between the two proteins, we performed co-immunoprecipitation experiment in U2OS cells. As shown in Figure 3A, ΔNp63α was found in p300 immunocomplexes, showing that the two proteins can associate in human cells.

Lysine K164 of the p53 protein, conserved in p63 and p73, is acetylated by p300 (38). In the ΔNp63α protein this residue corresponds to K193 (Supplementary Material, Fig. S3), mutated in patients affected by SHFM-IV (i.e. K193E) (7,8). We set forth to establish whether K193 was acetylated by p300, by carrying out *in vitro* acetylation assays using recombinant p300 protein and a set of synthetic p63 peptides centered on K193. A p53 synthetic peptide containing lysine K164 known to be acetylated by p300 (38) was used as a positive control. The results show that the p63 peptide centered on K193 was acetylated *in vitro* and the levels of acetylation are similar to those obtained with the p53 peptide (Fig. 3B).

In the same assay we also analyzed mutant p63 peptides carrying K193 and K194 substitutions into arginine, either one at a time or simultaneously, to determine which one (or both) could be target of the p300 acetyl-transferase activity. As shown in Figure 3B, p300 acetylates lysine K193: indeed the levels of acetylation of the p63-K193R mutant were reduced. However we cannot exclude that also K194 could be acetylated by p300 since we observed a modest decrease in the level of acetylation of the p63-K194R mutant peptide compared with the wild-type peptide. Finally, p300 overexpression in U2OS cells did not induce stabilization of the ΔNp63α-K193R and of the natural ΔNp63α-K193E mutant, while the ΔNp63α protein was stabilized (Fig. 3C), indicating that the integrity of K193 is required to induce p300-dependent stabilization of ΔNp63α. Moreover, in contrast to what observed for the wild-type ΔNp63α, the half-life of the ΔNp63α-K193R mutant was not enhanced upon p300 overexpression in U2OS cells (Fig. 3D).

FGF8 positively regulates ΔNp63α protein stability inducing its interaction with c-Abl and promoting ΔNp63α acetylation

During embryonic development, FGF8 acts as a signaling peptide essential for growth, morphogenesis and patterning of the limb buds (9,19–22). We have recently shown that FGF8 exerts a

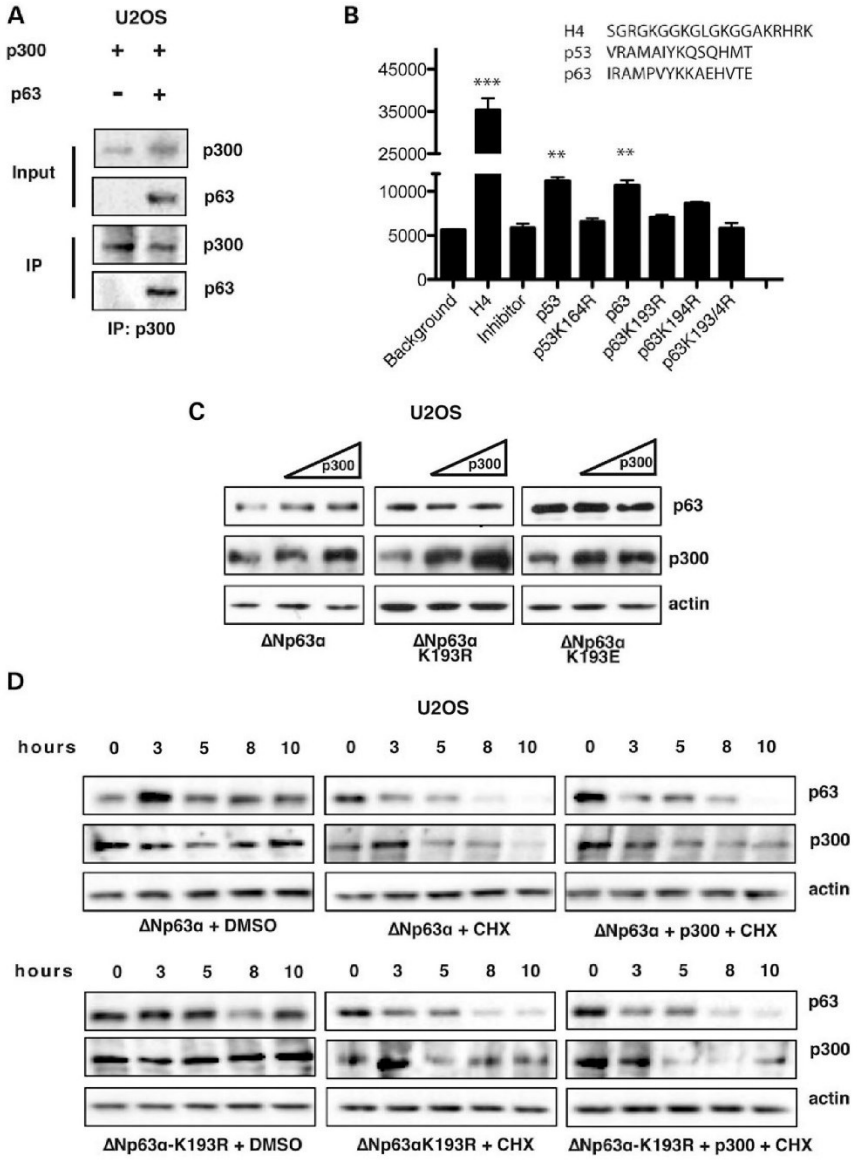

Figure 3. p300 interacts with ΔNp63α in human cells and catalizes *in vitro* acetylation of lysine K193. (**A**) U2OS whole cell extracts transiently co-transfected with ΔNp63α and p300 were analyzed by immunoprecipitation with an anti-p300 antibody followed by WB analysis with an anti-p63 antibody. U2OS cells, not transfected with p63 encoding plasmid were used as negative control. (**B**) *In vitro* acetylation assay performed according to the HAT assay kit protocol (Active Motif) with an H4 peptide and p53 peptides as positive controls, H4 plus anacardic acid 15 μM (an inhibitor of acetyl-transferase activity used as a negative control) and p63 peptides (peptide sequences are indicated). (**C**) WB analysis of U2OS whole cell extracts transiently co-transfected with ΔNp63α, ΔNp63α-K193E, ΔNp63α-K193R expression vectors (30 ng) and increasing amounts of p300 encoding plasmid (10 and 20 ng). (**D**) WB analysis of U2OS whole cell extracts transiently co-transfected with ΔNp63α, ΔNp63α-K193R and p300 expression vectors (30 ng and 5 ng respectively). 24 h after transfection protein half-life was measured by treating cells with 10 μg/ml of CHX.

stabilizing function on the ΔNp63α protein, by preventing its interaction with Pin1 that targets ΔNp63α protein for proteasomal degradation (23). We raised the hypothesis that FGF8 may stabilize the ΔNp63α protein, via p300-mediated acetylation of ΔNp63α, and that the limb malformation-associated p63 K193E mutation may pose an obstacle to this regulation.

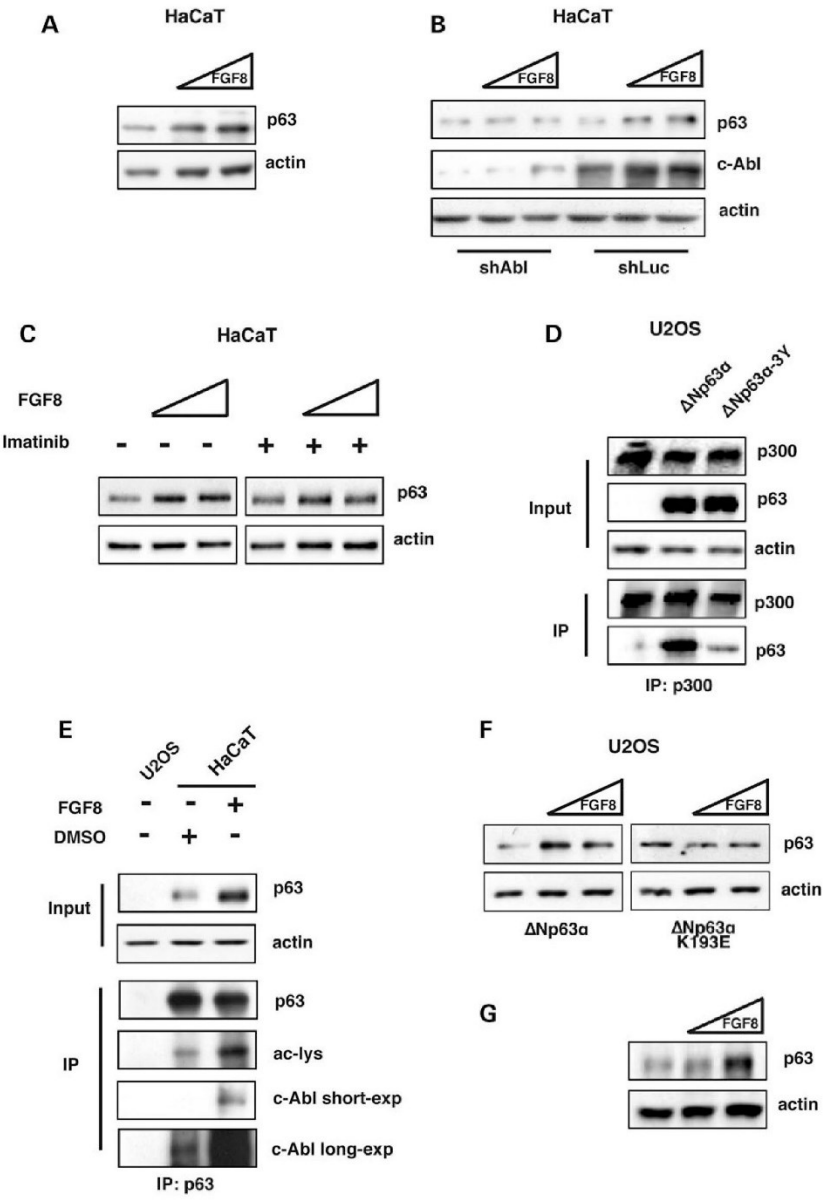

Figure 4. FGF8 positively regulates ΔNp63*α* protein stability inducing its interaction with c-Abl and promoting ΔNp63*α* acetylation. (**A**) WB analysis of HaCaT whole cell extracts treated with increasing amounts of FGF8 (0.5 ng/ml and 1 ng/ml) for 3 h. (**B**) WB analysis of HaCaT whole cell extracts stably transfected with an shRNA against c-Abl or shLuc plasmids, treated with increasing amounts of FGF8 (0.5 ng/ml and 1 ng/ml) for 3 h. (**C**) WB analysis of HaCaT cells treated with increasing amounts of FGF8 (0.5 ng/ml and 1 ng/ml) or pre-treated for 30 min with Imatinib (10 μM) followed by FGF8 treatment for 3 h. (**D**) U2OS whole cell extracts transiently co-transfected with either ΔNp63*α* or ΔNp63*α*-3Y (10 μg) and p300 (5 μg), and then analyzed by immunoprecipitation with an anti-p300 antibody followed by WB analysis with an anti-p63 antibody. (**E**) HaCaT whole cell extracts treated with FGF8 (0.5 ng/ml) or DMSO for 3 h were analyzed by immunoprecipitation with anti-p63 antibodies followed by WB analysis with the indicated antibodies. U2OS cells, not expressing p63 were used as negative control. (**F**) WB analysis of U2OS whole cell extracts transiently transfected with ΔNp63*α* or ΔNp63*α*-K193E encoding plasmids (30 ng). 24 h after transfection U2OS cells were treated with increasing amounts of FGF8 for 2 h (0.5 ng/ml and 1 ng/ml). (**G**) WB analysis of total proteins extracts from forelimbs isolated from wild-type mouse embryos at E11.5, cultured whole-mount for 48 h in the absence or presence of recombinant FGF8 (0.5 μg/ml and 1 μg/ml).

First, we treated HaCaT cells with increasing amounts of soluble FGF8 that resulted in efficient ΔNp63α protein stabilization as expected (Fig. 4A).

One of the down-stream effector of FGFs is the tyrosine kinase c-Abl: indeed, c-Abl is activated by FGF2 treatment (40). c-Abl is also a key regulator of the p53 family members (29,37,41–45). To verify whether c-Abl was required to induce the observed FGF8-mediated stabilization of ΔNp63α, we stably silenced endogenous c-Abl expression in HaCaT cells and then treated these cells with either FGF8 or FGF2. c-Abl silencing abolished ΔNp63α stabilization induced by either FGF8 (Fig. 4B) or FGF2 (data not shown), suggesting that FGFs stabilization of ΔNp63α requires the presence of the c-Abl protein. In order to verify whether the tyrosine kinase activity of c-Abl was required for the FGF8-mediated stabilization of ΔNp63α, we treated HaCaT cells with Imatinib, an inhibitor of c-Abl tyrosine kinase activity. As shown in Figure 4C, FGF8-mediated stabilization of ΔNp63α was prevented by Imatinib pre-treatment. Furthermore, the ΔNp63α-3Y mutant protein, with the three tyrosines known to be phopshorylated by c-Abl mutated into phenylalanin (44,45), was not stabilized by FGF8 treatment (Supplementary Material, Fig. S4).

To verify whether c-Abl was promoting the interaction between ΔNp63α and p300, we performed co-immunoprecipitation experiments of p300 with wild-type ΔNp63α or with the ΔNp63α-3Y mutant. As shown in Figure 4D, the ΔNp63α-3Y mutant displayed a drastically reduced interaction with p300 compared with wild-type ΔNp63α. Furthermore p300 overexpression did not modulate ΔNp63α-3Y protein levels (Supplementary Material, Fig. S5).

In order to verify whether FGF8, c-Abl and p300 were linked together in the same regulatory pathway, promoting ΔNp63α stabilization, we treated HaCaT cells with FGF8 and performed co-immunoprecipitation of ΔNp63α; we observed a great increase in ΔNp63α-c-Abl interaction and in the levels of ΔNp63α acetylation upon FGF8 treatment (Fig. 4E). Interestingly, we found that the signaling cascade activated by FGF8 was not active on the SHFM-IV-causing ΔNp63α-K193E mutant protein. Indeed as shown in Figure 4F, FGF8 treatment in U2OS cells did not induce ΔNp63α-K193E stabilization, clearly resembling the results obtained by p300 overexpression on this mutant (Fig. 3C). All these results indicate that c-Abl and p300 are linked together in a cascade, activated by FGF8, regulating ΔNp63α protein stability.

To verify if FGF8 and c-Abl are required to modulate not only ΔNp63α protein stability, but also its transcriptional activity, we performed luciferase assay in U2OS cells transiently transfected with the *DLX5* promoter, a known ΔNp63α transcriptional target in the AER cells of developing limbs (46). FGF8, Imatinib and Imatinib followed by FGF8 treatment were used. Interestingly, when we inhibited c-Abl kinase activity, ΔNp63α was unable to transactivate the *DLX5* promoter even in the presence of FGF8 treatment (Supplementary Material, Fig. S6). These data suggest that the c-Abl kinase activity was required to transduce the signal induced by FGF8 leading to ΔNp63α stabilization and transcriptional activation. Similar results were also obtained with the EGFR promoter (18, data not shown).

Finally, in order to assess if such mechanism could be relevant *in vivo*, e.g. the developing limb bud, we adopted an *ex vivo* method by culturing the embryonic limb buds obtained from wild-type mouse embryos at the age E10.5, and maintained whole-mount for 48 h (47). During the culture time, purified recombinant FGF8 was added to the medium at physiological doses, then the tissues were collected and analyzed by Western blot analyses for the abundance of ΔNp63α protein. Compared with untreated limbs, addition of FGF8 resulted in a clear accumulation of the ΔNp63α protein (Fig. 4G), indicating that FGF8 efficiently stabilizes, and most likely activates, ΔNp63α in the context of the limb embryonic tissue.

The K193E mutation alters ΔNp63α transcriptional activity in a promoter-specific manner

In order to verify whether p300 could act as a ΔNp63α co-activator we performed luciferase-reporter assays with the *DLX5* promoter. Interestingly, we observed that p300 co-transfection greatly enhanced the transcriptional activity of ΔNp63α, while the transcriptional activity of the ΔNp63α-K193E mutant could not be enhanced by p300 overexpression (Fig. 5A).

ΔNp63α transcriptional activity was impaired by the K193E mutation also on other ΔNp63α target genes involved in development, *EGFR* and *DLX6* (Fig. 5B) (18,46). We then examined whether the K193E mutation could alter ΔNp63α transcriptional activity on genes not directly required for limb development; for this aim we used the *p57KIP2* and *ADA* promoters, known to be involved in p63-dependent cell-cycle regulation (48,49). Interestingly, we found that the ΔNp63α-K193E mutant behaved as the wild-type ΔNp63α protein on both promoters (Fig. 5C), suggesting that the K193E mutation selectively alters ΔNp63α transcriptional activity.

To further characterize the transcriptional activity of the ΔNp63α-K193E mutant, we performed real-time, quantitative qPCR analyses in U2OS cells stably transfected with either the wild-type ΔNp63α or the ΔNp63α-K193E expression vectors. Interestingly, we confirmed that the ΔNp63α-K193E mutant overexpression results in altered expression of ΔNp63α target genes involved in development and apoptosis such as *PERP*, *CASP10*, *EGFR* (18,50) while it behaves like the wild-type ΔNp63α on *p53* (Fig. 6A). Taken together, these data clearly show that the K193E mutation alters the transcriptional activity of ΔNp63α in a gene-specific manner.

Next we tested whether the ΔNp63α-K193E mutant displayed altered DNA binding ability by Chromatin Immunoprecipitation (ChIP) assay of U2OS cells stably transfected with the wild-type ΔNp63α or with the ΔNp63α-K193E expressing vectors; the proteins were correctly expressed (Fig. 6B). We observed that the ΔNp63α-K193E mutant was not efficiently recruited on the Responsive Elelments (RE) of genes relevant for developmental and apoptotic processes (*PERP*, *CASP10* and *EGFR*) while it was normally recruited on RE of the *p53* gene, involved in cell cycle regulation (Fig. 6C).

In conclusion, the K193E mutation alters the ability of ΔNp63α to bind specific RE sequences resulting in altered transcriptional regulation of genes involved in the regulation of development and apoptotic processes.

Discussion

The p63 transcription factor is emerging as a master regulator of development and differentiation of ectoderm derived cells and tissues. In the last few years much attention has been paid to the analysis and identification of p63 transcriptional targets, their tissue and process specificity and how mutations in p63 affect its down-stream transcriptional properties (16–18,51,52). Clearly, this is only part of the full story. Indeed, more recently several p63 post-translational modifications have been recognized, acting either during response to DNA damage, differentiation or embryonic development (24–27). The full spectrum of these modifications, likely able to regulate stability and activity of the ΔNp63α protein, are not fully understood.

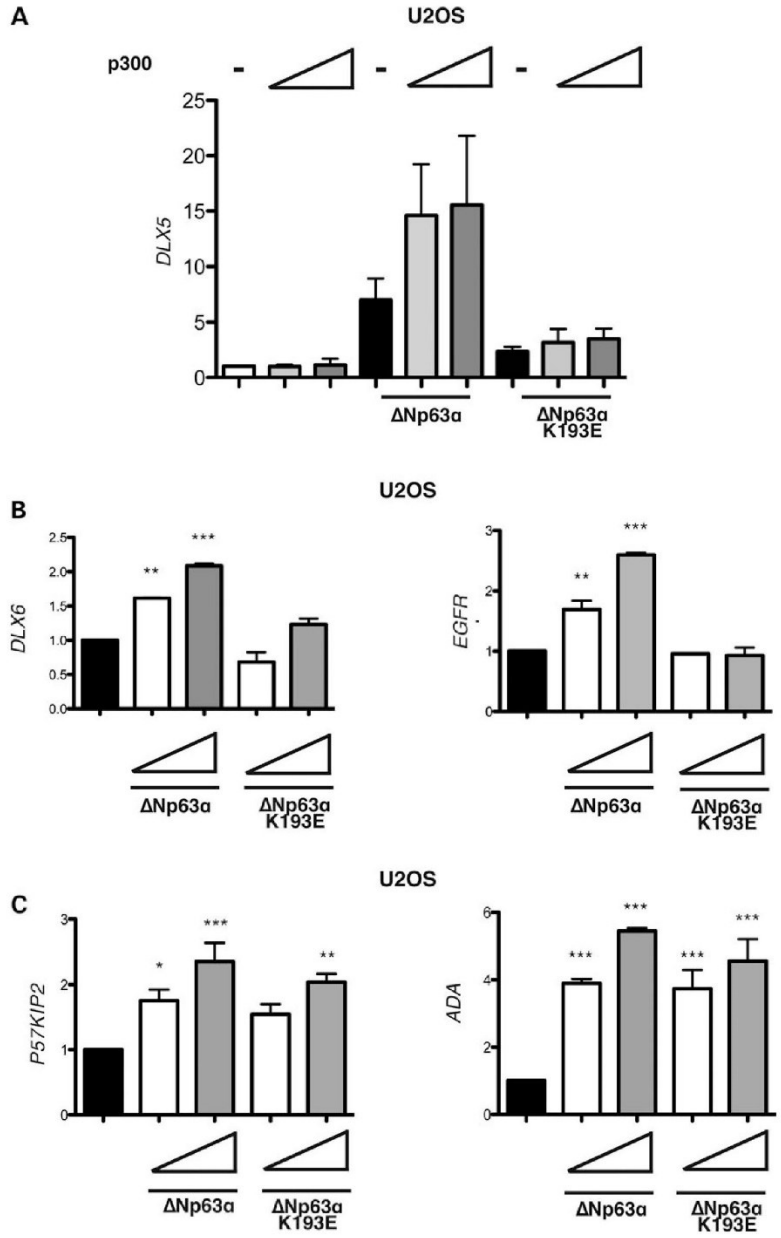

Figure 5. The K193E mutation alters ΔNp63α transcriptional activity in a promoter-specific manner. (**A**) Luciferase assay performed on U2OS cells transiently co-transfected with the −1200 bp *DLX5* promoter (200 ng) in the presence of ΔNp63α or ΔNp63α-K193E (50 ng) with increasing amounts of p300 (10 and 20 ng) expression vectors. Each histogram bar represents the mean of three indipendent transfection duplicates. Standard deviation are indicated. (**B**) Luciferase assay performed in U2OS cells transiently co-transfected with the *DLX6*, and *EGFR* reporter promoters (200 ng) in the presence of increasing amounts of ΔNp63α or ΔNp63α-K193E (50 and 100 ng) plasmids. (**C**) Luciferase assay performed on U2OS cells transiently co-transfected with the *p57kip2*, and ADA reporter promoters (200 ng) in the presence of increasing amounts of ΔNp63α or ΔNp63α-K193E (50 and 100 ng) plasmids. For (A–C) cells were lysed 24 h after transfection and luciferase activity was determined. The basal activity of the reporter plasmid was set to 1. Data are presented as fold activation/repression relative to the sample without effector. Each histogram bar represents the mean of three independent transfection duplicates. Standard deviations are indicated.

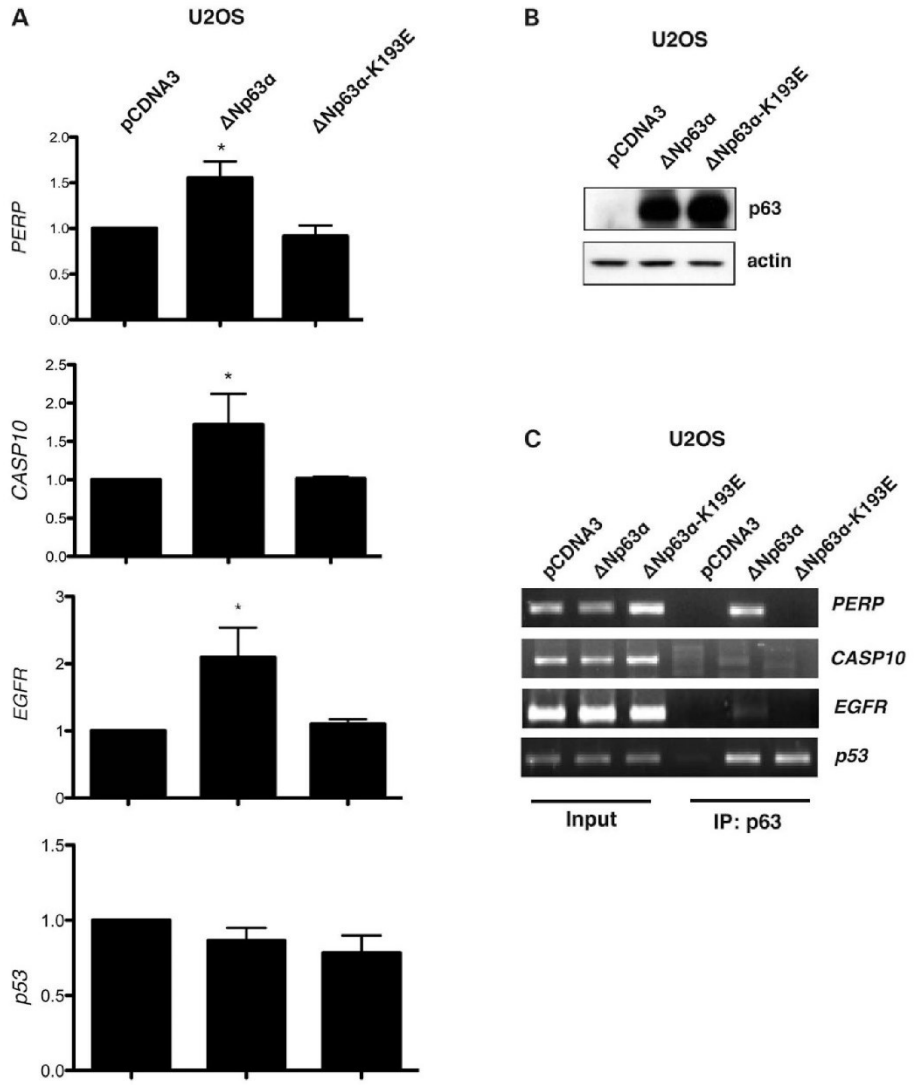

Figure 6. The ΔNp63α-K193E mutant displays an altered DNA binding activity and transcriptional activity on developmental related genes. (**A**) Expression of *CASP10*, *EGFR*, *PERP* and *p53* was analyzed by Real-Time qPCR in U2OS cells stably transfected with pCDNA3 (empty vector), ΔNp63α or ΔNp63α-K193E cDNAs. (**B**) ΔNp63α and ΔNp63α-K193E proteins expression was confirmed by WB analysis. (**C**) Cells used in A and B were subjected to ChIP analysis, and the recovered chromatin was amplified with *PERP*, *EGFR*, *p53* and *CASP10*-specific primers.

Here we report that FGF8, c-Abl, p300 and ΔNp63α are functionally linked in a molecular pathway modulating ΔNp63α activity and stability. Our data show that treatments with FGF8, a signaling molecule essential for limb outgrowth and patterning, result in increased ΔNp63α protein stability, both in cultured cells and in embryonic mouse limb buds *ex vivo*. Based on these data and previous findings from our team (23), we propose a model in which FGF8 promotes the interaction of c-Abl and ΔNp63α, and that this interaction is required for the consequent association of ΔNp63α with p300, leading to ΔNp63α acetylation (scheme in Fig. 7). When such acetylation is inefficient, due to reduced *FGF8* expression or to mutation of the p300 target lysine K193 in ΔNp63α, limb developmental defects ensue.

Based on our data, p300 appears to be an important regulator of ΔNp63α function during limb development, and in particular the results point to the possibility that p300 is required to selectively induce and activate with ΔNp63α a set of genes required to warrant correct limb development. No direct evidence of this is available,

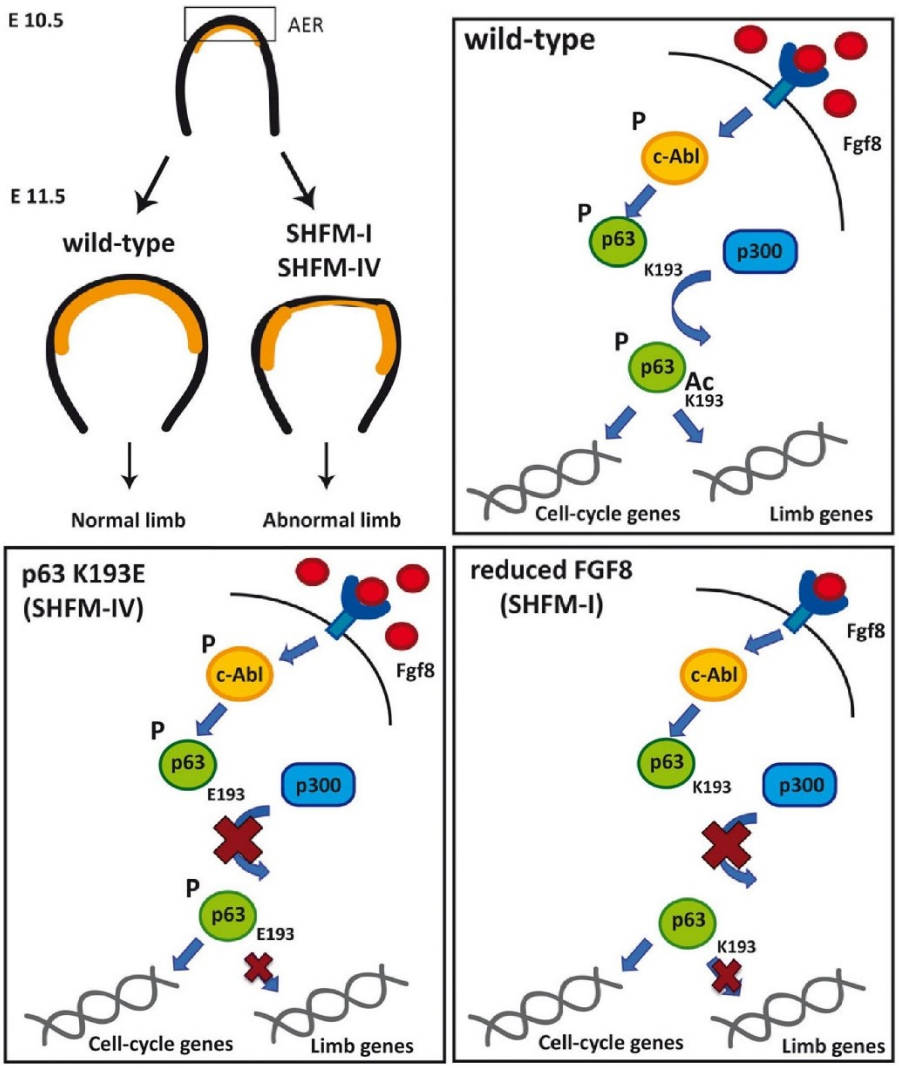

Figure 7. FGF8 positively regulates ΔNp63α protein stability in mice embryonic limb buds. FGF8, c-Abl and p300 are component of a regulatory pathway that leads to ΔNp63α stabilization and transcriptional activation in embryonic limb buds. Exposure of AER cells to FGF8 induces a signaling intracellular cascade that activates c-Abl causing ΔNp63α phosphorylation on tyrosine residues. This phosphorylation event is indispensable for the interaction of ΔNp63α with the p300 acetyl-transferases; acetylation of ΔNp63α result in its stabilization and transcriptional activation. In the absence of FGF8, or in the presence of p63 mutations, like the SHFM-associated K193E mutation, this signaling pathway is not active leading to improper expression of genes involved in limb development. This pathway could be relevant for correct AER stratification (in the scheme marked in yellow) ensuring correct limb outgrowth.

in fact the disruption of the *p300* gene in the mouse model is embryonic lethal and $p300^{-/-}$ mice arrest their development prior to the limb bud stage (53). Conversely, the role of acetylation and deacetylation on ΔNp63α are better known, indeed mice double knock-out for *Histone Deacetylase-1 and -2* (*HDAC1/HDAC2*) display developmental limb malformations similar to those observed in *p63* null mice (54). HDAC1 and HDAC2 mediate the repressive function of ΔNp63α on some of its transcriptional targets (like *14-3-3σ*, *p16/Ink4a*, *p19/ARF*) whose down-modulation is essential to ensure correct development (54). On the other hand, it's possible to speculate that Histone acetyl-transferases, such as p300, are needed to activate p63 target gene expression in concert with ΔNp63α. Indeed, luciferase-reporter assays indicated that p300 acetylation on K193 of ΔNp63α is required to guarantee an efficient transcription of genes involved in limb development, such as human *DLX5* and *DLX6* (46,55) (Fig. 5A, B).

We show here that lysine K193 of ΔNp63α is acetylated by p300, in human cells and *in vitro*.

This has important implications in the pathogenesis of the SHFM-IV syndrome, since this residue is found mutated into glutamic acid (K193E) in patients affected by this syndrome (7,8). Indeed, we found that the K193E mutant ΔNp63α protein is unable to activate p63 target genes required for developmental (such as *PERP*, *EGFR*) or apoptotic processes (*CASP10*). Indeed, programed cell death and cell differentiation are relevant to ensure correct shape of the limb (56). In particular, at early stages of limb development, the anterior and posterior necrotic zones are essential regions regulating the number of digits (57). On the other hand, the ΔNp63α-K193E mutant correctly induced the expression of genes connected to cell-cycle regulation (such as *p53* and *p57KIP2*) efficiently as the wild-type ΔNp63α protein. We found that, the altered transactivation activity of mutant ΔNp63α-K193E on target genes involved in developmental or apoptotic processes, is possibly due to a significant decrease in the DNA binding activity on the RE of such promoters, while this natural mutant was found to bind normally to the promoter of the *p53* gene. However, it is not clear how this mutation could alter the binding of ΔNp63α in a promoter-specific manner.

The role of FGF signaling in the SHFM malformation has been partly clarified. It is well established that FGF10 and FGF8 signaling are essential for AER induction and maintenance and that FGF8, expressed by the AER cells, is the key morphogen for limb bud outgrowth and patterning. Indeed FGF8 knock-out mice display severe defects in skeletal and limb development (19–22). The complete loss of *p63*, or the knock-in mouse model for the R279H mutation, associated to the EEC syndrome, leads to an evident downregulation of *FGF8* expression in the AER cells (3,4,9,46 and data not shown). Likewise, FGF8 is downregulated in the AER of embryos carrying the combined loss of *Dlx5*; *Dlx6*; two transcription factors causally implicated in SHFM type-I (55). Dlx5 and Dlx6 proteins co-localize with ΔNp63α in the AER cells and are direct ΔNp63α targets (46). Hence, the emerging picture is that FGF8 serves a double function, (a) a morphogen driving limb growth and patterning, via its actions on mesenchymal cells (paracrine) and AER cells (autocrine), (b) as stabilizer of ΔNp63α, to ensure the transitory stratification of the AER cells and the expression of limb-related p63 target genes.

In summary, the work presented here sheds new light on an important regulatory loop activated by FGF8 essential for ΔNp63α activation and stabilization in cell cultures and in mice limb buds and on the molecular mechanism that could be at the bases of the SHFM-IV pathogenesis.

Experimental procedures

Plasmids

All expression vectors encoding ΔNp63α wild-type and mutant proteins, p300 cDNAs, c-Abl and shAbl have been previously described (36,58). The shRNA against p300 (shp300) and control shRNA (shLuc) were purchased from Origene.

Cell culture and transfection

U2OS and HaCaT cells were kept in DMEM supplemented with 10% FBS (Euroclone) at 37°C in a humified atmosphere of 5% (v/v) CO_2 in air.

For transient transfection, 50 000 cells were seeded into 24-multiwell plates and on the next day transfected with Lipofectamine 2000 (Invitrogen) or Lipofectamine LTX (Invitrogen) for HaCaT cell, under the conditions suggested by the manufacturer. Transfection efficiency was checked by transfection of β-gal or GFP expression vectors. The total amount of transfected DNA (500 ng for 50 000 cells) was kept constant using empty vector as necessary.

For stable transfection 300 000 HaCaT or U2OS cells were plated in six wells and on the next day, HaCaT cells were transfected with 3 μg of shAbl or 3 μg of shLuc using Lipofectamine LTX (Invitrogen). After 24 h, cells were trypsinized and plated in a medium containing puromycin (0.8 μg/ml; Sigma). After 8 days of selection, clones were pooled and kept in puromycin. U2OS cells were transfected with 3 μg of ΔNp63α or ΔNp63α-K193E using Lipofectamine LTX (Invitrogen). After 24 h, cells were trypsinized and plated in medium containing Neomicin (G-418, 600 μg/ml). After 3 weeks of selection, clones were pooled and kept in Neomicinat 300 μg/ml.

U2OS and HaCaT cells were treated with 0.5 or 1 mM Valproic-Acid (VPA), 5 ng/ml or 10 ng/ml Trichostatin (TSA), 0.5 or 1 ng/ml FGF8 or FGF2, 10 μM CHX for the indicated times. For FGF2 or FGF8 treatments, cells were starved for 12 h before treatments using DMEM supplemented with 0.5% of FBS. HaCaT and U2OS cells were treated with 5 μM or 10 μM Imatinib, (Sigma) for the indicated times.

Western blot and antibodies

24 h after transfection, cells were lysed in 100 μl of Loading Buffer 2X (2% sodium dodecyl sulfate, 30% glycerol, 144 mM β-mercaptoethanol, 100 mM Tris–HCl pH 6.8 and 0.1% Bromo-Phenol Blue). Samples were incubated at 98°C for 10 min and resolved by SDS-PAGE. Proteins were transferred to a nitrocellulose membrane (Protran, Millipore). The blots were incubated with the following antibodies (p63 4A4 sc-8431, Santa Cruz Biotechnology), p300 (p300 C-20 sc-585, Santa Cruz Biotechnology), c-Abl (A5844, Sigma), acetylated lysine (#9441, Cell-Signaling) and actin (A2066, Sigma). We used the following secondary antibodies: α-mouse (sc-2005, Santa Cruz Biotechnology), α-rabbit (sc-2030, Santa Cruz Biotechnology). Proteins were visualized by an enhanced chemi-luminescence method (Genespin) according to manufacturer's instructions.

Luciferase activity assay

For reporter promoter assays, cells were transiently co-transfected with the *DLX5*, *DLX6*, *ADA*, *EGFR* and *p57KIP2* luciferase-reporter plasmids (23,46–48) and expression plasmids encoding for ΔNp63α, ΔNp63α-K193E and p300. Cells were seeded in 24-well plates and transfected using Lipofectamine 2000 (Invitrogen, Life Sciences). At 24 h post-transfection, cell extracts were prepared with Luciferase lysis buffer (1% Triton X-100, 25 mM Gly-Gly pH 7.8, 15 mM $MgSO_4$, 4 mM EDTA), and the luciferase activity was measured using the Beetle Luciferin Kit (Promega Inc.) on a TD 20/20 luminometer (Turner design).

The results are expressed as relative luciferase activity after normalization with the beta-Galactosidase plasmid as internal control. Basal activity of the reporter was set to 1. Each histogram bar represents the mean of three independent transfection experiments performed in triplicate. Standard deviations are indicated.

Co-immunoprecipitation

U2OS and HaCaT cells (1.25×10^6/100 mm plate) were transfected with the indicated vectors. 24 h after transfection cells were harvested for whole-cell lysates preparation using RIPA buffer (10 mM Tris–HCl pH 8, 2 mM EDTA, 0.1% SDS, 0.1% sodium deoxycholate, 140 mM NaCl, 1X Triton X-100, supplemented with

1 mM phenylmethylsulfonylfluoride and cocktail protease inhibitors, Sigma). Cell lysates were incubated on ice for 20 min, vortexed, then centrifuged at 6600 g for 20 min to remove cell debris. Protein concentration was determined with the Bradford Reagent (Sigma). 2 mg of cell lysates were incubated overnight at 4°C with 2 μg of anti-p63 (H-129 sc-8344, Santa Cruz Biotechnology) and anti-p300 (p300 C-20 sc-585, Santa Cruz Biotechnology). The immuno-complexes were collected by incubating with a mix of Protein A Agarose and Protein G Sepharose (Sigma) overnight at 4°C. The beads were washed three times: the first wash with RIPA buffer and the others with PBS. The beads were then re-suspended in 2X Loading buffer, heated at 98°C and loaded on a SDS polyacrylamide gel and subjected to western blotting with the indicated antibodies.

RNA extraction and real-time qPCR

For quantitative Real-Time qPCR total RNA was extracted from U2OS cells with the TRI Reagent (Sigma). 1 μg of total RNA was reverse-transcribed using SuperScriptIII cDNA Preparation Kit (Life-Technology). Real-Time quantitative PCR (qPCR) was performed with SybrGreen supermix (BIORAD). Tubulin mRNA was used for normalization. For Real-Time qPCR reaction the sequence of the primer pairs are described in Supplementary Material, Table S1.

ChIP assay

U2OS cells were used for ChIP assays performed as previously described (51). Briefly, after fixing in 1% formaldehyde, cells were lysed for 5 min in 50 mM Tris pH 8.0, 2 mM EDTA, 0.1% NP-40, 10% glycerol and supplemented with protease inhibitors (all from Sigma). Nuclei were re-suspended in 50 mM Tris pH8.0, 1% SDS and 5 mM EDTA. Chromatin was sheared by sonication, centrifuged and diluted 10-fold in 50 mM Tris, pH 8.0, 0.5% NP-40, 0.2 M NaCl and 0.5 mM EDTA. After pre-clearing with a 50% suspension of salmon sperm-saturated protein A, lysates were incubated at 4°C overnight with anti-p63 (H137 sc-8343, Santa-Cruz). Immune complexes were collected with sperm-saturated protein A, washed three times with high salt buffer (20 mM Tris pH 8.0, 0.1% SDS, 1% NP-40, 2 mM EDTA and 500 mM NaCl), and three times with Tris/EDTA (TE). Immune complexes were extracted in TE containing 1% SDS, and protein–DNA cross-links were reverted by heating at 65°C overnight. DNA was extracted by phenol–chloroform, and the immunoprecipitated DNA was used in PCR reaction. PCR reactions were performed for 25–35 cycles of denaturation at 95°C for 45 s, annealing at 55–57°C for 45 s and extension at 72°C for 45 s. Primer sequences are reported in Supplementary Material, Table S2.

In vitro acetylation assay

In vitro acetylation assay was performed following instructions provided by Fluorescent HAT Assay Kit (Active Motif, 56100). The purified recombinant p300 catalitic domain was incubated with acetyl-CoA and specific synthetic substrate peptides. All peptides were provided by GeneScript. Sequences are reported in Figure 3B. For fluorescence reading, a BF10000 Fluorocount was used.

Statistical analysis

Statistical analyses were performed with one-way ANOVA followed by Dunnett's Multiple Comparison post-test, when needed, using GraphPad PRISM version 5.0 (GraphPad, San Diego, CA, USA). In the graphs, * and ** mark statistically significant data with a $P < 0.05$ and <0.01, respectively. Statistically highly significant data, with a $P < 0.001$, are marked by ***.

Supplementary Material

Supplementary Material is available at *HMG* online.

Conflict of Interest statement. None declared.

Funding

This work was supported by the Telethon Foundation: grant number GGP11097 to L.G., A.C. and G.R.M. Funding to pay the Open Access publication charges for this article was provided by the Telethon Foundation.

References

1. Koster, M.I., Kim, S., Mills, A.A., DeMayo, F.J. and Roop, D.R. (2004) p63 is the molecular switch for initiation of an epithelial stratification program. *Genes Dev.*, **18**, 126–133.
2. Yang, A., Kaghad, M., Wang, Y., Gillett, E., Fleming, M.D., Dötsch, V., Andrews, N.C., Caput, D. and McKeon, F. (1998) p63, a p53 homolog at 3q27-29, encodes multiple products with transactivating, death-inducing, and dominant-negative activities. *Mol. Cell*, **2**, 305–316.
3. Mills, A.A., Zheng, B., Wang, X.J., Vogel, H., Roop, D.R. and Bradley, A. (1999) p63 is a p53 homologue required for limb and epidermal morphogenesis. *Nature*, **398**, 708–713.
4. Yang, A., Schweitzer, R., Sun, D., Kaghad, M., Walker, N., Bronson, R.T., Tabin, C., Sharpe, A., Caput, D., Crum, C. and McKeon, F. (1999) p63 is essential for regenerative proliferation in limb, craniofacial and epithelial development. *Nature*, **398**, 714–718.
5. Bokhoven, H.V. and Brunner, H.G. (2002) Splitting p63. *Am. J. Hum. Genet.*, **71**, 1–13.
6. Brunner, H.G., Hamel, B.C.J. and Bokhoven, H.V. (2002) p63 gene mutations and human developmental syndromes. *Am. J. Med. Genet.*, **112**, 284–290.
7. Duijf, P.H., Bokhoven, H.V. and Brunner, H.G. (2003) Pathogenesis of split-hand/split-foot malformation. *Hum. Mol. Genet.*, **12**, 51–60.
8. Ianakiev, P., Kilpatrick, M.W., Toudjarska, I., Basel, D., Beighton, P. and Tsipouras, P. (2000) Split-hand/split-foot malformation is caused by mutations in the p63 Gene on 3q27. *Am. J. Hum. Genet.*, **67**, 59–66.
9. Guerrini, L., Costanzo, A. and Merlo, G.R. (2011) A symphony of regulations centered on p63 to control development of ectoderm-derived structures. *J. Biomed. Biotechnol.*, 864904, doi:10.1155/2011/864904.
10. Murray-Zmijewski, F., Lane, D.P. and Bourdon, J.C. (2006) p53/p63/p73 isoforms: an orchestra of isoforms to harmonise cell differentiation and response to stress. *Cell Death Differ.*, **13**, 962–972.
11. Mangiulli, M., Valletti, A., Caratozzolo, M.F., Tullo, A., Sbisà, E., Pesole, G. and D'Erchia, A.M. (2009) Identification and functional characterization of two new transcriptional variants of the human p63 gene. *Nucleic Acids Res.*, **37**, 6092–6104.
12. Harms, K.L. and Chen, X. (2006) The functional domains in p53 family proteins exhibit both common and distinct properties. *Cell Death Differ.*, **13**, 890–897.

13. Yang, A. and McKeon, F. (2000) p63 and p73: p53 mimics, menaces and more. *Nat. Rev. Mol. Cell. Biol.*, **1**, 199–207.
14. Yang, A., Kaghad, M., Caput, D. and McKeon, F. (2002) On the shoulder of giants: p63, p73 and the rise of p53. *Trends Genet.*, **18**, 90–95.
15. Irwin, M.S. and Kaelin, W.G. (2001) p53 family update: p73 and p63 develop their own identities. *Cell Growth Differ.*, **1**, 337–349.
16. Pozzi, S., Zambelli, F., Merico, D., Pavesi, G., Robert, A., Maltère, P., Gidrol, X., Mantovani, R. and Vigano, M.A. (2009) Transcriptional Network of p63 in human keratinocytes. *PLoS ONE*, **4**, e5008.
17. Viganò, M.A. and Mantovani, R. (2007) Hitting the numbers: the emerging network of p63 targets. *Cell Cycle*, **3**, 233–239.
18. Testoni, B., Borrelli, S., Tenedini, E., Alotto, D., Castagnoli, C., Piccolo, S., Tagliafico, E., Ferrari, S., Viganò, M.A. and Mantovani, R. (2006) Identification of new p63 targets in human keratinocytes. *Cell Cycle*, **5**, 2805–2811.
19. Yu, K. and Ornitz, D.M. (2008) FGF signaling regulates mesenchymal differentiation and skeletal patterning along the limb bud proximodistal axis. *Development*, **135**, 483–491.
20. Boulet, A.M., Moon, A.M., Arenkiel, B.R. and Capecchi, M.R. (2004) The roles of Fgf4 and FGF8 in limb bud initiation and outgrowth. *Dev. Biol.*, **273**, 361–372.
21. Moon, A.M. and Capecchi, M.R. (2000) FGF8 is required for outgrowth and patterning of the limbs. *Nat. Genet.*, **26**, 455–459.
22. Lewandoski, M., Sun, X. and Martin, G.R. (2004) FGF8 signalling from the AER is essential for normal limb development. *Nat. Genet.*, **4**, 460–463.
23. Restelli, M., Lopardo, T., Lo Iacono, N., Garaffo, G., Conte, D., Rustighi, A., Napoli, M., Del Sal, G., Perez-Morga, D., Costanzo, A., Merlo, G.R. and Guerrini, L. (2014) DLX5, FGF8 and the Pin1 isomerase control ΔNp63α protein stability during limb development: a regulatory loop at the basis of the SHFM and EEC congenital malformations. *Hum. Mol. Genet.*, **23**, 3830–3842.
24. Ghioni, P., D'Alessandra, Y., Mansueto, G., Jaffray, E., Hay, R.T., La Mantia, G. and Guerrini, L. (2005) The protein stability and transcriptional activity of p63alpha are regulated by SUMO-1 conjugation. *Cell Cycle*, **1**, 183–190.
25. Galli, F., Rossi, M., D'Alessandra, Y., De Simone, M., Lopardo, T., Haupt, Y., Alsheich-Bartok, O., Anzi, S., Shaulian, E., Calabrò, V., La Mantia, G. and Guerrini, L. (2010) MDM2 and Fbw7 cooperate to induce p63 protein degradation following DNA damage and cell differentiation. *J. Cell Sci.*, **123**, 2423–2433.
26. Di Costanzo, A., Festa, L., Duverger, O., Vivo, M., Guerrini, L., La Mantia, G., Morasso, M.I. and Calabrò, V. (2009) Homeodomain protein Dlx3 induces phosphorylation-dependent p63 degradation. *Cell Cycle*, **8**, 1185–1195.
27. Papoutsaki, M., Moretti, F., Lanza, M., Marinari, B., Sartorelli, V., Guerrini, L., Chimenti, S., Levrero, M. and Costanzo, A. (2005) A p38-dependent pathway regulates ΔNp63 DNA binding to p53-dependent promoters in UV-induced apoptosis of keratinocytes. *Oncogene*, **24**, 6970–6975.
28. Brooks, C.L. and Gu, W. (2003) Ubiquitination, phosphorylation and acetylation: the molecular basis for p53 regulation. *Curr. Opin. Cell Biol.*, **15**, 164–171.
29. Pietsch, E.C., Sykes, S.M., McMahon, S.B. and Murphy, M.E. (2008) The p53 family and programmed cell death. *Oncogene*, **50**, 6507–6521.
30. Gu, B. and Zhu, W.G. (2012) Surf the post-translational modification network of p53 regulation. *Int. J. Biol. Sci.*, **8**, 672–684.
31. Brooks, C.L. and Gu, W. (2011) The impact of acetylation and deacetylation on the p53 pathway. *Protein Cell*, **2**, 456–462.
32. Gu, W. and Roeder, R.G. (1997) Activation of p53 sequence-specific DNA binding by acetylation of the p53 C-terminal domain. *Cell*, **90**, 595–606.
33. Luo, J., Li, M., Tang, Y., Laszkowska, M., Roeder, R.G. and Gu, W. (2004) Acetylation of p53 augments its site-specific DNA binding both in vitro and in vivo. *Proc. Natl. Acad. Sci. U.S.A.*, **101**, 2259–2264.
34. Marmorstein, R. and Roth, S.Y. (2001) Histone acetyltransferases: function, structure, and catalysis. *Curr. Opin. Genet. Dev.*, **11**, 155–161.
35. Zeng, X., Li, X., Miller, A., Yuan, Z., Yuan, W., Kwok, R.P., Goodman, R. and Lu, H. (2000) The N-terminal domain of p73 interacts with the CH1 domain of p300/CREB binding protein and mediates transcriptional activation and apoptosis. *Mol. Cell Biol.*, **20**, 1299–1310.
36. Costanzo, A., Merlo, P., Pediconi, N., Fulco, M., Sartorelli, V., Cole, P.A., Fontemaggi, G., Fanciulli, M., Schiltz, L., Blandino, G., Balsano, C. and Levrero, M. (2002) DNA damage-dependent acetylation of p73 dictates the selective activation of apoptotic target genes. *Mol. Cell*, **9**, 175–186.
37. Mantovani, F., Piazza, S., Gostissa, M., Strano, S., Zacchi, P., Mantovani, R., Blandino, G. and Del Sal, G. (2004) Pin1 links the activities of c-Abl and p300 in regulating p73 function. *Mol. Cell*, **14**, 625–636.
38. Tang, Y., Zhao, W., Chen, Y., Zhao, Y. and Gu, W. (2008) Acetylation is indispensable for p53 activation. *Cell*, **133**, 612–626.
39. Chae, Y.S., Kim, H., Kim, D., Lee, H. and Lee, H.O. (2012) Cell density-dependent acetylation of ΔNp63α is associated with p53-dependent cell cycle arrest. *FEBS Lett.*, **8**, 1128–1134.
40. Yan, W., Bentley, B. and Shao, R. (2008) Distinct angiogenic mediators are required for basic fibroblast growth factor- and vascular endothelial growth factor-induced angiogenesis: the role of cytoplasmic tyrosine kinase c-Abl in tumor angiogenesis. *Mol. Biol. Cell*, **19**, 2278–2288.
41. Agami, R., Blandino, G., Oren, M. and Shaul, Y. (1999) Interaction of c-Abl and p73alpha and their collaboration to induce apoptosis. *Nature*, **399**, 809–813.
42. Sanchez-Prieto, R., Sanchez-Arevalo, V.J., Servitja, J.M. and Gutkind, J.S. (2002) Regulation of p73 by c-Abl through the p38 MAP kinase pathway. *Oncogene*, **21**, 974–979.
43. Levav-Cohen, Y., Goldberg, Z., Zuckerman, V., Grossman, T., Haupt, S. and Haupt, Y. (2005) C-Abl as a modulator of p53. *Biochem. Biophys. Res. Commun.*, **331**, 737–749.
44. Gonfloni, S., Di Tella, L., Caldarola, S., Cannata, S.M., Klinger, F.G., Di Bartolomeo, C., Mattei, M., Candi, E., De Felici, M., Melino, G. and Cesareni, G. (2009) Inhibition of the c-Abl-TAp63 pathway protects mouse oocytes from chemotherapy-induced death. *Nat. Med.*, **15**, 1179–1185.
45. Yuan, M., Luong, P., Hudson, C., Gudmundsdottir, K. and Basu, S. (2010) c-Abl phosphorylation of ΔNp63α is critical for cell viability. *Cell Death Dis.*, doi: 10.1038/cddis.2009.15.
46. Lo Iacono, N., Mantero, S., Chiarelli, A., Garcia, E., Mills, A.A., Morasso, M.I., Costanzo, A., Levi, G., Guerrini, L. and Merlo, G.R. (2008) Regulation of Dlx5 and Dlx6 gene expression by p63 is involved in EEC and SHFM congenital limb defects. *Development*, **135**, 1377–1388.
47. Lussier, M., Canoun, C., Ma, C., Sank, A. and Shuler, C. (1993) Interdigital soft tissue separation induced by retinoic acid in mouse limbs cultured in vitro. *Int. J. Dev. Biol.*, **4**, 555–564.

48. Beretta, C., Chiarelli, A., Testoni, B., Mantovani, R. and Guerrini, L. (2005) Regulation of the cyclin-dependent kinase inhibitor p57Kip2 expression by p63. *Cell Cycle*, **4**, 1625–1631.
49. Sbisà, E., Mastropasqua, G., Lefkimmiatis, K., Caratozzolo, M.F., D'Erchia, A.M. and Tullo, A. (2006) Connecting p63 to cellular proliferation: the example of the adenosine deaminase target gene. *Cell Cycle*, **2**, 205–212.
50. Ihrie, R.A., Marques, M.R., Nguyen, B.T., Horner, J.S., Papazoglu, C., Bronson, R.T., Mills, A.A. and Attardi, L.D. (2005) Perp is a p63-regulated gene essential for epithelial integrity. *Cell*, **120**, 843–856.
51. Marinari, B., Ballaro, C., Koster, M.I., Giustizieri, M.L., Moretti, F., Crosti, F., Papoutsaki, M., Karin, M., Alema, S., Chimenti, S., Roop, D.R. and Costanzo, A. (2009) IKKalpha is a p63 transcriptional target involved in the pathogenesis of ectodermal dysplasias. *J. Invest. Dermatol.*, **129**, 60–69.
52. Lopardo, T., Lo Iacono, N., Marinari, B., Giustizieri, M.L., Cyr, D.G., Merlo, G., Crosti, F., Costanzo, A. and Guerrini, L. (2008) Claudin-1 is a p63 target gene with a crucial role in epithelial development. *PLoS ONE*, doi: 10.1371/journal.pone.0002715.
53. Yao, T.P., Oh, S.P., Fuchs, M., Zhou, N.D., Chng, L.E., Newsome, D., Bronson, R.T., Li, E., Livingston, D.M. and Eckner, R. (1999) Gene dosage-dependent embryonic development and proliferation defects in mice lacking the transcriptional integrator p300. *Cell*, **93**, 361–372.
54. LeBoeuf, M., Terrell, A., Trivedi, S., Sinha, S., Epstein, J.A., Olson, E.N., Morrisey, E.E. and Millar, S.E. (2010) Hdac1 and Hdac2 act redundantly to control p63 and p53 functions in epidermal progenitor cells. *Dev. Cell*, **19**, 807–818.
55. Merlo, G.R., Paleari, L., Mantero, S., Genova, F., Beverdam, A., Palmisano, G.L., Barbieri, O. and Levi, G. (2002) Mouse model of split hand/foot malformation type I. *Genesis*, **33**, 97–101.
56. Chimal-Monroy, J., Abarca-Buis, R.F., Cuervo, R., Díaz-Hernández, M., Bustamante, M., Rios-Flores, J.A., Romero-Suárez, S. and Farrera-Hernández, A. (2011) Molecular control of cell differentiation and programmed cell death during digit development. *Iubmb Life*, **10**, 922–929.
57. Nomura, N., Yokoyama, H. and Tamura, K. (2014) Altered developmental events in the anterior region of the chick forelimb give rise to avian-specific digit loss. *Dev. Dyn.*, **6**, 741–752.
58. Ghioni, P., Bolognese, F., Duijf, P.H., Van Bokhoven, H., Mantovani, R. and Guerrini, L. (2002) Complex transcriptional effects of p63 isoforms: identification of novel activation and repression domains. *Mol. Cell. Biol.*, **22**, 8659–8668.

Supplementary material

Figure S1. WB analysis of U2OS cell extracts transfected with ΔNp63α expression vector (30 ng) and then treated with increasing amounts of Trichostatin (TSA) (5 ng/ml and 10 ng/ml) for 5 hours or Valproic acid (VPA) (0,5 mM and 1 mM) for 3 hours.

Figure S2. WB analysis of HaCaT whole cell extracts transiently co-transfected with shp300 and shLuc expression vectors (80 ng). 48 hours after transfection protein half-life was measured by treating cells with 10 μg/ml of Cycloheximide (CHX).

Figure S3. Alignment of the human and mouse p53 protein region flanking K164 with human p63 and p73 sequences. The conserved lysine is marked in bold (h: human; m: mouse)

Figure S4. WB analysis of U2OS whole cell extracts transiently transfected with ΔNp63α or ΔNp63α-3Y expression vectors (30 ng) and treated with FGF8 (0.5 ng/ml) for 2 hours.

Figure S5. WB analysis of U2OS whole cell extracts transiently co-transfected with ΔNp63α or ΔNp63α-3Y expression vectors (30 ng) and increasing amount of p300 (10 and 20 ng) encoding plasmids.

Figure S6. Luciferase assay performed on U2OS cells transiently co-transfected with the -1200 bp *DLX5* promoter (200 ng) and ΔNp63α. 24 hours after transfection U2OS cells were treated with FGF8 (0,5 ng/ml) for 2 hours, or Imatinib (5 μM) alone for 2 hours and 30 minutes, or pretreated with Imatinib for 30 minutes then followed by FGF8 treatment for 2 hours. Standard deviations are indicated.

Fig. S1

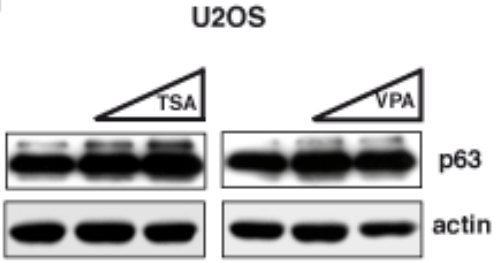

Fig. S2

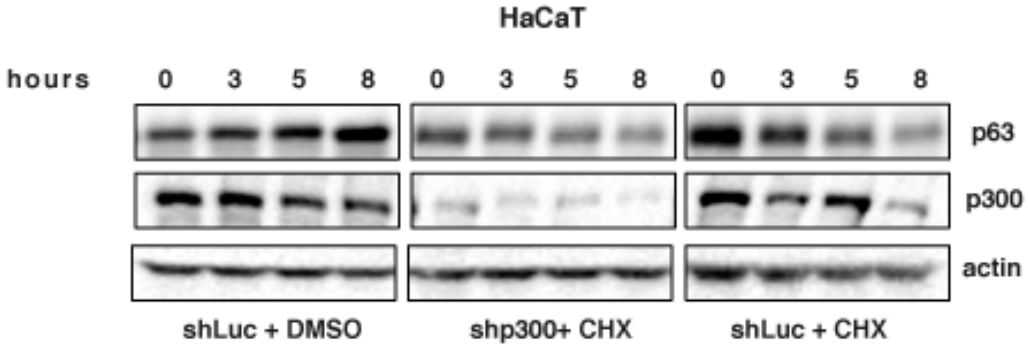

Fig. S3

h	p53	154	GTRVRAMAIY**K**QSQHMTEVVR	174
m	p53	151	GSRVRAMAIY**K**KSQHMTEVVR	171
h	p63	183	GAVIRAMPVY**K**KAEHVTDVVK	203
h	p73	172	GTAIRAMPVY**K**KAEHVTDVVK	192

Fig. S4

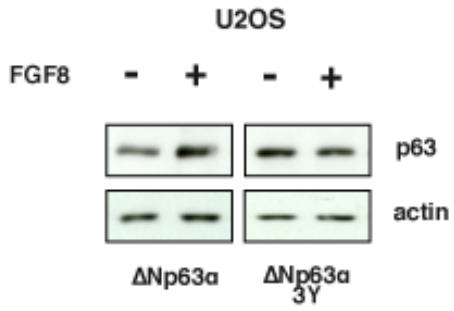

Fig. S5

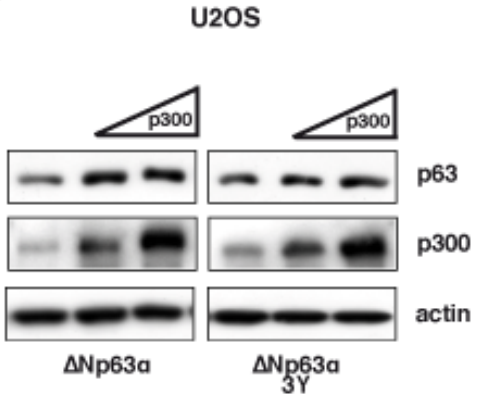

Fig. S6

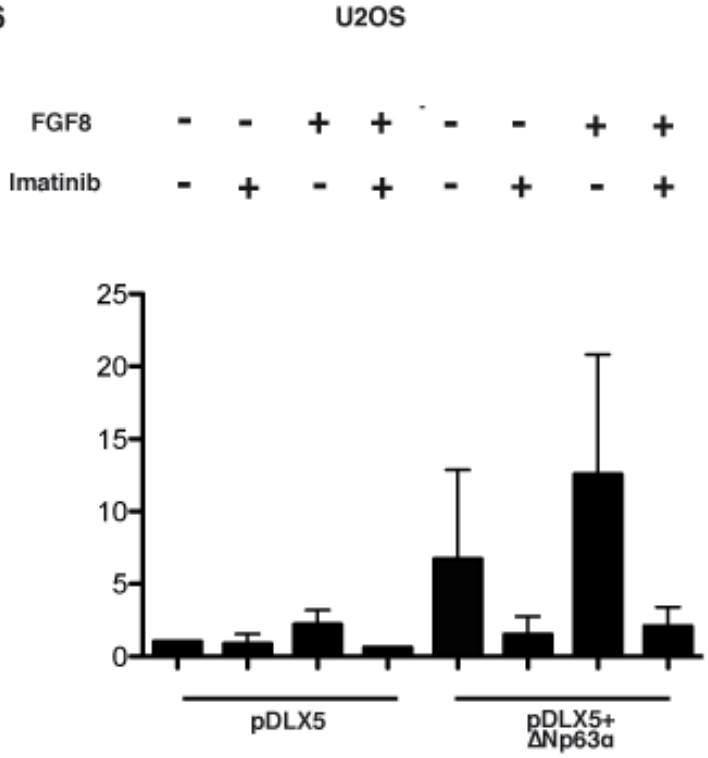

T1

PRIMERS FOR REAL-TIME qPCR

Gene (human)	Sequence (5' to 3')
Tubulin For	CTTCAGTGAGACGGGCGCTGGCAAGCAC
Tubulin Rev	TGATGAGCTGCTCAGGGTGGAA
Ikka For	TTCGGGAACGTCTGTCTGTACC
Ikka Rev	GGCACCATCGTTCTCTGTTT
Perp For	GACCCCAGATGCTTGTCTTC
Perp Rev	AAAGCCGTAGGCCCAGTTAT
p53 For	ACATGACGGAGGTTGTGAGG
p53 Rev	CCAAATACTCCACACGCAAA
Casp10 For	ACCCGACAAAGGGTTTCTCT
Casp10 Rev	GCCAGGAAACTTAGGGAGGT
EgfR For	CCCAGTACCTGCTCAACTGGT
Egfr Rev	TGCCAGGTCGCGGTG

T2

PRIMERS FOR ChIP

Gene (human)	Sequence (5' to 3')
p21 For	(see ref. 57)
p21 Rev	(see ref. 57)
Perp For	AGGTGGAACACCACACCCTA
Perp Rev	CGGGGATATTGGCAGAACTA
p53 For	AGAGTGTGGGATTCGTGAGC
p53 Rev	CCAGGGACGAGTGTGGATAC
Casp10 For	GAACAGGCAAAGAAGGTGGT
Casp10 Rev	AGGTTGCAGTGAGCCAAAAT
EgfR For	AATGGAAGAATCGGGTGTTG
Egfr Rev	AAAGAGGAGCTGCCCTAACC

Part III

ΔNp63α is a new molecular target of thalidomide teratogenicity

Elisa Molinari[1*], Hideki Ando[2*], Teresa Lopardo[1], Marco De Simone[1], Hiroshi Handa[2], Luisa Guerrini[1°]

[1] Department of Biosciences, Università degli Studi di Milano, 20133 Milano, Italy

[2] Department of Nanoparticle Translational Research, Tokyo Medical University, Shinjuku-ku, Tokyo, 160-8402, Japan

[*] Co-first authors

° Corresponding author:

Luisa Guerrini, Department of Biosciences, Università degli Studi di Milano

Via Celoria 26, 20133 Milan, Italy

Tel +39-02 50315000 Fax +39-02 50315044

e-mail: luisa.guerrini@unimi.it

Abstract

The transcription factor p63 plays a key role in limb, epithelial and cranio-facial development and *p63* mutations can cause severe limb malformations; in some cases, the clinical features of *p63* patients were similar to thalidomide-induced malformations. Thalidomide was largely prescribed against morning sickness in the early 1950s to pregnant women, causing a worldwide epidemic of newborn defects. Because of thalidomide potent teratogenic effects, the drug was withdrawn from the market but its use has been recently approved in the treatment of leprosy and multiple myeloma. It is therefore important to describe the molecular mechanism at the basis of thalidomide teratogenicity. Our data indicate that ΔNp63α is a new molecular target of thalidomide teratogenicity. Here we report that thalidomide induces proteasome-mediated degradation of ΔNp63α via the activity of GSK3 kinase and FBWX7 E3 ubiquitin ligase. Moreover, we show that, in zebrafish embryos, the restoration of normal levels of p63 is sufficient and necessary to readjust the general perturbation induced by thalidomide in fin development. Our results, by demonstrating that the downregulation of ΔNp63α protein levels is at the basis of thalidomide-induced pectoral fin malformations, provide a fundamental missing piece in the description of the molecular mechanisms of thalidomide teratogenicity.

Introduction

The p63 transcription factor, homolog to the p53 tumor suppressor, plays a pivotal role in limb, epithelial and cranio-facial development (1,2). A tight regulation of p63 activity and stability is indispensable to maintain its correct function during development. This control is achieved through a wide spectrum of post-translational modifications that can modulate p63 half-life, localization and interactions under specific stimuli (3–6). Indeed, we previously reported that, upon DNA damage or keratinocytes differentiation, ΔNp63α can be ubiquitinated and targeted for degradation by the FBW7 E3-ubiquitin ligase. Efficient degradation of ΔNp63α by FBWX7 requires GSK3 kinase activity, which phosphorylates p63 on serine 383 (S383) residue (7).

The *p63* gene encodes for at least ten protein isoforms, which differ in their amino and carboxy-terminal regions as a consequence of alternative transcription start site and alternative splicing, respectively (8,9), with ΔNp63α being the most expressed isoform in the embryonic ectoderm. ΔNp63α is at the centre of a complex molecular network that controls Apical Ectodermal Ridge (AER) function and maintenance via transcriptional regulation of the *DLX5* and *DLX6* genes that are in turn regulators of the essential morphogenetic factor FGF8 (10–12). Accordingly, p63 homozygous mutant mice show severe defects affecting their limbs, skin and craniofacial skeleton. In $p63^{-/-}$ new-born animals, the hindlimbs are absent whereas the forelimbs are severely truncated in their distal segment (1,2). The limb defects observed in $p63^{-/-}$ mice are highly reminiscent of the phenotype of patients affected by conditions due to specific mutations in *p63* gene, such as Ectrodactyly-Ectodermal dysplasia-Clefting (EEC) syndrome (MIM 604292), Limb-Mammary Syndrome (LMS [MIM 603543]), Acro-Dermato-Ungual Lacrimal-Tooth (ADULT) syndrome (MIM 103285), and nonsyndromic Split-Hand/Foot Malformation (SHFM) type 4 (13,14).

The limb defects presented by EEC, LMS, ADULT and SHFM4 patients show a striking resemblance with the malformations induced by the teratogenic drug thalidomide. It has occurred that EEC patients have been wrongly referred as possible victims of thalidomide (15). In 1950s, prescription of the sedative drug thalidomide (α-(N-phthalimido)glutarimide) caused a worldwide epidemic of multiple birth defects and it was soon withdrawn from the market. The uptake of thalidomide by pregnant women during their first trimester of gestation caused in the newborns multiple defects such as limb, ear, cardiac, and gastrointestinal malformations. The limb malformations, known as phocomelia and amelia, are characterized, respectively, by severe shortening or complete absence of legs and/or arms (16–18). The fact that, on the contrary, no remarkable toxicity was observed when the drug was tested on rodents is probably due to the species-specificity of thalidomide teratogenicity; the drug is able to

induce limb/fin deformities in humans, monkeys, rabbits, chicks, and zebrafish (*Danio rerio*) but not in rats and mice (19).

In 1965 there was a renewal of the interest in thalidomide, as it was shown to have immunomodulatory and anti-inflammatory properties in patients with Erythema Nodosum Leprosum (ENL), a painful complication of leprosy (20). Thalidomide was also found to inhibit the basic Fibroblast Growth Factor (bFGF)-induced formation of new blood vessels (21) and the production of vascular endothelial growth factor (22). These findings prompted clinical trials exploring thalidomide use for anti-angiogenic cancer therapy. The efficacy of thalidomide and its derivatives lenalidomide and pomalidomide (collectively known as IMiDs) has since been demonstrated for several haematological cancers such as multiple myeloma (23,24). The anti-proliferative and immunomodulatory effects of IMiDs have recently been linked to drug-induced ubiquitination and degradation of the transcription factors IKZF1 and IKZF3, two specific B cell transcription factors, involved in the onset of multiple myeloma (25,26).

With respect to ENL and myeloma, thalidomide was approved for use by the US FDA in 1998 and 2006, respectively (19). However, due to its serious teratogenicity, the prescription of thalidomide is strictly controlled by the System for Thalidomide Education and Prescribing Safety (STEPS) program (27). It is therefore very important to describe in detail the mechanism of action of the drug. In fact, the elucidation of the molecular basis of thalidomide teratogenicity can lead to the elimination of its side effects and to the development of thalidomide derivatives and related compounds devoid of teratogenic activity. Moreover, by further investigating the targets of thalidomide therapeutic activity, it may be possible to expand the spectrum of pathological conditions in which the drug can be used.

However, despite the many efforts that were spent during the last 50 years trying to elucidate thalidomide mechanism of action, the details remain still elusive. Previous studies have proposed that thalidomide-induced oxidative stress might be at the basis of thalidomide teratogenicity (28,29). Another supported thesis states that thalidomide anti-angiogenic properties might mediate its teratogenic effects (21,30). Only recently has been identified a primary target for thalidomide teratogenicity: the thalidomide-binding protein CEREBLON (CRBN), which is a substrate receptor in the (31). However, the ubiquitously expressed CRBN protein cannot account alone for the tissue-specificity of thalidomide teratogenicity and other components are likely to contribute to the effects of the drug.

In the present study, we report that thalidomide is able to promote FBWX7 mediated ubiquitination and proteasome mediated degradation of ΔNp63α. To do so, it requires the activity of Glycogen Synthase Kinase 3 (GSK3), which phosphorylates ΔNp63α on residues S383 and threonine 397 (T397), whose integrity is required for thalidomide action on ΔNp63α. Moreover, our data

demonstrate that thalidomide-induced downregulation of ΔNp63α in zebrafish embryos is at the basis of thalidomide-induced fin defects, providing a description of the molecular basis of thalidomide teratogenicity.

Results

Thalidomide induces ΔNp63α degradation

The phenotypic similarity between thalidomide-induced malformations and those due to mutations in *p63* gene prompted us to determine whether p63 could be a molecular target of the drug. We treated human keratinocytes (HaCaT) cells, which endogenously express the ΔNp63α isoform, with thalidomide (10 μM). Indeed, thalidomide treatment resulted in a drastic decrease of ΔNp63α protein expression levels (Fig. 1). RT-PCR performed on total RNA from these cells revealed that thalidomide-induced ΔNp63α protein downregulation was not accompanied by a decrease in *p63* mRNA levels, indicating that thalidomide acts at a protein level to modulate ΔNp63α expression (Fig. 2). In order to understand how the drug induces a decrease in ΔNp63α levels, we treated HaCaT cells with thalidomide in the presence or absence of the proteasome inhibitor MG132 (5 μM). Interestingly, the treatment with MG132 blocked the effects of thalidomide on ΔNp63α protein levels, indicating that thalidomide treatment induces proteasome-mediated degradation of ΔNp63α (Fig. 1).

Thalidomide treatment alters the transcriptional activity of ΔNp63α in a promoter-specific manner

p63 is essential for epidermal differentiation and limb development. In order to assess the impact of thalidomide treatment on p63 downstream pathway(s), we treated HaCaT cells with thalidomide (10 μM) and analysed by semi-quantitative RT-PCR the expression levels of a particular set of p63 target genes: *IKKα*, which is involved in epidermal development (32,33), *PERP*, which is essential for epithelial integrity (34), *DLX5* and *DLX6* which are downstream to p63 in the regulation of limb development (10) and *REDD1*, involved in the response to reactive oxygen species (35). Interestingly, upon thalidomide treatment, the transcription levels of the p63 target genes *IKKα*, *PERP*, *DLX5* and *DLX6* were drastically reduced, whilst the expression levels of *REDD1* remained unaltered (Fig. 2), indicating that thalidomide-induced p63 degradation results specifically in an alteration of p63 function on developmentally-related target genes.

Thalidomide treatment specifically induces the degradation of the ΔNp63α and ΔNp63β isoforms and requires the activity of FBWX7 E3 ubiquitin ligase and GSK3 kinase to promote the degradation

The p53-related *p63* gene can be transcribed in several isoforms that differ not only in their structure but also in function (13,36). In order to analyse the response of the different p63 isoforms to thalidomide, we transiently transfected human osteosarcoma (U2OS) cells, which do not endogenously express p63, with either ΔNp63α, ΔNp63β or ΔNp63γ isoforms and treated the cells with thalidomide (10 μM). Thalidomide treatment efficiently leads to a downregulation of ΔNp63α and ΔNp63β isoforms but does not alter ΔNp63γ protein levels. Interestingly, thalidomide acts specifically on the p63 transcription factor, since the protein levels of NF-Y and p53 transcription factors were not altered by the treatment (Fig. 3A).

The C-terminal region of p63 is absent in the ΔNp63γ isoform and therefore may be required for thalidomide-induced p63 degradation. To further narrow-down the region of p63 required for thalidomide action, we employed several truncated mutants of ΔNp63 with stop codon inserted at different positions within the common region shared by ΔNp63α and ΔNp63β isoforms (data not shown). Interestingly, in the region that was found to be necessary for mediating thalidomide-induced degradation were present two residues, S383 and T397, which we previously identified as important sites for p63 degradation (5,7). To verify whether these two residues are involved in thalidomide-induced degradation, we treated with thalidomide (10 μM) U2OS cells transfected with either the ΔNp63αS383A, the ΔNp63αT397A or the ΔNp63αS383A/T397A mutants. Interestingly, the single mutants ΔNp63αS383A and ΔNp63αT397A appeared to be partially resistant to thalidomide treatment, whilst the double mutant ΔNp63αS383A/T397A was completely resistant (Fig. 3B).

S383 and T397 residues are centered on two predicted phosphodegrons for the FBWX7 E3 ubiquitin ligase, which promotes the degradation of ΔNp63α and ΔNp63β isoforms upon DNA damage or keratinocytes differentiation. FBWX7 binds to its targets in a phosphorylation-dependent manner and most of its known substrates are phosphorylated by GSK3 (7).

Strikingly, silencing of endogenous *FBWX7* in HaCaT cells abolished ΔNp63α protein modulation upon thalidomide treatment (Fig. 4A). Moreover, inhibition of GSK3 kinase activity with the specific inhibitor SB216763 (10 μM) led to a complete resistance of ΔNp63α protein to thalidomide treatment (Fig. 4B), indicating that the thalidomide-induced downregulation of ΔNp63α is mediated by the activity of FBWX7 E3 ubiquitin ligase and GSK3 kinase.

Thalidomide treatment downregulates p63 protein levels *in vivo* in zebrafish embryos

Thalidomide, along with its anti-angiogenic, anti-neoplastic and anti-rheumatic properties, displays dangerous teratogenic effects. In particular, thalidomide is teratogenic in rabbits and chicks, but not in mice and rats. Recently, thalidomide was reported to be teratogenic in zebrafish where it causes severe reduction in the length of pectoral fins, which are homolog structures to tetrapod limbs with respect to early patterning and gene expression (31,37). In order to verify in an *in vivo* model whether thalidomide treatment results in a downregulation of p63 protein levels, we treated zebrafish embryos with thalidomide (400 μM) and allowed them to grow for 24, 48 or 72 hours post fertilization (hpf). Indeed, thalidomide treatment induces a downregulation of p63 protein levels in zebrafish embryos along with a severe impairment of pectoral fin development (Fig 5A). p63 is an important regulator of correct fin development also in zebrafish (38–40). To further characterize the effects of thalidomide on the fin developmental pathway which is downstream to p63, we analysed the protein levels of dlx5 which is a p63 target gene involved in the development of zebrafish pectoral fins (10,40). Interestingly, protein levels of dlx5 were reduced in zebrafish embryos treated with thalidomide (400μM) (Fig. 5B), suggesting that thalidomide-induced downregulation of p63 results in a general impairment of the downstream fin developmental pathway.

Thalidomide-induced defects are rescued by p63 overexpression in zebrafish embryos

In order to verify whether the reduction of p63 protein levels could be linked to thalidomide tereatogenicity, we microinjected either *zp63*-mRNA or control-mRNA into zebrafish embryos that were subsequently treated with thalidomide (400 μM) and let them develop for 72 hpf.

Strikingly, the injection of *zp63*-mRNA was able to rescue the thalidomide-induced defects in pectoral fin development, observed in the embryos injected with control-mRNA (Fig. 6A, 6B). This result strongly suggests that the restoration of normal p63 levels is able to rescue the phenotypical defects induced by thalidomide treatment in fin development.

Furthermore, to verify if the phenotypical rescue that we obtained by microinjecting *zp63*-mRNA was accompanied by a general restoration of the fin developmental pathway, we analysed by Real-Time qPCR the expression levels of *tbx5a* and *prrx1a*, two genes essential for correct fin development in zebrafish embryos (41–43). Our analysis on total RNA from zebrafish embryos at 49 hpf revealed that the microinjection of *zp63*-mRNA is able to restore the levels of *tbx5a* and *prxx1a* transcript otherwise altered by thalidomide treament (Fig. 6C).

All these results indicate that the restoration of p63 levels can rescue thalidomide-induced alterations in fin development both at a phenotypical and at a molecular level, suggesting that thalidomide-

induced teratogenesis is indeed mediated by p63 protein downregulation, which perturbs the downstream developmental pathway.

Discussion

Here we report that thalidomide is able to induce developmental defects by promoting protesome-mediated degradation of ΔNp63α and demonstrate that ΔNp63α is a new molecular target of thalidomide teratogenicity.

p63 transcription factor plays a key role in limb development and *p63*$^{-/-}$ mice display absence or severe truncations of the limbs (1,2). Moreover, mutations in *p63* gene can cause several syndromic or non-syndromic conditions, some of them characterized by severe defects in the limbs, such as ectrodactyly and syndactyly (13,14). The clinical features of patients affected by these mutations are very reminiscent of thalidomide-induced defects. Indeed, it has occurred that EEC patients have been wrongly referred as possible victims of thalidomide (15).

Thalidomide causes multiple birth defects of the ear, eye, internal organs, and central nervous system but the most frequent malformations induced by the drug are by far phocomelia and amelia (16–18). These two pathological conditions consist, respectively, in the severe shortening or in the complete absence of legs and/or arms.

Since the first discovery of thalidomide teratogenic effects in 1961, numerous efforts were made trying to understand the molecular mechanisms of action of the drug. It was proposed that thalidomide teratogenic activity is linked to its ability to inhibit bFGF-induced angiogenesis; thalidomide antiangiogenic effects might be at the basis of limb defects, since blood vessel formation is crucial for limb development (21). In 1999, Parman et al. suggested that thalidomide causes limb deformities through a mechanism involving oxidative stress; thalidomide generates reactive oxygen species (ROS) and oxidative stress might downregulate essential limb growth factors (28,29).

However, only recently it has been identified a primary target for thalidomide teratogenicity: the thalidomide-binding protein CEREBLON (CRBN), which is a substrate receptor in the E3 ubiquitin ligase complex CRL4 (31). Ito et al. proposed that thalidomide causes limb malformations by inhibiting CRBN E3 ubiquitin ligase activity. CRBN has an important role in central nervous system development, especially in memory and learning and is linked to Autosomal Recessive NonSyndromic mild Mental Retardation (ARNSMR) (44). Nevertheless, there is no evidence of a primary role for the ubiquitously expressed CRBN protein in limb development. Therefore, CRBN can hardly account alone for the tissue-specificity of thalidomide teratogenicity and other components are likely to contribute to the effects of the drug.

Our results indicate that thalidomide treatment is able to induce teratogenicity by reducing ΔNp63α protein levels, both *in vitro* and *in vivo*. Based on our data, we propose a model in which thalidomide is able to promote ΔNp63α ubiquitination through the action of the E3 ubiquitin ligase FBWX7, consequently leading to the proteasomal degradation of ΔNp63α and to a downregulation of its target genes. To induce ΔNp63α degradation, thalidomide requires the activity of GSK3 kinase which phosphorylates p63 on residues S383 and T397 and this phosphorylation is recognized as a signal by FBWX7 (Fig.7).

Thalidomide, by altering the otherwise tightly regulated levels of p63, overall disregulates the pathways that drive the development of zebrafish pectoral fins and perturbs the expression levels of p63 targets involved in development such as dlx5.

Most importantly, we demonstrate that the microinjection of *p63*-mRNA into 2-cells stage zebrafish embryos phenotypically rescues thalidomide-induced alterations in fin formation. Moreover, this phenotypical rescue is accompanied at a molecular level by a restoration of normal expression levels of *tbx5a* and *prrx1a*, two genes essential for correct fin development in zebrafish embryos (41–43), indicating that the microinjection of *p63*-mRNA is sufficient and necessary to readjust the general perturbation induced by thalidomide in fin development.

All these data indicate that thalidomide-induced p63 downregulation is at the basis of the fin defects induced by the drug.

However, there is no clear evidence of a direct interaction between thalidomide and ΔNp63α. It is possible that thalidomide primary target CRBN can mediate the effect of the drug on ΔNp63α.

It is also possible that thalidomide acts on ΔNp63α independently from CRBN, by directly binding to ΔNp63α, GSK3 kinase and/or FBWX7 ubiquitin ligase. Thalidomide might, for example, facilitate the interaction between FBWX7 E3 ubiquitin ligase and ΔNp63α, inducing ΔNp63α ubiquitination and consequent degradation. Fisher et al. suggested a similar mechanism for the lenalidomide-induced degradation of IKZF1 and IKZF3, two essential factors in the onset of multiple myeloma; the thalidomide analogue lenalidomide is able to bring IKZF1 and IKZF3 in the vicinity of CRL4 CRBN E3 ubiquitin ligase, thus promoting their ubiquitination (45).

The employment of thalidomide in the treatment of multiple myeloma and leprosy (20,23) requires a precise description of its molecular mechanism of action. A better understanding of thalidomide mechanism of action might allow a rational design of novel related compounds with equal therapeutic properties but devoid of thalidomide teratogenic activity.

The present work demonstrates that thalidomide induces limb/fin defects by reducing ΔNp63α protein levels, providing a fundamental missing piece in the description of the molecular mechanisms at the basis of thalidomide teratogenicity.

Moreover, the capability of thalidomide to downregulate ΔNp63α protein levels has a therapeutic relevance per se. In fact, despite its pivotal role in development, ΔNp63α was also shown to be involved in several types of cancer such as squamous cell carcinoma (SCC), pediatric neuroblastoma and osteosarcoma (46,47). It is demonstrated that, in these pathological conditions, ΔNp63α upregulation induces the expression of crucial angiogenic factors and promotes tumour development. Moreover, cells overexpressing ΔNp63α display a selective advantage in osteorsarcoma metastasis, underlining ΔNp63α central role in the tumour progression and dissemination (46).
Thus, our discovery of the effects of thalidomide on ΔNp63α levels not only clarifies the molecular mechanisms of thalidomide teratogenic effects on limb/fin development, but also paves the way for a potential powerful use of thalidomide and its derivatives in the treatment of neoplastic conditions where ΔNp63α is overexpressed.

Experimental procedures

Plasmids

All expression vectors encoding p63 cDNAs have been previously described (48). The sh*LUC*, sh*FBWX7* and ΔNp63αS383A/T397A constructs also have been previously described (7,49).

Cell culture, transfection and treatments

U2OS and HaCaT cells were kept in DMEM supplemented with 10% FBS (Euroclone) at 37°C in a humified atmosphere of 5% (v/v) CO_2 in air. For transient transfection, 50000 cells were seeded into 24-multiwell plates and on the next day transfected with Lipofectamine 2000 (Invitrogen) or Lipofectamine LTX (Invitrogen) for HaCaT cells, under the conditions suggested by the manufacturer. Transfection efficiency was checked by transfection of β-gal or GFP expression vectors. The total amount of transfected DNA (500 ng for 50 000 cells) was kept constant using empty vector as necessary. U2OS and HaCaT cells were treated with 10 μM thalidomide (Sigma-Aldrich), 10 μM SB216763 (Sigma-Aldrich) or 5 μM MG132 (Sigma-Aldrich) for the indicated times.

Zebrafish maintenance and treatments

Current Italian national rules: no approval needs to be given for research on zebrafish embryos. Wild-type zebrafish of the AB strain were raised and maintained according to established techniques (50). Embryos were collected by natural spawning. Thalidomide treatment was performed as previously described (31).

Western blot and antibodies

24 h after transfection or at the indicated times after treatments, cells were lysed in 100 µl of Loading Buffer 2X (2% sodium dodecyl sulfate, 30% glycerol, 144 mM β-mercaptoethanol, 100 mM Tris HCl pH 6.8 and 0.1% Bromo-Phenol Blue).
Zebrafish total extracts were obtained by mechanical disgregation of the embryos into RIPA Buffer (50 mM Tris HCl pH 8.0, 150 mM NaCl, 0.1% SDS, 0.1% NP-40, 0.5% sodium deoxycholate). PMSF and cocktail protease inhibitors (Sigma-Aldrich) were added according to the manufacturer's instruction.
Cell and zebrafish embryo samples were incubated at 98°C for 10 min and resolved by SDS-PAGE. Proteins were transferred to a nitrocellulose membrane (Protran, Millipore). The blots were incubated with the following antibodies: p63 (mouse monoclonal 4A4 sc-8431, Santa Cruz Biotechnology), dlx5 (goat polyclonal Y-20 sc-18151, Santa Cruz Biotechnology), p53 (mouse monoclonal DO1, Genespin) and actin (A2066, Sigma), NF-YA (rabbit polyclonal sc-10779, Santa Cruz Biotechnology). We used the following secondary antibodies: goat α-mouse (sc-2005, Santa Cruz Biotechnology), goat α-rabbit (sc-2030, Santa Cruz Biotechnology) and rabbit α-goat (sc-2768, Santa Cruz Biotechnology). Proteins were visualized by an enhanced chemi-luminescence method (Biorad) according to manufacturer's instructions.

Microinjection of capped mRNAs

Microinjection into one-cell stage embryos was carried out as previously described (51) using a nitrogen gas-pressure microinjector IM 300 (Narishige) at 15 picosiemens for 30-50 ms. Capped mRNAs were synthesized *in vitro* using the mMESSAGE mMACHINE SP6 in vitro transcription kit (Ambion). RNAs were dissolved in nuclease-free water at 350 ng/µl immediately before use.

RNA extraction and RT-PCR

Total RNA was extracted from HaCaT cells using the TRI-Reagent (Sigma), as indicated by the supplier. 1 µg of RNA was reverse-transcribed using SuperScript III (Life Technology), following the manufacturer's instuctions. Total cDNA was used for amplification with the primers described in Table 1. GAPDH mRNA was used for normalization.

RNA extraction and Real-Time qPCR from zebrafish extracts

Total RNA was extracted from zebrafish embryos at 49 hpf using NucleoSpin® RNA XS (MACHEREY-NAGEL) as indicated by the supplier. 1 µg of RNA was reverse-transcribed using SuperScript III (Life Technology), following the manufacturer's instuctions. Real-Time quantitative PCR (qPCR) was performed with SybrGreen supermix (Biorad). GAPDH mRNA was used for normalization. The sequences of the primers are reported in Table 2.

Table 1. Primers for semi-quantitative RT-PCR on HaCaT cell extracts

	Forward	Reverse
ΔNp63α	5'-GTCTCCATCTTCATATGGTAA-3'	5'-CACACTGACTGTAGAGGCA-3'
DLX5	5'-CTACAACCGCGTCCCAAG-3'	5'-CACCTGTGTTTGTGTCAATCC-3'
DLX6	5'-CCTCGGACCATTTATTCCAG-3'	5'-TTGTTCTGAAACCATATCTTCACC-3'
IKKα	5'-TTCGGGAACGTCTGTCTGTACC-3'	5'-GGTTTGTTGAGCAGCTTTCGGAG-3'
GAPDH	5'-TCACCAGGGCTGCTTTTAAC-3'	5'-TGGAAGATGGTGATGGGATT-3'
PERP	5'-GTGGAAATGCTCCCAAGAGG-3'	5'-TCCAATCACTCCAGGAAGACA-3'
REDD1	5'-GAACTCCCACCCCAGATCGG-3'	5'-CGAGGGTCAGCTGGAAGGTG-3'

Table 2. Primers for Real-Time qPCR on zebrafish extracts

	Forward	Reverse
gapdh	5'-CGCTGGCATCTCCCTCAA-3'	5'-TCAGCAACACGATGGCTGTAG-3'
tbx5a	5'-CCACTGCATCAAGAGGAAAGT-3'	5'-CCACATACGGCTTCTTCTTATAGGG-3'
prrx1a	5'-AGCGACACTACACAGCAGGA-3'	5'-CGCCTCTGTTTACGCTTCT-3'

References

1. Mills AA, Zheng B, Wang XJ, Vogel H, Roop DR, Bradley A. p63 is a p53 homologue required for limb and epidermal morphogenesis. Nature. 1999 Apr 22;398(6729):708–13.

2. Yang A, Schweitzer R, Sun D, Kaghad M, Walker N, Bronson RT, et al. p63 is essential for regenerative proliferation in limb, craniofacial and epithelial development. Nature. 1999 Apr 22;398(6729):714–8.

3. Ghioni P, D'Alessandra Y, Mansueto G, Jaffray E, Hay RT, La Mantia G, et al. The protein stability and transcriptional activity of p63alpha are regulated by SUMO-1 conjugation. Cell Cycle Georget Tex. 2005 Jan;4(1):183–90.

4. Papoutsaki M, Moretti F, Lanza M, Marinari B, Sartorelli V, Guerrini L, et al. A p38-dependent pathway regulates DeltaNp63 DNA binding to p53-dependent promoters in UV-induced apoptosis of keratinocytes. Oncogene. 2005 Oct 20;24(46):6970–5.

5. Di Costanzo A, Festa L, Duverger O, Vivo M, Guerrini L, La Mantia G, et al. Homeodomain protein Dlx3 induces phosphorylation-dependent p63 degradation. Cell Cycle Georget Tex. 2009 Apr 15;8(8):1185–95.

6. Restelli M, Molinari E, Marinari B, Conte D, Gnesutta N, Costanzo A, et al. FGF8, c-Abl and p300 participate in a pathway that controls stability and function of the ΔNp63α protein. Hum Mol Genet. 2015 Aug 1;24(15):4185–97.

7. Galli F, Rossi M, D'Alessandra Y, De Simone M, Lopardo T, Haupt Y, et al. MDM2 and Fbw7 cooperate to induce p63 protein degradation following DNA damage and cell differentiation. J Cell Sci. 2010 Jul 15;123(Pt 14):2423–33.

8. Murray-Zmijewski F, Lane DP, Bourdon J-C. p53/p63/p73 isoforms: an orchestra of isoforms to harmonise cell differentiation and response to stress. Cell Death Differ. 2006 Jun;13(6):962–72.

9. Mangiulli M, Valletti A, Caratozzolo MF, Tullo A, Sbisà E, Pesole G, et al. Identification and functional characterization of two new transcriptional variants of the human p63 gene. Nucleic Acids Res. 2009 Oct;37(18):6092–104.

10. Lo Iacono N, Mantero S, Chiarelli A, Garcia E, Mills AA, Morasso MI, et al. Regulation of Dlx5 and Dlx6 gene expression by p63 is involved in EEC and SHFM congenital limb defects. Dev Camb Engl. 2008 Apr;135(7):1377–88.

11. Guerrini L, Costanzo A, Merlo GR. A symphony of regulations centered on p63 to control development of ectoderm-derived structures. J Biomed Biotechnol. 2011;2011:864904.

12. Restelli M, Lopardo T, Lo Iacono N, Garaffo G, Conte D, Rustighi A, et al. DLX5, FGF8 and the Pin1 isomerase control ΔNp63α protein stability during limb development: a regulatory loop at the basis of the SHFM and EEC congenital malformations. Hum Mol Genet. 2014 Jul 15;23(14):3830–42.

13. van Bokhoven H, Brunner HG. Splitting p63. Am J Hum Genet. 2002 Jul;71(1):1–13.

14. van Bokhoven H, McKeon F. Mutations in the p53 homolog p63: allele-specific developmental syndromes in humans. Trends Mol Med. 2002 Mar;8(3):133–9.

15. Stephens TD, Bunde CJ, Fillmore BJ. Mechanism of action in thalidomide teratogenesis. Biochem Pharmacol. 2000 Jun 15;59(12):1489–99.

16. Knobloch J, Rüther U. Shedding light on an old mystery: thalidomide suppresses survival pathways to induce limb defects. Cell Cycle Georget Tex. 2008 May 1;7(9):1121–7.

17. Franks ME, Macpherson GR, Figg WD. Thalidomide. Lancet Lond Engl. 2004 May 29;363(9423):1802–11.

18. Vargesson N. Thalidomide-induced limb defects: resolving a 50-year-old puzzle. BioEssays News Rev Mol Cell Dev Biol. 2009 Dec;31(12):1327–36.

19. Ito T, Ando H, Handa H. Teratogenic effects of thalidomide: molecular mechanisms. Cell Mol Life Sci CMLS. 2011 May;68(9):1569–79.

20. Sheskin J. THALIDOMIDE IN THE TREATMENT OF LEPRA REACTIONS. Clin Pharmacol Ther. 1965 Jun;6:303–6.

21. D'Amato RJ, Loughnan MS, Flynn E, Folkman J. Thalidomide is an inhibitor of angiogenesis. Proc Natl Acad Sci U S A. 1994 Apr 26;91(9):4082–5.

22. Yabu T, Tomimoto H, Taguchi Y, Yamaoka S, Igarashi Y, Okazaki T. Thalidomide-induced antiangiogenic action is mediated by ceramide through depletion of VEGF receptors, and is antagonized by sphingosine-1-phosphate. Blood. 2005 Jul 1;106(1):125–34.

23. Singhal S, Mehta J, Desikan R, Ayers D, Roberson P, Eddlemon P, et al. Antitumor activity of thalidomide in refractory multiple myeloma. N Engl J Med. 1999 Nov 18;341(21):1565–71.

24. Pan B, Lentzsch S. The application and biology of immunomodulatory drugs (IMiDs) in cancer. Pharmacol Ther. 2012 Oct;136(1):56–68.

25. Krönke J, Udeshi ND, Narla A, Grauman P, Hurst SN, McConkey M, et al. Lenalidomide causes selective degradation of IKZF1 and IKZF3 in multiple myeloma cells. Science. 2014 Jan 17;343(6168):301–5.

26. Lu G, Middleton RE, Sun H, Naniong M, Ott CJ, Mitsiades CS, et al. The myeloma drug lenalidomide promotes the cereblon-dependent destruction of Ikaros proteins. Science. 2014 Jan 17;343(6168):305–9.

27. Zeldis JB, Williams BA, Thomas SD, Elsayed ME. S.T.E.P.S.: a comprehensive program for controlling and monitoring access to thalidomide. Clin Ther. 1999 Feb;21(2):319–30.

28. Parman T, Wiley MJ, Wells PG. Free radical-mediated oxidative DNA damage in the mechanism of thalidomide teratogenicity. Nat Med. 1999 May;5(5):582–5.

29. Hansen JM, Harris C. A novel hypothesis for thalidomide-induced limb teratogenesis: redox misregulation of the NF-kappaB pathway. Antioxid Redox Signal. 2004 Feb;6(1):1–14.

30. Therapontos C, Erskine L, Gardner ER, Figg WD, Vargesson N. Thalidomide induces limb defects by preventing angiogenic outgrowth during early limb formation. Proc Natl Acad Sci U S A. 2009 May 26;106(21):8573–8.

31. Ito T, Ando H, Suzuki T, Ogura T, Hotta K, Imamura Y, et al. Identification of a primary target of thalidomide teratogenicity. Science. 2010 Mar 12;327(5971):1345–50.

32. Candi E, Terrinoni A, Rufini A, Chikh A, Lena AM, Suzuki Y, et al. p63 is upstream of IKK alpha in epidermal development. J Cell Sci. 2006 Nov 15;119(Pt 22):4617–22.

33. Marinari B, Ballaro C, Koster MI, Giustizieri ML, Moretti F, Crosti F, et al. IKKalpha is a p63 transcriptional target involved in the pathogenesis of ectodermal dysplasias. J Invest Dermatol. 2009 Jan;129(1):60–9.

34. Ihrie RA, Marques MR, Nguyen BT, Horner JS, Papazoglu C, Bronson RT, et al. Perp is a p63-regulated gene essential for epithelial integrity. Cell. 2005 Mar 25;120(6):843–56.

35. Ellisen LW, Ramsayer KD, Johannessen CM, Yang A, Beppu H, Minda K, et al. REDD1, a developmentally regulated transcriptional target of p63 and p53, links p63 to regulation of reactive oxygen species. Mol Cell. 2002 Nov;10(5):995–1005.

36. Sethi I, Romano R-A, Gluck C, Smalley K, Vojtesek B, Buck MJ, et al. A global analysis of the complex landscape of isoforms and regulatory networks of p63 in human cells and tissues. BMC Genomics. 2015;16:584.

37. Ito T, Handa H. Deciphering the mystery of thalidomide teratogenicity. Congenit Anom. 2012 Mar;52(1):1–7.

38. Bakkers J, Hild M, Kramer C, Furutani-Seiki M, Hammerschmidt M. Zebrafish DeltaNp63 is a direct target of Bmp signaling and encodes a transcriptional repressor blocking neural specification in the ventral ectoderm. Dev Cell. 2002 May;2(5):617–27.

39. Lee H, Kimelman D. A dominant-negative form of p63 is required for epidermal proliferation in zebrafish. Dev Cell. 2002 May;2(5):607–16.

40. Kouwenhoven EN, van Heeringen SJ, Tena JJ, Oti M, Dutilh BE, Alonso ME, et al. Genome-wide profiling of p63 DNA-binding sites identifies an element that regulates gene expression during limb development in the 7q21 SHFM1 locus. PLoS Genet. 2010 Aug;6(8):e1001065.

41. Pi-Roig A, Martin-Blanco E, Minguillon C. Distinct tissue-specific requirements for the zebrafish tbx5 genes during heart, retina and pectoral fin development. Open Biol. 2014;4:140014.

42. Parrie LE, Renfrew EM, Wal AV, Mueller RL, Garrity DM. Zebrafish tbx5 paralogs demonstrate independent essential requirements in cardiac and pectoral fin development. Dev Dyn Off Publ Am Assoc Anat. 2013 May;242(5):485–502.

43. Hernández-Vega A, Minguillón C. The Prx1 limb enhancers: targeted gene expression in developing zebrafish pectoral fins. Dev Dyn Off Publ Am Assoc Anat. 2011 Aug;240(8):1977–88.

44. Higgins JJ, Rosen DR, Loveless JM, Clyman JC, Grau MJ. A gene for nonsyndromic mental retardation maps to chromosome 3p25-pter. Neurology. 2000 Aug 8;55(3):335–40.

45. Fischer ES, Böhm K, Lydeard JR, Yang H, Stadler MB, Cavadini S, et al. Structure of the DDB1-CRBN E3 ubiquitin ligase in complex with thalidomide. Nature. 2014 Aug 7;512(7512):49–53.

46. Bid HK, Roberts RD, Cam M, Audino A, Kurmasheva RT, Lin J, et al. ΔNp63 promotes pediatric neuroblastoma and osteosarcoma by regulating tumor angiogenesis. Cancer Res. 2014 Jan 1;74(1):320–9.

47. Hibi K, Trink B, Patturajan M, Westra WH, Caballero OL, Hill DE, et al. AIS is an oncogene amplified in squamous cell carcinoma. Proc Natl Acad Sci U S A. 2000 May 9;97(10):5462–7.

48. Ghioni P, Bolognese F, Duijf PHG, Van Bokhoven H, Mantovani R, Guerrini L. Complex transcriptional effects of p63 isoforms: identification of novel activation and repression domains. Mol Cell Biol. 2002 Dec;22(24):8659–68.

49. Anzi S, Finkin S, Shaulian E. Transcriptional repression of c-Jun's E3 ubiquitin ligases contributes to c-Jun induction by UV. Cell Signal. 2008 May;20(5):862–71.

50. Westerfield M. The zebrafish book. A guide for the laboratory use of zebrafish (Danio rerio). 4th ed. University of Oregon Press; 2000.

51. Ando H, Furuta T, Okamoto H. Photo-mediated gene activation by using caged mRNA in zebrafish embryos. Methods Cell Biol. 2004;77:159–71.

Figure legends

Figure 1. The ΔNp63α protein is downregulated by thalidomide treatment in human keratinocytes. Western Blot (WB) analysis of whole HaCaT cell extracts treated with DMSO, 5 μM MG132, 10 μM thalidomide, or 10 μM thalidomide concomitantly with 5 μM MG132, for the indicated times.

Figure 2. Expression of *ΔNp63α* and of its target genes in HaCaT cells upon thalidomide treatment. RT-PCR semiquantitative analysis of *ΔNp63α, REDD1, IKKα, PERP, DLX5* and *DLX6* mRNAs on whole HaCaT cell extracts treated with DMSO or 10 μM thalidomide for the indicated times. *GAPDH* mRNA was used for normalization.

Figure 3. Thalidomide degrades specifically isoforms ΔNp63α and ΔNp63β and requires integrity of S383 and T397 residues. (**A**) WB analysis of whole extracts from U2OS cells transiently co-transfected with either ΔNp63α, ΔNp63β or ΔNp63γ expression vectors (30 ng) and then treated with DMSO or 10 μM thalidomide for the indicated times. Endogenous NF-Y and p53 protein levels are also shown. (**B**) WB analysis of whole extracts from U2OS cells transiently transfected with either ΔNp63α or ΔNp63αS383A-T397A mutant expression vectors (30 ng) and then treated with DMSO or 10 μM thalidomide for the indicated times.

Figure 4. Thalidomide requires FBWX7 and GSK3 activity. (**A**) WB analysis of whole HaCaT cell extracts transiently transfected with sh*FBWX7* or sh*LUC* (40 ng) and treated with DMSO or 10 μM thalidomide for the indicated times. (**B**) WB analysis of whole HaCaT cell extracts treated with DMSO, 10 μM SB216763, 10 μM thalidomide or 10 μM thalidomide concomitantly with 10 μM SB216763.

Figure 5. Thalidomide downregulates p63 and its target dlx5 in zebrafish embryos. (**A**) WB analysis of whole zebrafish embryos extracts treated with DMSO or 400 μM thalidomide. The embryos were analysed for p63 protein expression levels at the stages of 24, 48 and 72 hpf. (**B**) WB analysis of whole zebrafish embryos extracts treated with DMSO or 400 μM thalidomide. The embryos were analysed for dlx5 protein expression levels at the stage of 48 hpf.

Figure 6. Microinjection of *zp63*-mRNA is able to rescue thalidomide-induced defects both at a phenotypical and at a molecular level. (**A**) Dorsal views of pectoral fins of 72-hpf embryos treated with DMSO or 400 μM thalidomide. Pectoral fins are indicated by arrowheads. Green arrowheads

indicate normal fins, red arrowheads indicate short fins. Where indicated, *egfp*-mRNA or *egfp:zp63*-mRNA was injected into one-cell stage embryos. (**B**) Percentage of embryos treated with DMSO or 400 μM thalidomide displaying Normal, Mild or Severe phenotype. Where indicated, *egfp*-mRNA or *egfp:zp63*-mRNA was injected into one-cell stage embryos. The embryos were classified on the basis of the pectoral fins length. Normal class embryos displayed normal fins, Mild class embryos displayed shorter, non-protruding fins, Severe class embryos did not display a proper fin fold but a fin bud, or complete absence of the fin. (**C**) Expression of *tbx5a* and *prrx1a* was analyzed by Real-Time qPCR in zebrafish embryos at 49 hpf treated with DMSO or thalidomide. Where indicated, *egfp*-mRNA or *egfp:zp63*-mRNA was injected into one-cell stage embryos.

Figure 7. ΔNp63α is a molecular target of thalidomide teratogenicity. Based on our data, we propose a model in which thalidomide induces teratogenicity by promoting a series of ΔNp63α post-translational modifications that lead to the proteasomal degradation of the protein. To induce ΔNp63α degradation, thalidomide requires the activity of GSK3 kinase which phosphorylates p63 on residues S383 and T397 and this phosphorylation is recognized as a signal by FBWX7. Thalidomide-induced ΔNp63α degradation leads to a lack of activation of ΔNp63α target genes involved in limb/fin development, such as *dlx5*.

Figures

Fig. 1

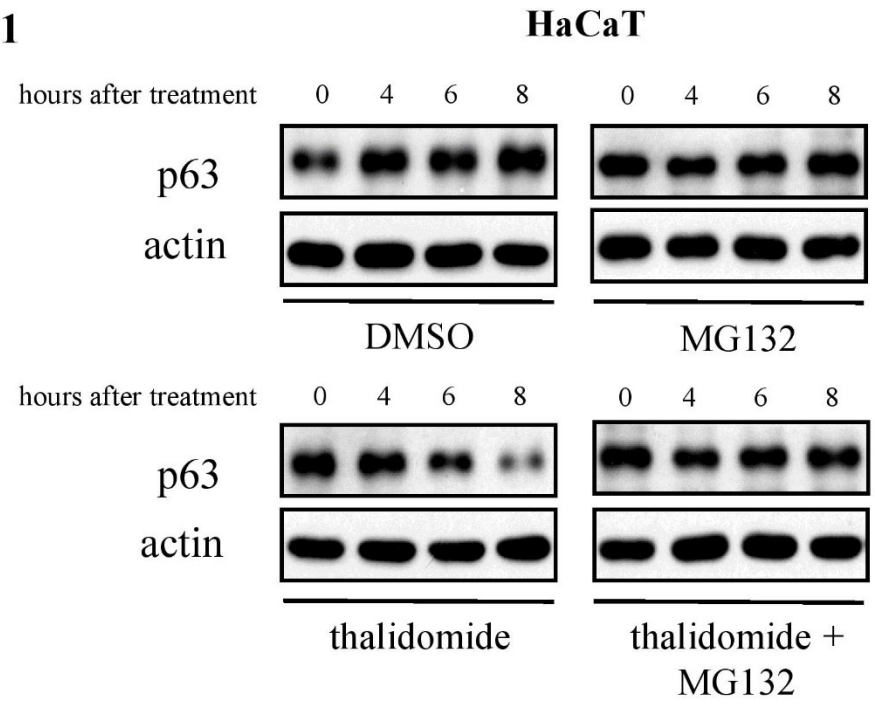

Fig. 2

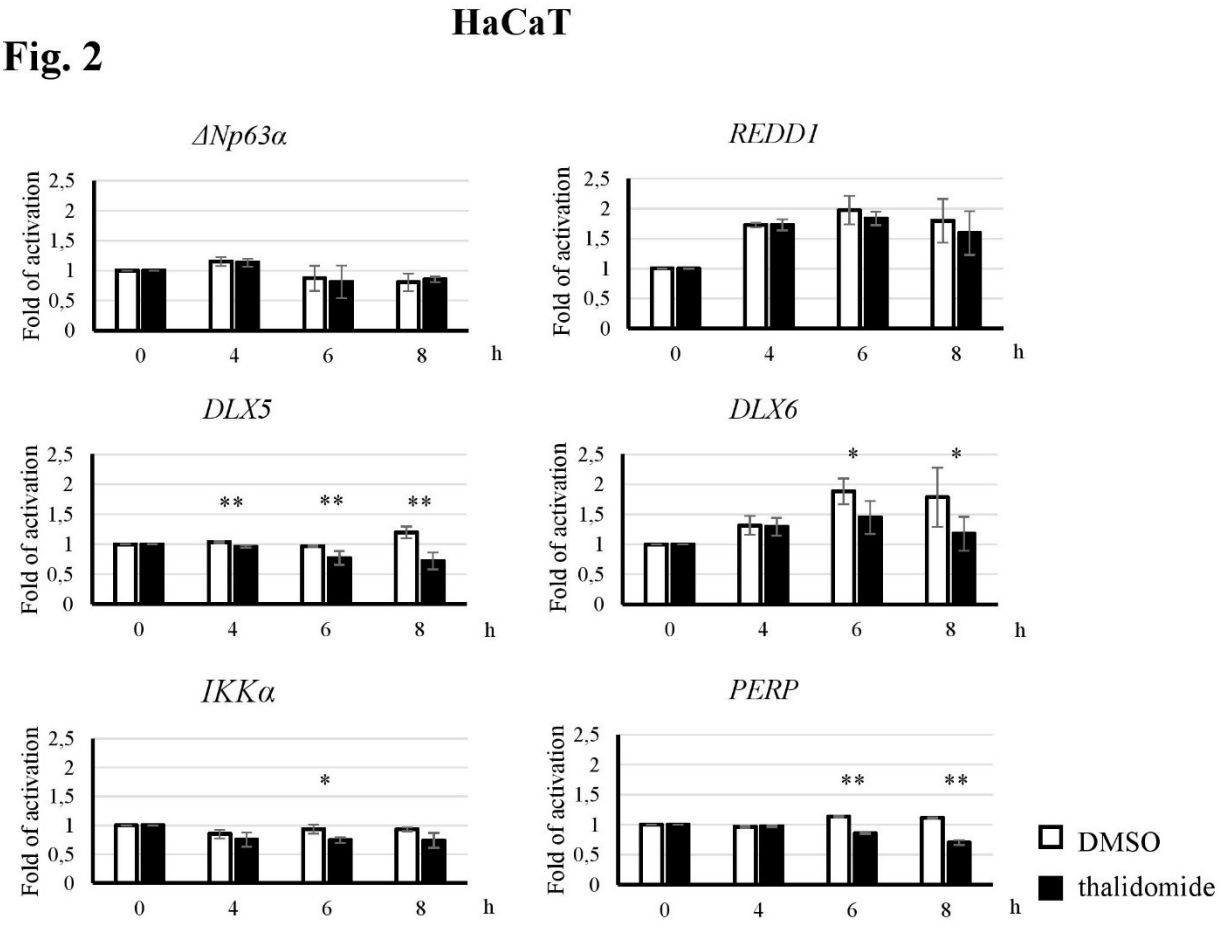

Fig. 3

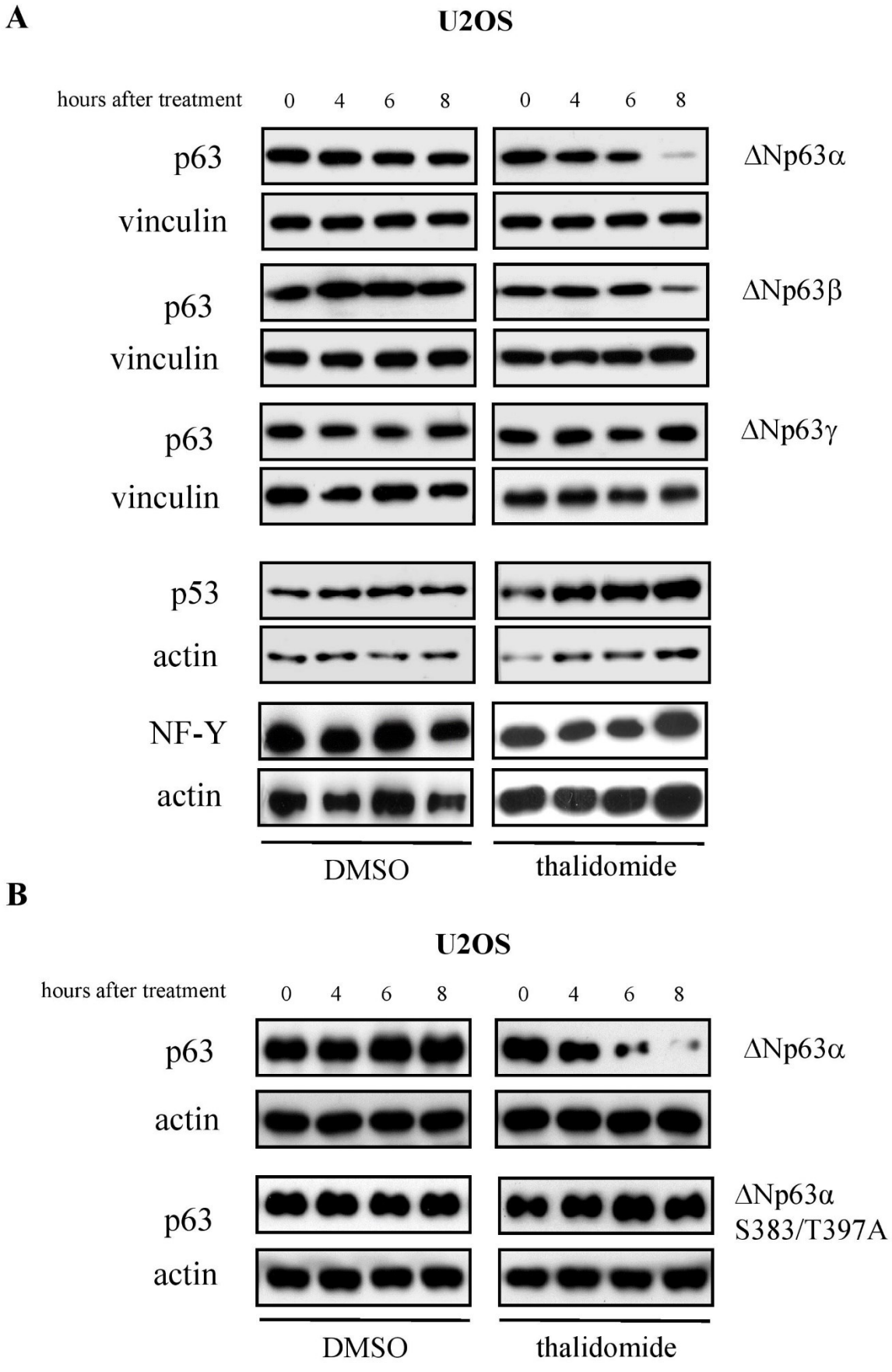
A
U2OS
hours after treatment
0 4 6 8 0 4 6 8
p63
vinculin
ΔNp63α
p63
vinculin
ΔNp63β
p63
vinculin
ΔNp63γ
p53
actin
NF-Y
actin
DMSO
thalidomide
B
U2OS
hours after treatment
0 4 6 8 0 4 6 8
p63
actin
ΔNp63α
p63
actin
ΔNp63α
S383/T397A
DMSO
thalidomide

Fig. 4

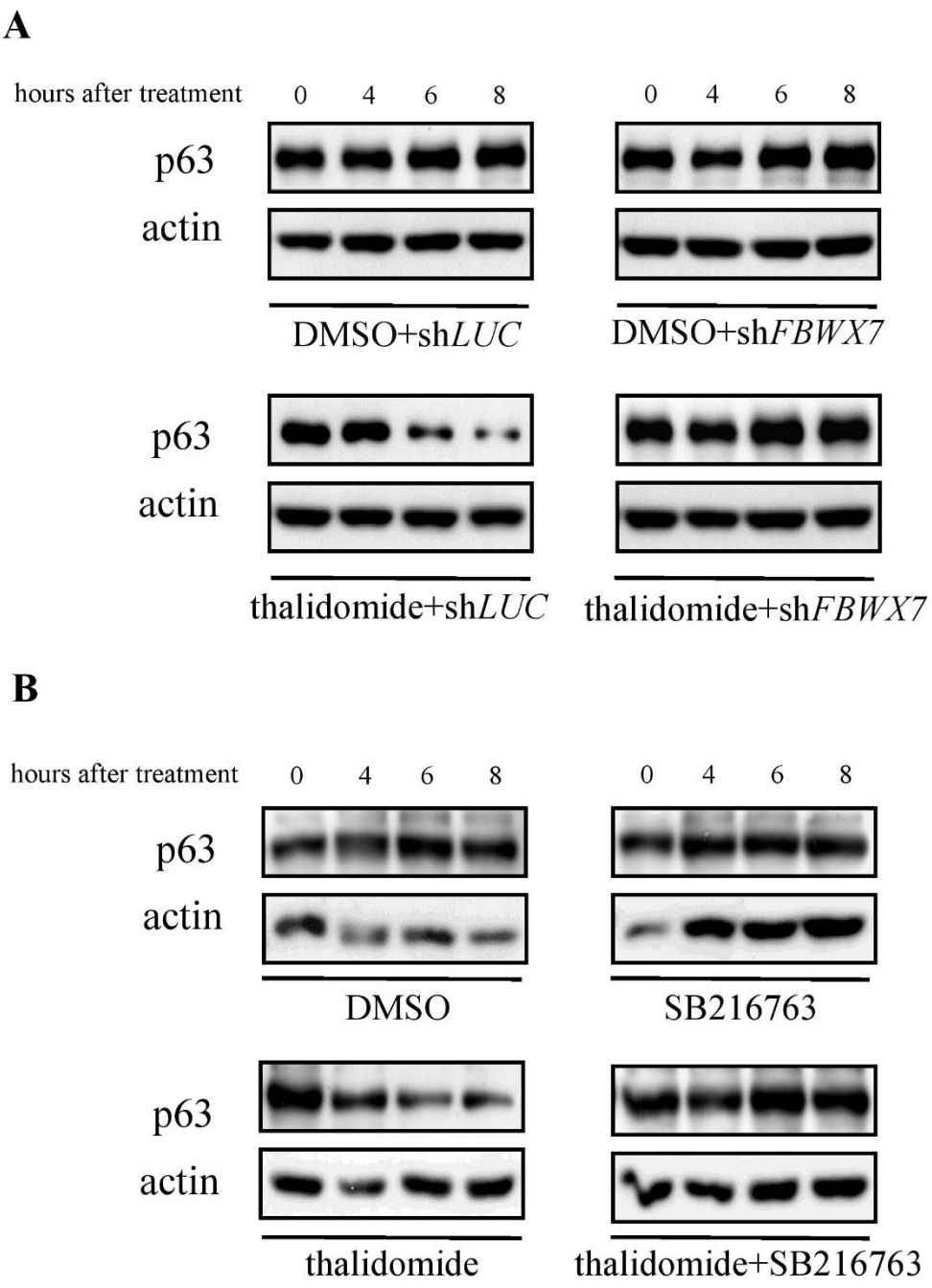
A
hours after treatment
0 4 6 8
0 4 6 8
p63
actin
DMSO+sh*LUC*
DMSO+sh*FBWX7*
p63
actin
thalidomide+sh*LUC*
thalidomide+sh*FBWX7*
B
hours after treatment
0 4 6 8
0 4 6 8
p63
actin
DMSO
SB216763
p63
actin
thalidomide
thalidomide+SB216763

Fig. 5

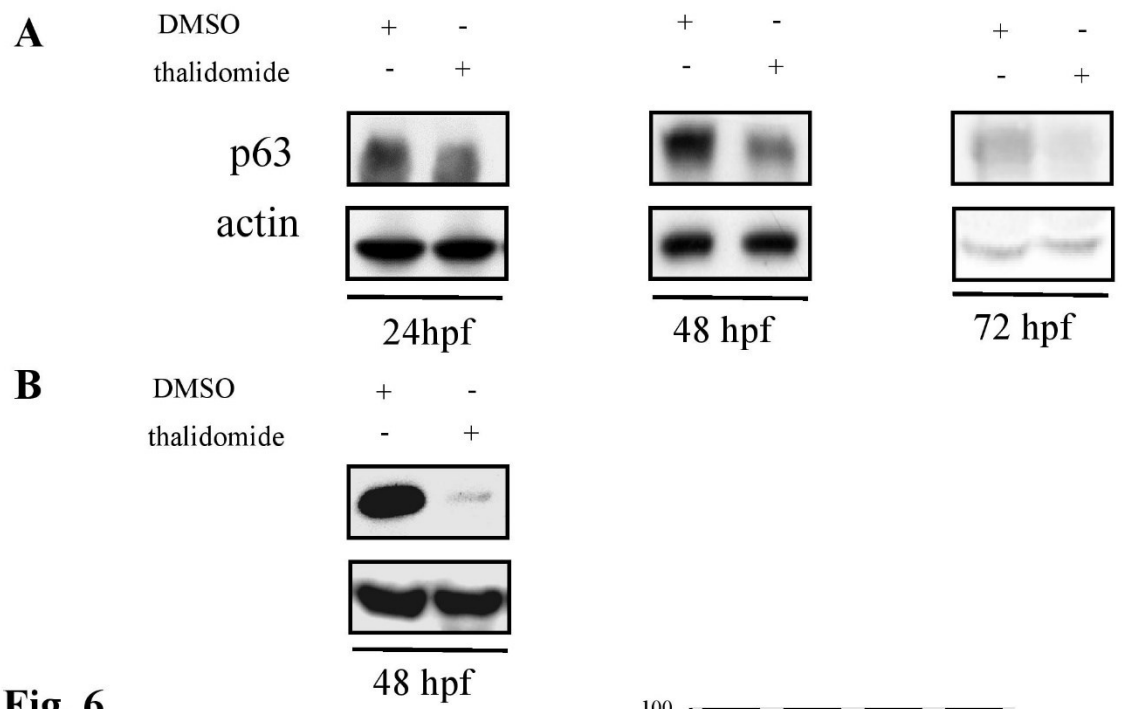
A
DMSO
thalidomide
p63
actin
24hpf
48 hpf
72 hpf
B
DMSO
thalidomide
48 hpf

Fig. 6

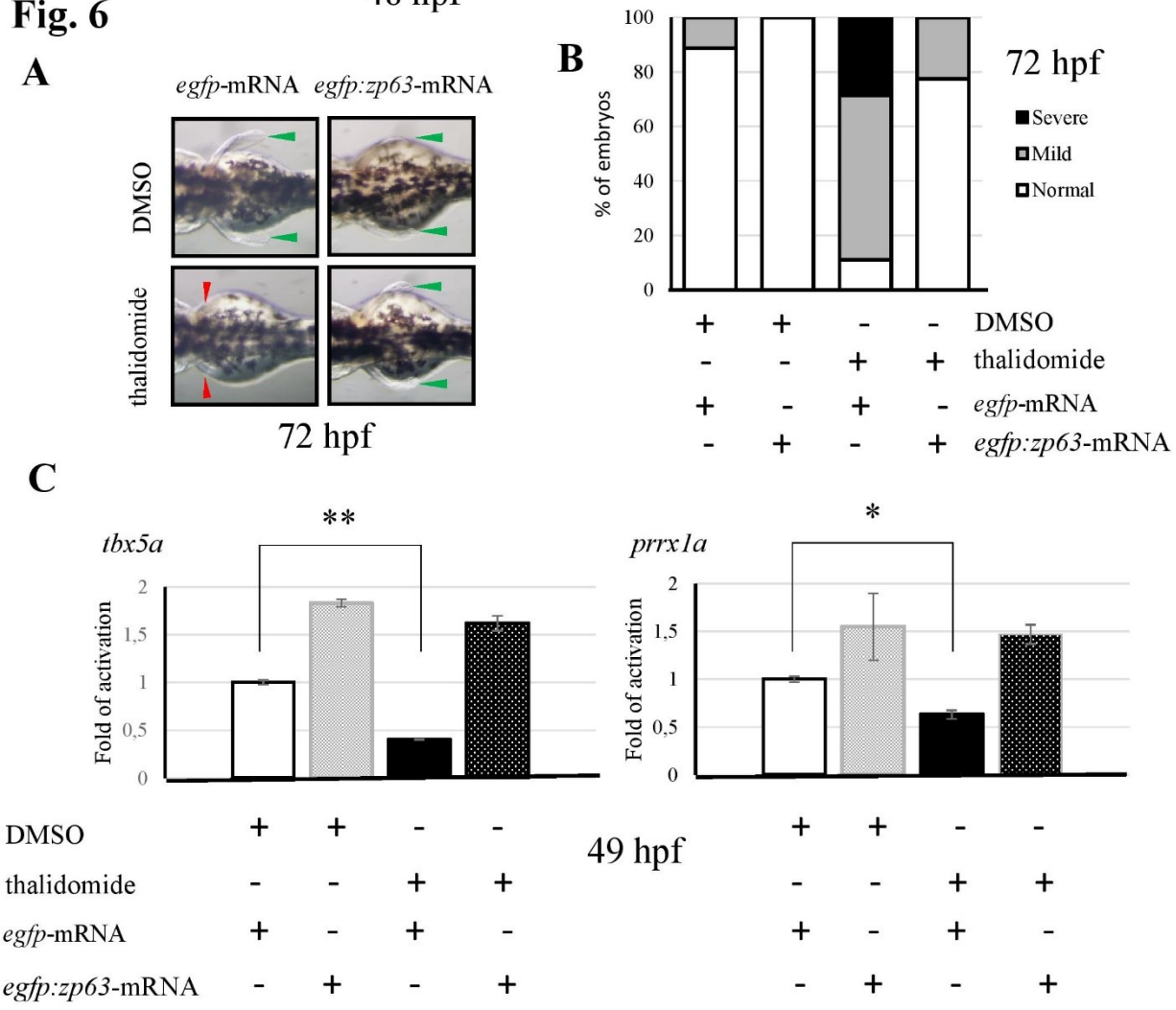
A
egfp-mRNA
egfp:zp63-mRNA
DMSO
thalidomide
72 hpf
B
% of embryos
72 hpf
Severe
Mild
Normal
DMSO
thalidomide
egfp-mRNA
egfp:zp63-mRNA
C
tbx5a
prrx1a
Fold of activation
49 hpf
DMSO
thalidomide
egfp-mRNA
egfp:zp63-mRNA

Fig. 7

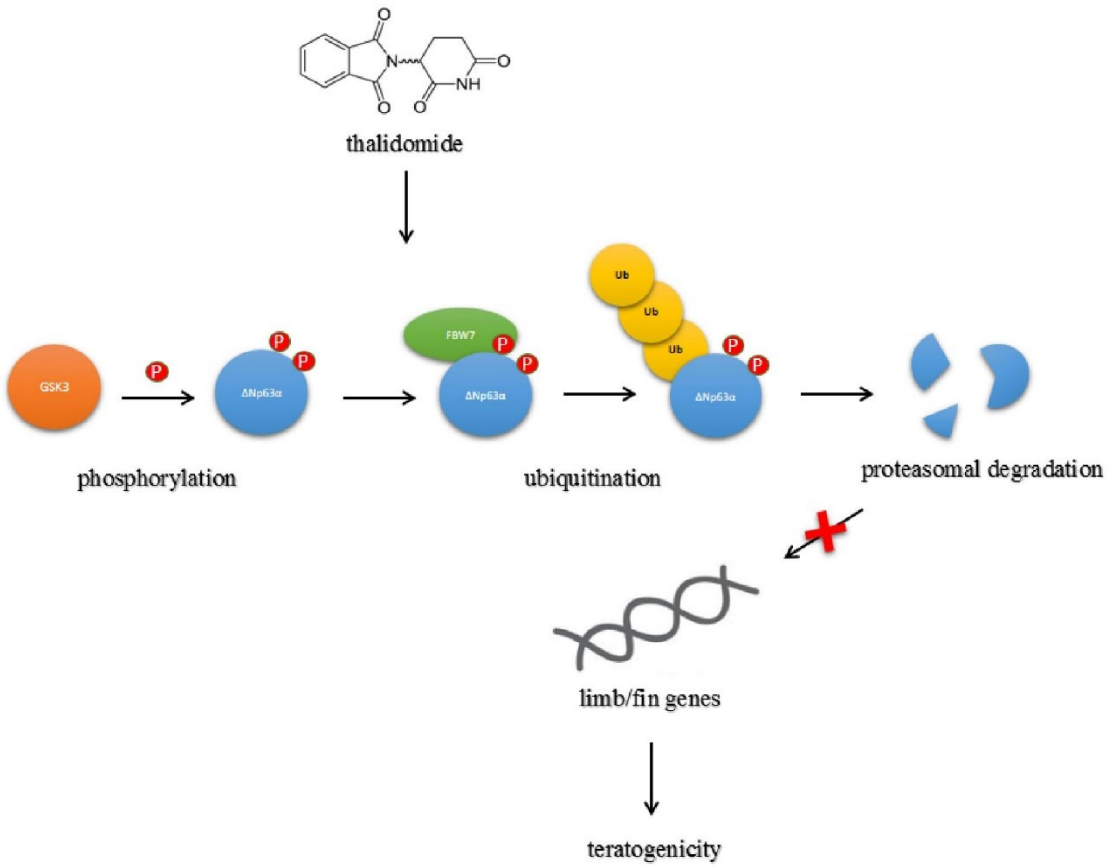
thalidomide
GSK3
ΔNp63α
FBW7
Ub
phosphorylation
ubiquitination
proteasomal degradation
limb/fin genes
teratogenicity

CRBN is a negative regulator of ΔNp63α protein

Introduction

In the last 50 years many efforts were spent trying to unravel the molecular mechanism of action of the teratogenic drug thalidomide.

Only in 2010 Ito et al. identified the primary target of thalidomide teratogenicity. By employing high-performance affinity ferriteglycidyl methacrylate (FG) beads, covalently conjugated to the carboxylic thalidomide derivative FR259625, they were able to purify from HeLa cell extracts a direct target of thalidomide drug. By mass spectrometry, it was possible to identify this protein as CEREBLON (CRBN), a protein made up of 442 amino acids, evolutionarily conserved from plants to humans (1). *CRBN* was first reported in 2004 and was originally identified as an Autosomal Recessive NonSyndromic mild Mental Retardation (ARNSMR) gene, which is located at 3p25-pter and plays an important role in central nervous system development, being involved in memory and learning (2,3). However, CRBN also possesses intrinsic ubiquitination activity and co-precipitates with all the components of the Cullin 4 (CUL4)-based E3 ubiquitin protein ligase complex. CRBN is a subunit of the CUL4-based E3 ubiquitin ligase complex where it functions as a substrate receptor (1). CUL4-based E3 ubiquitin ligases have been shown to be important for DNA repair (4–10), DNA replication (11–14), transcription (15) and development (1).

Thalidomide is able to inhibit CRBN autoubiquitination *in vitro*, suggesting that thalidomide is an inhibitor of its E3 ubiquitin ligase activity. The *CRBN Y384A/ W386A* (CRBNYW/AA) double point mutant, unable to bind to thalidomide, does not display loss of autoubiquitination activity upon drug treatment, suggesting that thalidomide inhibits E3 function of the CRBN-containing complex by directly binding to CRBN. *In vivo* studies on zebrafish embryos revealed that the microinjection in 2 cells-stage embryos of the mRNA encoding for *CRBN Y384A/ W386A*, rescues the defects otherwise induced by thalidomide in ear and pectoral fin development (1).

Collectively, all these pieces of evidence suggest that thalidomide exerts its teratogenic effects by binding to CRBN and inhibiting its function, indicating that CRBN is a primary target of thalidomide teratogenicity. In particular, it was proposed that thalidomide initiates teratogenic effects by inhibiting CRBN E3 ubiquitin ligase function, leading to the accumulation of unknown substrates that might be negative regulators of essential factors that drive correct limb/fin development, such as fgf8 (1).

In 2013 it has been demonstrated that also thalidomide analogue lenalidomide is able to bind CRBN protein and this binding mediates the therapeutic effects of the drug against Multiple Myeloma (MM), a malignancy of immunoglobulin producing plasma cells. Lu et al. and Krönke et al. demonstrated

that, after direct binding, lenalidomide is able to activate the E3 ligase activity of CRBN, which acquires the ability to selectively target for proteasomal degradation the zinc finger-containing transcription factors Ikaros (IKZF1) and Aiolos (IKZF3), which are highly expressed in B cell malignancies, including MM (16–21).

Studies on the crystallized structure of *Gallus gallus* (chicken) CRBN bound to thalidomide or lenalidomide revealed that the drugs bind to CRBN at the canonical substrate-binding site. As thalidomide and lenalidomide occupy the binding site of CRBN, they simultaneously confer to the E3 complex new substrate specificity while interfering with the recruitment of endogenous substrates (22). Therefore thalidomide and lenalidomide appear to be not only CRBN antagonists, as proposed by Ito et al. (1), instead, they more generally alter the substrate specificity of CRBN to include proteins important in MM.

Rationale

CRBN is a primary target of thalidomide teratogenicity (1). However, the highly conserved and ubiquitously expressed CRBN protein cannot account alone for the species-specificity and tissue-specificity of thalidomide teratogenicity and other components, perhaps downstream targets of CRBN, are likely to contribute to the effects of the drug. Moreover, the CRBN substrates that mediate the teratogenic cascade initiated by thalidomide have not been identified yet.

p63 is a key regulator of limb/fin development (23–26) and in the previous chapter we reported that it is an essential mediator of thalidomide teratogenicity. We proposed that thalidomide leads to FBWX7-mediated degradation of p63 and that thalidomide-induced depletion of p63 is both sufficient and necessary for the drug to initiate its teratogenic effects (Molinari et al., in preparation). However, it is not clear whether thalidomide directly interacts with p63 or its action on p63 is mediated by other components. We here aim at elucidating if CRBN is involved in mediating thalidomide-induced downregulation of p63 and if p63 is a substrate of CRBN E3 ubiquitin ligase activity.

Results

CRBN overexpression leads to ΔNp63α proteasome-mediated degradation

In order to assess whether ΔNp63α could be a substrate of thalidomide direct target CRBN, we transfected in human osteosarcoma (U2OS) cells, which do not endogenously express p63, the ΔNp63α isoform together with increasing quantities of CRBN. Overexpression of CRBN results in a dose-dependent decrease of ΔNp63α protein levels. Interestingly, this effect was blocked when the cells where concomitantly treated with the proteasome inhibitor MG132, suggesting that the overexpression of CRBN promotes a proteasome-mediated degradation of ΔNp63α (Fig. 1A). On the contrary, transient silencing of *CRBN* in U2OS cells, transfected with ΔNp63α, resulted in an upregulation of ΔNp63α protein levels (Fig. 1B), confirming that CRBN acts as a negative regulator on ΔNp63α.

Fig. 1

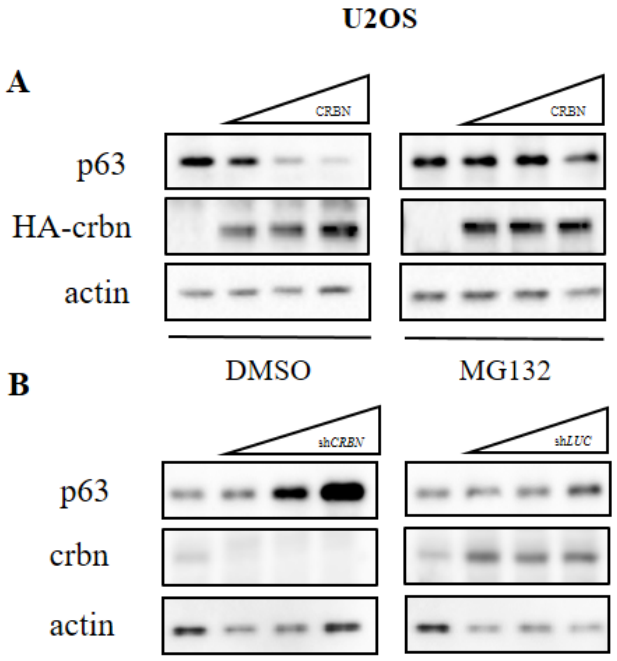

Figure 1. CRBN overexpression leads to ΔNp63α proteasome-mediated degradation. (**A**) The ΔNp63α protein is downregulated by CRBN overexpression in human U2OS. Western Blot (WB) analysis of whole U2OS cell extracts transiently co-transfected with ΔNp63α (30 ng) and increasing quantities (30, 60, 90 ng) of CRBN expression vectors and then treated with DMSO (left) or 5 μM MG 132 (right). (**B**) The ΔNp63α protein is upregulated upon *CRBN* silencing. WB analysis of whole U2OS cell extracts transiently co-transfected with ΔNp63α and sh*CRBN* or sh*LUC*.

CRBN overexpression specifically induces protein downregulation of ΔNp63α and ΔNp63β but not of ΔNp63γ

In order to analyse the response of the different p63 isoforms to CRBN overxpression, we transiently transfected U2OS cells with either ΔNp63α, ΔNp63β or ΔNp63γ isoforms together with increasing quantities of CRBN. CRBN overexpression resulted in a dose-dependent reduction of ΔNp63α and ΔNp63β, but not of ΔNp63γ (Fig. 2A). Very interestingly, ΔNp63γ resistance to CRBN overexpression reflects ΔNp63γ resistance to thalidomide treatment (see previous chapter), indicating that the C-terminal missing portion in ΔNp63γ is required both for thalidomide- and CRBN-induced p63 downregulation.

Moreover, CRBN overexpression was found able to alter specifically the levels of p63 transcription factor, since the protein levels of p53 did not change in presence of increasing quantities of CRBN (Fig 2B).

Fig. 2

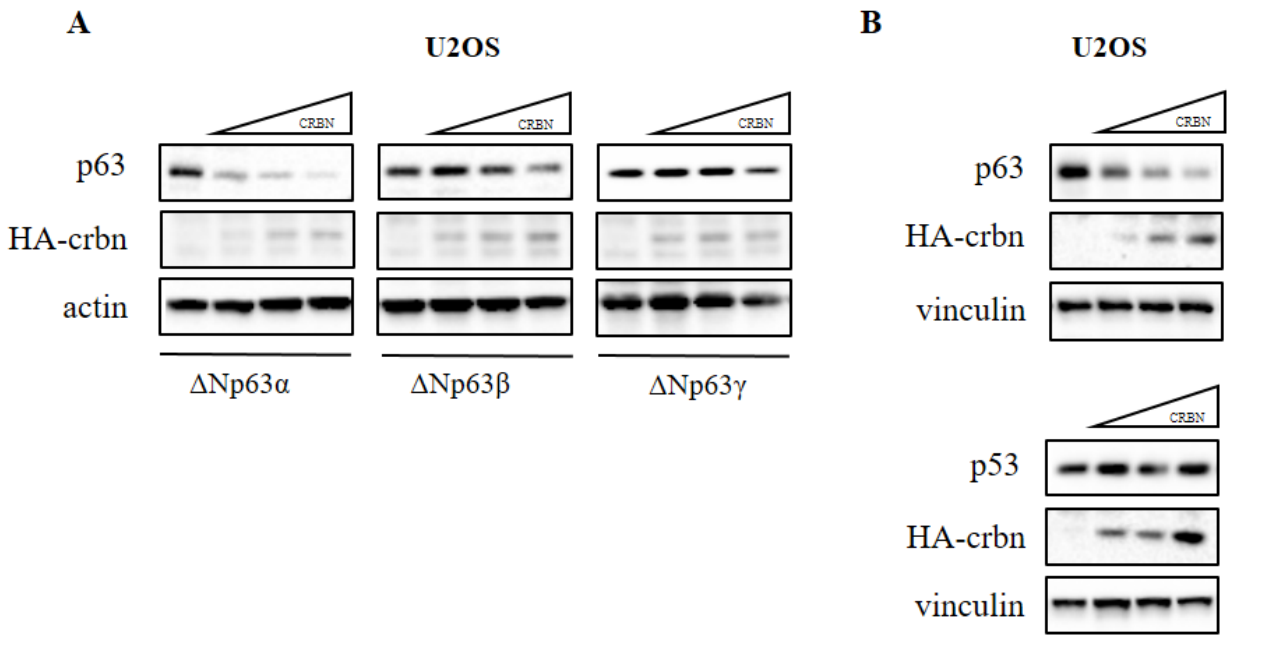

Figure 2. CRBN overexpression specifically induces protein downregulation of ΔNp63α and ΔNp63β isoforms. (**A**) WB analysis of whole extracts from U2OS cells transiently co-transfected with either ΔNp63α, ΔNp63β (30 ng) or ΔNp63γ (15 ng) expression vectors and with increasing quantities (30, 60, 90 ng) of CRBN expression vector. (**B**) CRBN overexpression efficiently induces ΔNp63α protein downergulation, whilst it does not alter the levels of p53 protein.

Crbn knockdown results in an upregulation of p63 protein in zebrafish embryos

To confirm whether crbn is able to perturb p63 protein levels also *in vivo*, we transiently knocked down *zcrbn* in zebrafish embryos by microinjecting a *zcrbn*-specific morpholino (*zcrbn*-MO) and let the embryos develop for 72 hours post fertilization (hpf). The morphant embryos displayed mild fin defects in a *zcrbn*-MO dose-dependent manner (Fig. 3A, 3B), similarly as previously showed by Ito et al. (1). We then checked the protein levels of p63 from control and morphant whole embryos extracts. Interestingly, also in zebrafish embryos, the knockdown of *crbn* is able to promote a dose-dependent upregulation of p63 protein, indicating that crbn acts as a negative regulator of p63 also *in vivo* in zebrafish embryos (Fig. 3C).

Fig. 3

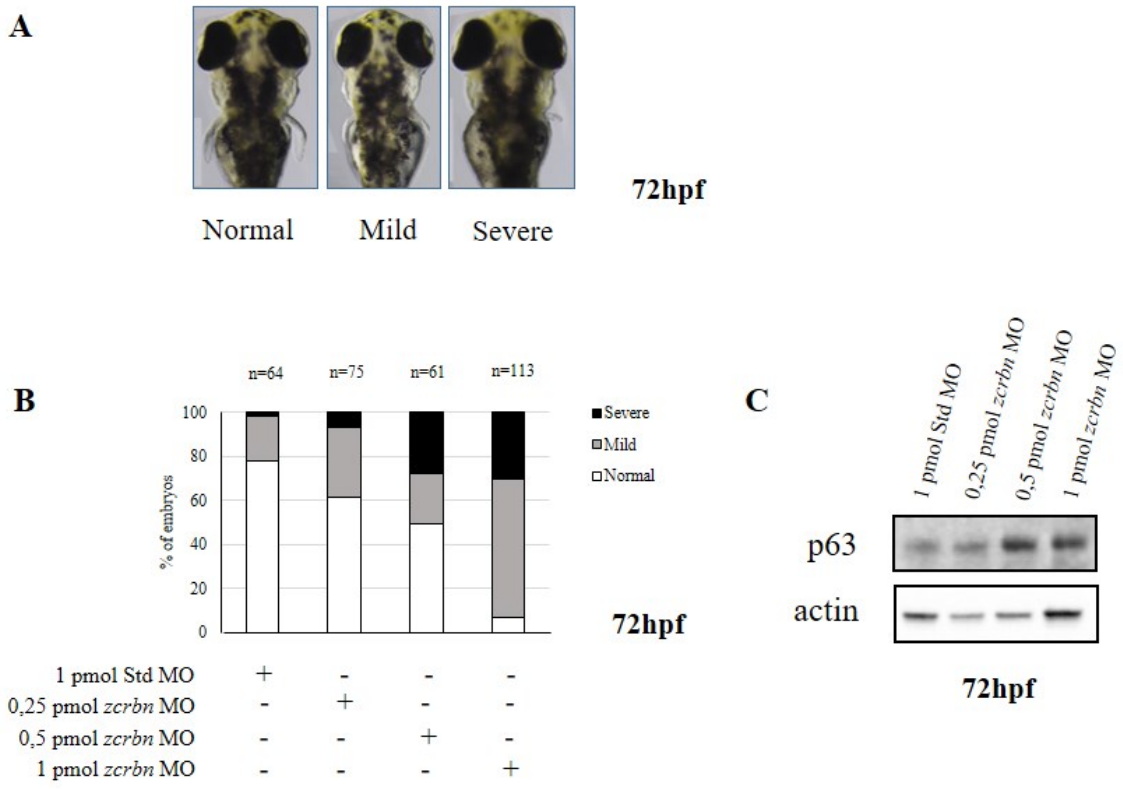

Figure 4. *Crbn* knockdown results in an upregulation of p63 protein in zebrafish embryos. (**A**) Microinjected embryos with *zcrbn*-MO displayed mild fin defects in a dose-dependent manner. Dorsal views of pectoral fins of 72 hpf embryos. The embryos were classified on the basis of the pectoral fins length. Normal class embryos displayed normal fins, Mild class embryos displayed shorter, non-protruding fins, Severe class embryos did not display a proper fin fold but a fin bud, or complete absence of the fin. (**B**) Percentage of embryos displaying Normal, Mild or Severe phenotype for each dose of control-MO (Std-MO) or *zcrbn*-MO injected. (**C**) WB analysis of whole extracts from zebrafish embryos microinjected

with Std-MO or with increasing doses of *zcrbn*-MO. The embryos were analysed for p63 protein expression levels at the stage of 72-hpf.

Mouse CRBN is not able to induce ΔNp63α protein downregulation in murine cells

Thalidomide is able to induce developmental malformations in human, chimps, rabbit, chicken and zebrafish but not in mouse and rat and the reasons for the species-specificity of thalidomide teratogenicity are still unknown (27). CRBN is highly conserved from fish to mammals and the residues Y384 and W386, identified by Ito et al. as responsible for thalidomide binding (1), are also present in the murine protein. Thus, CRBN alone can hardly explain the species-specificity of thalidomide teratogenicity and it is possible that other molecules, perhaps downstream targets of CRBN, may define the specificity of thalidomide teratogenicity.

We raised the hypothesis that the species-specificity of thalidomide teratogenicity might be explained by the differential ability of CRBN orthologues from different species to induce ΔNp63α protein downregulation. To test this hypothesis we firstly expressed in U2OS cells ΔNp63α together with increasing quantities of either *Homo sapiens* (human) or *Mus musculus* (mouse) CRBN. The human and mouse CRBN orthologues did not display differential efficiency in inducing ΔNp63α downregulation (Fig. 4A). However, when we repeated the experiment in a murine context, by overexpressing either human or mouse CRBN in ΔNp63α transfected murine embryo fibroblasts NIH 3T3 cells, mouse CRBN displayed a significant lower efficiency in promoting ΔNp63α downregulation compared to its human orthologous (Fig. 4B).

Fig. 4

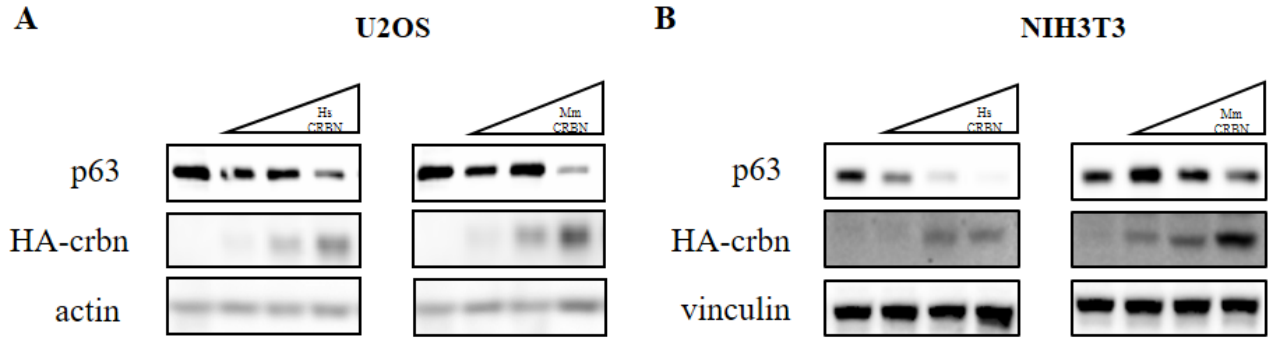

Figure 5. Mouse CRBN is not able to induce ΔNp63α protein downregulation in murine cells. (**A**) WB analysis of whole extracts from U2OS cells transiently co-transfected with ΔNp63α (30 ng) and increasing quantities (30, 60, 90 ng) of either human (Hs) or mouse (Mm) CRBN expression vectors. (**B**) WB analysis of whole extracts from NIH 3T3 cells transiently co-transfected with ΔNp63α (30 ng) and increasing quantities (30, 60, 90 ng) of either human (Hs) or mouse (Mm) CRBN expression vectors

Human and mouse CRBN display a differential ability to interact with ΔNp63α in a murine context

In order to verify if the effect of CRBN on ΔNp63α levels is due to a physical interaction between the two proteins, we transfected U2OS cells with ΔNp63α, together with either human or mouse CRBN, immunoprecipitated HA-CRBN from these cell extracts and checked whether ΔNp63α was able to co-immunoprecipitate with CRBN. Indeed, ΔNp63α co-immunoprecipitated with both human and mouse CRBN (Fig. 5A). We then repeated the same assay in NIH 3T3 cells. In murine context, ΔNp63α displayed a strikingly reduced ability to co-immunoprecipitate with mouse CRBN, whilst it still efficiently interacted with human CRBN (Fig. 5B).

Should ΔNp63α be a downstream target of CRBN in thalidomide teratogenic cascade, the differential ability of CRBN orthologues from different species to interact with ΔNp63α might provide a hint into the species-specificity of thalidomide teratogenicity.

Fig. 5

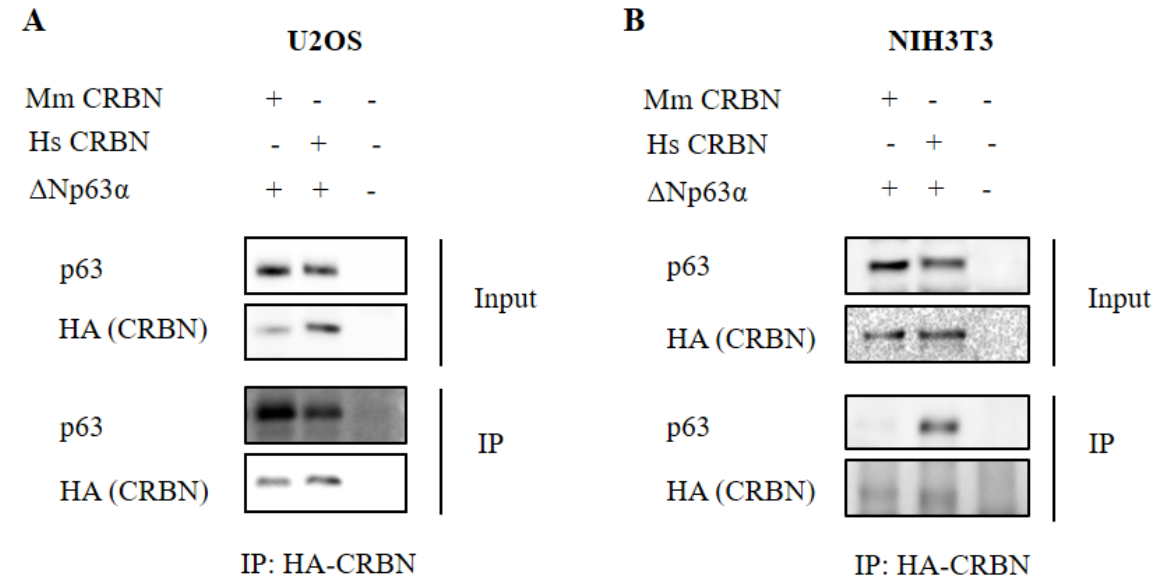

Figure 5. ΔNp63α and CRBN belong to the same immunocomplex. (**A**) U2OS whole cell extracts transiently co-transfected with ΔNp63α (10 µg) and either mouse (Mm) or human (Hs) HA-CRBN (10 µg) were analyzed by immunoprecipitation with anti-HA antibody followed by WB analysis with anti-p63 antibody. U2OS cells not transfected were used as negative control. (**B**) NIH 3T3 whole cell extracts transiently co-transfected with ΔNp63α (10 µg) and either mouse (Mm) or human (Hs) HA-CRBN (10 µg) were analyzed by immunoprecipitation with anti-HA antibody followed by WB analysis with anti-p63 antibody. NIH 3T3 cells not transfected were used as negative control.

Discussion and future perspectives

CRBN is the only direct target of thalidomide identified so far (1). However, the highly conserved and ubiquitariously expressed CRBN protein can hardly explain alone the species- and tissue-specificity of thalidomide teratogenicity and other components are likely to be involved in the teratogenic process.

Ito et al., proposed that thalidomide initiates its teratogenic effects by inhibiting CRBN ubiquitin ligase activity on unknown substrates that might be negative regulators of factors essential for limb/fin development, such as fgf8 (1). Nevertheless, the direct substrates of CRBN in the teratogenic cascade have not been identified yet.

We showed in the previous chapter that ΔNp63α is a target of thalidomide teratogenicity, as thalidomide induces a reduction of ΔNp63α protein levels *in vitro* and *in vivo* and this effect is, at least in part, at the basis of the developmental defects induced by the drug (Molinari et al., in preparation). However, it is not clear how thalidomide induces a reduction of ΔNp63α; whether it directly acts on ΔNp63α or on other components upstream to ΔNp63α in the teratogenic cascade.

The preliminary data that we are here reporting indicate that also CRBN is able to promote a downregulation of ΔNp63α protein. CRBN is a substrate receptor in CUL4-based E3 ubiquitin ligase complex (1). Our data are compatible with the hypothesis that ΔNp63α could be a substrate of CRBN ubiquitin ligase activity. Thalidomide, which is known to alter the activity and substrate specificity of CRBN (16,17,22), might promote a reduction of ΔNp63α protein levels by activating CRBN ubiquitin ligase activity towards ΔNp63α.

ΔNp63α, which is an essential factor that drives correct limb and fin development, might represent a good candidate for mediating the teratogenic effects triggered by the binding of thalidomide to CRBN and could define the tissue-specificity of the malformations induced by the drug. Moreover, we found that, unlike its human orthologous, mouse CRBN is poorly efficient in co-immunoprecipitating with ΔNp63α and in inducing its downregulation in murine cells. Should ΔNp63α be a downstream target of CRBN in thalidomide teratogenic cascade, the differential sensitivity of ΔNp63α to CRBN orthologues from different species might explain the species-specificity of thalidomide teratogenicity.

However, many questions remain to be addressed:

a) does CRBN mediate thalidomide action on ΔNp63α?

To verify if CRBN is indeed involved in thalidomide-induced degradation of ΔNp63α we plan to analyse the effects of thalidomide-treatment on ΔNp63α protein levels in cells where CRBN has been silenced or overexpressed.

b) does CRBN directly ubiquitinate ΔNp63α or does it act indirectly via a regulator of ΔNp63α stability?
c) we showed in the previous chapter that thalidomide promotes p63 degradation via FBWX7 ubiquitin ligase activity (Molinari et al., in preparation). Provided that CRBN contributes to thalidomide-induced ΔNp63α downregulation, does it interact with FBWX7 or does it function through an independent pathway?
d) Finally, we plan to investigate the reasons of the reduced interaction between mouse CRBN and ΔNp63α protein in murine cells.

Thalidomide is now used for treatment of MM and leprosy (28,29): a better understanding of its mechanism of action might pave the way for the design of related compounds with equal therapeutic properties but devoid of teratogenic activity. Moreover, it has been shown that the ability of thalidomide and its analogues to alter CRBN substrates specificity mediates not only the teratogenicity but also the therapeutic properties of these drugs (16,17,30). Therefore, elucidating whether ΔNp63α is a real substrate of CRBN and whether thalidomide is able to alter CRBN function on ΔNp63α might have a therapeutic relevance in those malignant conditions in which p63 is overexpressed.

Experimental procedures

Plasmids

All expression vectors encoding p63 cDNAs have been previously described (31). The CRBN constructs have also been previously described (1).

Cell culture, transfection and treatments

U2OS cells were kept in DMEM supplemented with 10% FBS (Euroclone) at 37°C in a humified atmosphere of 5% (v/v) CO_2 in air. For transient transfection, 50000 cells were seeded into 24-multiwell plates and on the next day transfected with Lipofectamine 3000 (Invitrogen) under the conditions suggested by the manufacturer. Transfection efficiency was checked by transfection of β-gal or GFP expression vectors. The total amount of transfected DNA (500 ng for 50 000 cells) was kept constant using empty vector as necessary. U2OS cells were treated with 5 μM MG132 (Sigma-Aldrich) for 3 h.

Zebrafish maintenance and treatments

Current Italian national rules: no approval needs to be given for research on zebrafish embryos. Wild-type zebrafish of the AB strain were raised and maintained according to established techniques (32). Embryos were collected by natural spawning.

Western blot and antibodies

24 h after transfection, cells were lysed in 100 µl of Loading Buffer 2X (2% sodium dodecyl sulfate, 30% glycerol, 144 mM β-mercaptoethanol, 100 mM Tris HCl pH 6.8 and 0.1% Bromo-Phenol Blue). Zebrafish total extracts were obtained by mechanical disgregation of the embryos into RIPA Buffer (50 mM Tris HCl pH 8.0, 150 mM NaCl, 0.1% SDS, 0.1% NP-40, 0.5% sodium deoxycholate). PMSF and cocktail protease inhibitors (Sigma-Aldrich) were added according to the manufacturer's instruction.

Cell and zebrafish embryo samples were incubated at 98°C for 10 min and resolved by SDS-PAGE. Proteins were transferred to a nitrocellulose membrane (Protran, Millipore). The blots were incubated with the following antibodies: p63 (mouse monoclonal 4A4 sc-8431, Santa Cruz Biotechnology) HA (rabbit polyclonal Y-11 sc-805, Santa Cruz Biotechnology), p53 (mouse monoclonal DO1, Genespin) and actin (A2066, Sigma). We used the following secondary antibodies: goat α-mouse (sc-2005, Santa Cruz Biotechnology) and goat α-rabbit (sc-2030, Santa Cruz Biotechnology). Proteins were visualized by an enhanced chemi-luminescence method (Biorad) according to manufacturer's instructions.

Microinjection of Morpholino

Injections were carried out on 1–2 cell-stage embryos (Eppendorf FemtoJet Micromanipulator 5171); the dye tracer, rhodamine dextran, was co-injected. A standard control morpholino (Std-MO) oligonucleotide specific for human β-thalassemia was used. *zcrbn* antisense ATG morpholino (*zcrbn*-MO) (Gene Tools) used in this study has been previously described (1).

Co-immunoprecipitation

U2OS cells (1.25×10^6/100mm plate) were transfected with the indicated vectors. 48 h after transfection, cells were harvested for whole-cell lysates preparation using RIPA buffer (10mM Tris–HCl pH 8, 2mM EDTA, 0.1% SDS, 0.1% sodium deoxycholate, 140 mM NaCl, 1X Triton X-100, supplemented with 1mM phenylmethylsulfonylfluoride and cocktail protease inhibitors, Sigma). Cell lysates were incubated on ice for 20 min, vortexed, then centrifuged at 6600 g for 20 min to remove cell debris. Protein concentration was determined with the Bradford Reagent (Sigma). 2 mg of cell

lysates were incubated overnight at 4°C with 2 µg of anti-HA (rabbit polyclonal Y-11 sc-805, Santa Cruz Biotechnology). The immuno-complexes were collected by incubating with a mix of Protein A Agarose and Protein G Sepharose (Sigma) overnight at 4°C. The beads were washed three times: the first wash with RIPA buffer and the others with PBS. The beads were then resuspended in 2X Loading buffer, heated at 98°C and loaded on a SDS polyacrylamide gel and subjected to western blotting with the indicated antibodies.

References

1. Ito T, Ando H, Suzuki T, Ogura T, Hotta K, Imamura Y, et al. Identification of a primary target of thalidomide teratogenicity. Science. 2010 Mar 12;327(5971):1345–50.

2. Higgins JJ, Rosen DR, Loveless JM, Clyman JC, Grau MJ. A gene for nonsyndromic mental retardation maps to chromosome 3p25-pter. Neurology. 2000 Aug 8;55(3):335–40.

3. Higgins JJ, Pucilowska J, Lombardi RQ, Rooney JP. A mutation in a novel ATP-dependent Lon protease gene in a kindred with mild mental retardation. Neurology. 2004 Nov 23;63(10):1927–31.

4. Groisman R, Kuraoka I, Chevallier O, Gaye N, Magnaldo T, Tanaka K, et al. CSA-dependent degradation of CSB by the ubiquitin-proteasome pathway establishes a link between complementation factors of the Cockayne syndrome. Genes Dev. 2006 Jun 1;20(11):1429–34.

5. Wang H, Zhai L, Xu J, Joo H-Y, Jackson S, Erdjument-Bromage H, et al. Histone H3 and H4 ubiquitylation by the CUL4-DDB-ROC1 ubiquitin ligase facilitates cellular response to DNA damage. Mol Cell. 2006 May 5;22(3):383–94.

6. Kapetanaki MG, Guerrero-Santoro J, Bisi DC, Hsieh CL, Rapić-Otrin V, Levine AS. The DDB1-CUL4ADDB2 ubiquitin ligase is deficient in xeroderma pigmentosum group E and targets histone H2A at UV-damaged DNA sites. Proc Natl Acad Sci U S A. 2006 Feb 21;103(8):2588–93.

7. Groisman R, Polanowska J, Kuraoka I, Sawada J, Saijo M, Drapkin R, et al. The ubiquitin ligase activity in the DDB2 and CSA complexes is differentially regulated by the COP9 signalosome in response to DNA damage. Cell. 2003 May 2;113(3):357–67.

8. Nag A, Bondar T, Shiv S, Raychaudhuri P. The xeroderma pigmentosum group E gene product DDB2 is a specific target of cullin 4A in mammalian cells. Mol Cell Biol. 2001 Oct;21(20):6738–47.

9. Chen X, Zhang Y, Douglas L, Zhou P. UV-damaged DNA-binding proteins are targets of CUL-4A-mediated ubiquitination and degradation. J Biol Chem. 2001 Dec 21;276(51):48175–82.

10. Sugasawa K, Okuda Y, Saijo M, Nishi R, Matsuda N, Chu G, et al. UV-induced ubiquitylation of XPC protein mediated by UV-DDB-ubiquitin ligase complex. Cell. 2005 May 6;121(3):387–400.

11. Liu C, Powell KA, Mundt K, Wu L, Carr AM, Caspari T. Cop9/signalosome subunits and Pcu4 regulate ribonucleotide reductase by both checkpoint-dependent and -independent mechanisms. Genes Dev. 2003 May 1;17(9):1130–40.

12. Bondar T, Ponomarev A, Raychaudhuri P. Ddb1 is required for the proteolysis of the Schizosaccharomyces pombe replication inhibitor Spd1 during S phase and after DNA damage. J Biol Chem. 2004 Mar 12;279(11):9937–43.

13. Higa LAA, Mihaylov IS, Banks DP, Zheng J, Zhang H. Radiation-mediated proteolysis of CDT1 by CUL4-ROC1 and CSN complexes constitutes a new checkpoint. Nat Cell Biol. 2003 Nov;5(11):1008–15.

14. Hu J, McCall CM, Ohta T, Xiong Y. Targeted ubiquitination of CDT1 by the DDB1-CUL4A-ROC1 ligase in response to DNA damage. Nat Cell Biol. 2004 Oct;6(10):1003–9.

15. Wertz IE, O'Rourke KM, Zhang Z, Dornan D, Arnott D, Deshaies RJ, et al. Human De-etiolated-1 regulates c-Jun by assembling a CUL4A ubiquitin ligase. Science. 2004 Feb 27;303(5662):1371–4.

16. Krönke J, Udeshi ND, Narla A, Grauman P, Hurst SN, McConkey M, et al. Lenalidomide causes selective degradation of IKZF1 and IKZF3 in multiple myeloma cells. Science. 2014 Jan 17;343(6168):301–5.

17. Lu G, Middleton RE, Sun H, Naniong M, Ott CJ, Mitsiades CS, et al. The myeloma drug lenalidomide promotes the cereblon-dependent destruction of Ikaros proteins. Science. 2014 Jan 17;343(6168):305–9.

18. Ferreirós-Vidal I, Carroll T, Taylor B, Terry A, Liang Z, Bruno L, et al. Genome-wide identification of Ikaros targets elucidates its contribution to mouse B-cell lineage specification and pre-B-cell differentiation. Blood. 2013 Mar 7;121(10):1769–82.

19. Thompson EC, Cobb BS, Sabbattini P, Meixlsperger S, Parelho V, Liberg D, et al. Ikaros DNA-binding proteins as integral components of B cell developmental-stage-specific regulatory circuits. Immunity. 2007 Mar;26(3):335–44.

20. Merkenschlager M. Ikaros in immune receptor signaling, lymphocyte differentiation, and function. FEBS Lett. 2010 Dec 15;584(24):4910–4.

21. Monticelli S, Sallusto F. Negative regulators take center stage. Nat Immunol. 2012 Aug;13(8):719–20.

22. Fischer ES, Böhm K, Lydeard JR, Yang H, Stadler MB, Cavadini S, et al. Structure of the DDB1-CRBN E3 ubiquitin ligase in complex with thalidomide. Nature. 2014 Aug 7;512(7512):49–53.

23. Mills AA, Zheng B, Wang XJ, Vogel H, Roop DR, Bradley A. p63 is a p53 homologue required for limb and epidermal morphogenesis. Nature. 1999 Apr 22;398(6729):708–13.

24. Yang A, Schweitzer R, Sun D, Kaghad M, Walker N, Bronson RT, et al. p63 is essential for regenerative proliferation in limb, craniofacial and epithelial development. Nature. 1999 Apr 22;398(6729):714–8.

25. Bakkers J, Hild M, Kramer C, Furutani-Seiki M, Hammerschmidt M. Zebrafish DeltaNp63 is a direct target of Bmp signaling and encodes a transcriptional repressor blocking neural specification in the ventral ectoderm. Dev Cell. 2002 May;2(5):617–27.

26. Lee H, Kimelman D. A dominant-negative form of p63 is required for epidermal proliferation in zebrafish. Dev Cell. 2002 May;2(5):607–16.

27. Ito T, Ando H, Handa H. Teratogenic effects of thalidomide: molecular mechanisms. Cell Mol Life Sci CMLS. 2011 May;68(9):1569–79.

28. Sheskin J. THALIDOMIDE IN THE TREATMENT OF LEPRA REACTIONS. Clin Pharmacol Ther. 1965 Jun;6:303–6.

29. Singhal S, Mehta J, Desikan R, Ayers D, Roberson P, Eddlemon P, et al. Antitumor activity of thalidomide in refractory multiple myeloma. N Engl J Med. 1999 Nov 18;341(21):1565–71.

30. Ito T, Handa H. Myeloid disease: Another action of a thalidomide derivative. Nature. 2015 Jul 9;523(7559):167–8.

31. Ghioni P, Bolognese F, Duijf PHG, Van Bokhoven H, Mantovani R, Guerrini L. Complex transcriptional effects of p63 isoforms: identification of novel activation and repression domains. Mol Cell Biol. 2002 Dec;22(24):8659–68.

32. Westerfield M. The zebrafish book. A guide for the laboratory use of zebrafish (Danio rerio). 4th ed. University of Oregon Press; 2000.